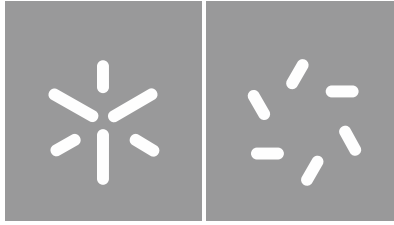


**Universidade do Minho**  
Escola de Ciências

José Miguel Marques Rios de Sá Rosas

**Genetic mechanisms involved in  
dormancy and flower induction of  
Fagaceae trees**





**Universidade do Minho**

Escola de Ciências

José Miguel Marques Rios de Sá Rosas

**Genetic mechanisms involved in  
dormancy and flower induction of  
Fagaceae trees**

Dissertação de Mestrado

Mestrado de Biologia Molecular, Biotecnologia e  
Bioempreendedorismo em Plantas

Trabalho efetuado sob a orientação de  
**Professora Doutora Maria Manuela  
Ribeiro Costa**

abril de 2023

## **Direitos de autor e condições de utilização do trabalho por terceiros**

Este é um trabalho académico que pode ser utilizado por terceiros desde que respeitadas as regras e boas práticas internacionalmente aceites, no que concerne aos direitos de autor e direitos conexos.

Assim, o presente trabalho pode ser utilizado nos termos previstos na licença [abaixo](#) indicada.

Caso o utilizador necessite de permissão para poder fazer um uso do trabalho em condições não previstas no licenciamento indicado, deverá contactar o autor, através do RepositóriUM da Universidade do Minho.

### ***Licença concedida aos utilizadores deste trabalho***



**Atribuição  
CC BY**

<https://creativecommons.org/licenses/by/4.0/>

## **Acknowledgements**

I would like to express my gratitude to Doctor Maria Manuela Ribeiro Costa for giving me the opportunity of developing this work, and for guiding me throughout this project giving her advice and sharing her scientific knowledge.

I would also like to thank all my colleagues in LBFP for showing me the ropes around the lab and creating a pleasant environment to work in. A special thanks to Ana Teresa for helping me throughout this journey, and for all the enriching debates.

To my family, thank you for always supporting and believing in me. Specially to my parents, Fátima and Luís, for always encouraging me and supporting my dreams in every step of the way. Thank you for instilling in me the curiosity, critical thinking and passion that led me down this path.

To my friends, for all the moments, debates, and friendship that helped me grow immeasurably as a person, you guys are the best, and so is Loftus.

Finally, to Marisa, for always being by my side and for all the love and unwavering support you gave throughout both easy and tougher times, thank with all my heart, this journey would not have been possible without your help and encouragement.

## **Statement of Integrity**

I hereby declare having conducted this academic work with integrity. I confirm that I have not used plagiarism or any form of undue use of information or falsification of results along the process leading to its elaboration.

I further declare that I have fully acknowledged the Code of Ethical Conduct of the University of Minho.

**Resumo:** Mecanismos genéticos envolvidos na regulação da dormência e floração em Fagaceae

As Fagaceae estão entre as árvores perenes mais importantes a nível económico e ecológico. Durante o inverno, estas árvores entram em estado de dormência de forma a proteger os meristemas e os órgãos primordiais do frio até que se verifiquem condições mais favoráveis à retoma do seu crescimento vegetativo e reprodutivo. Estes ciclos de crescimento/dormência dependem da combinação de respostas complexas a sinais ambientais mediadas por mecanismos reguladores moleculares. *Quercus robur* (carvalho roble) e *Quercus suber* (sobreiro) são fagáceas de grande relevância nos países mediterrânicos. Ambas espécies entram em dormência no outono, mantendo os gomos em estado dormente durante o inverno. Na primavera ocorre o abrolhamento nas duas espécies, com as flores monoicas masculinas (amentilhos) a surgirem pouco tempo depois. No entanto, o sobreiro apresenta um fenótipo único entre as fagáceas, uma vez que a sua floração masculina e feminina apresentam ampla separação física e temporal. Isto é, cada evento de floração ocorre com um intervalo de um a dois meses, e não há sinais de abortamento de estruturas reprodutoras do sexo oposto durante todo o desenvolvimento floral. Desvendar os mecanismos genéticos reguladores da dormência e da floração nestas espécies poderá demonstrar-se de grande interesse. Este trabalho visou a identificação e análise da expressão dos potenciais genes reguladores da dormência e floração em *Q. robur* e em *Q. suber* durante um ciclo anual de crescimento. Foi desenhado um *Yeast One-Hybrid assay* para testar a interação entre o gene *QsPI* e o seu potencial regulador QsHTH. Foi observado que o *QrFT* é sobreexpresso na fase de crescimento ativo e reprimido durante a dormência sugerindo a conservação do seu papel enquanto libertador da dormência e promotor do crescimento. Foram observados dois picos de expressão dos genes *QrSOC1*, *QrSPL4* e *QrSHP*, um durante a fase de “*bud swelling*” e outro antes da indução da dormência, sugerindo duas fases de indução das flores. *QrFLC* e *QrSVP1* registaram um pico de expressão em Outubro, sugerindo a participação destes genes na indução e/ou manutenção da dormência. A sequência codificante do QsHTH foi clonada no pGAD424 e o plasmídeo pAbai contendo parte da sequência do promotor *QsPI* foi integrado no genoma Y1Gold. Fornecendo, desta forma, todos os componentes necessários para testar a interação entre *QsPI* e QsHTH num ensaio Y1H. Esta tese proporcionou um útil ponto de vista sobre os mecanismos reguladores da dormência e floração em *Q. robur*, com importância para futuros estudos e em Fagaceae, e estabeleceu as etapas necessárias para futuras análises da regulação do QsPI e dos mecanismos que controlam a identidade dos sexual das flores.

**Palavras-chave:** Fagaceae; *Quercus robur*; *Quercus suber*; dormência; *FLOWERING LOCUS T*; *SHORT VEGETATIVE PHASE*; floração; unissexualidade; *PISTILLATA*; *HOTHEAD*

**Abstract:** Genetic mechanisms involved in dormancy and flower induction of Fagaceae trees

Fagaceae are amongst the most ecologically and economically relevant perennial tree species. During winter, these trees rely on dormancy to protect their meristems and organ primordia from the cold, until more favorable conditions are met and both vegetative and reproductive growth are resumed. These growth-dormancy cycles are tightly regulated by integration of responses to environmental cues with molecular regulatory mechanisms. *Quercus robur* and *Quercus suber* are two Fagaceae of utmost importance in Mediterranean countries, both species enter a dormancy in autumn, with the buds remaining dormant throughout the winter. Usually, in spring bud burst occurs in both species with monoecious flowers emerging shortly after, however, *Q. suber* flowering phenotype is particular among Fagaceae trees, as *Q. suber* male and female flowering exhibits a complete temporal and spatial separation, with both flowers being unisexual by inception, and each flowering event occurring one to two months apart. Thus, uncovering the genetic networks regulating dormancy and flowering in these two oak species is of great interest. In this work, identification and expression analysis of potential homologs of *Q. robur* and *Q. suber* dormancy and flowering time regulators was performed, and their expression analysis was performed by PCR, during one growing season. Furthermore, an Yeast One-Hybrid assay to test the interaction between B-class MADS-box gene *QsPI* and its potential regulator QsHTH was designed. *QrFT* was observed to be differentially overexpressed during phases of active growth and downregulated during dormancy, implying a possible role conservation as a dormancy release and growth promoter. *QrSOC1*, *QrSPL4* and *QrSHP* were observed to have two expression peaks, one during the buds swelling phase and other in late summer before dormancy induction, possibly indicating two flower induction events. *QrFLC* and *QrSVP1* displayed an expression peak in October, suggesting the involvement of these genes in dormancy induction and maintenance. *QsHTH* open reading frame was also successfully cloned into the pGAD424 vector, and the pAbai plasmid containing a fragment of *QsPI* promoter sequence was successfully integrated into the Y1Gold genome. Thus, providing all required components for testing the interaction between *QsPI* and QsHTH in an Y1H assay. This thesis provided a useful insight into the regulatory mechanisms of dormancy and flowering in *Q. robur*, which might be useful for future studies focused on other Fagaceae with similar reproductive habits, while setting required steps for further analysis of *QsPI* regulation, and to a further extent uncover the mechanisms controlling the flowers reproductive organ identity.

**Keywords:** Fagaceae; *Quercus robur*; *Quercus suber*; bud dormancy; *FLOWERING LOCUS T*; *SHORT VEGETATIVE PHASE*; flower induction; monoecy; unisexuality; *PISTILLATA*; *HOTHEAD*

## Table of contents

Direitos de autor e condições de utilização do trabalho por terceiros .....	ii
Statement of Integrity .....	iv
Resumo.....	v
Abstract.....	vi
Table of contents .....	vii
List of figures.....	x
List of tables .....	xvi
List of Abbreviations .....	xvi
<b>1. Introduction.....</b>	<b>1</b>
<b>1.1. Fagaceae .....</b>	<b>1</b>
1.1.1. <i>Quercus robur</i> .....	2
1.1.2. <i>Quercus suber</i> .....	4
<b>1.2. Bud dormancy and growth cycle.....</b>	<b>7</b>
1.2.1. Dormancy stages .....	9
<b>1.3. Dormancy and flower induction regulation .....</b>	<b>10</b>
1.3.2. Metabolism of carbohydrates .....	11
1.3.3. Phytohormones.....	11
1.3.4. Epigenetic regulation .....	12
1.3.5. Genetic regulation.....	13
<b>1.4. Flowering.....</b>	<b>16</b>
<b>1.5. Previous studies in <i>Q. suber</i> and its particular case of unisexuality and flower organ determination. ....</b>	<b>20</b>
<b>2. Objectives.....</b>	<b>23</b>
<b>3. Materials and Methods.....</b>	<b>24</b>
<b>3.1. Plant material .....</b>	<b>24</b>
<b>3.2. Phylogenetic analysis .....</b>	<b>24</b>

3.3.	RNA extraction .....	25
3.4.	DNase treatment .....	26
3.5.	cDNA synthesis .....	26
3.6.	Polymerase chain reaction (PCR).....	26
3.7.	Colony PCRs .....	27
3.8.	Scanning densitometry .....	28
3.9.	Molecular assays .....	29
3.9.1.	Bacterial/yeast material.....	29
3.9.1.1.	<i>Escherichia coli</i> .....	29
3.9.1.2.	<i>E. coli</i> competent cells.....	29
3.9.1.3.	<i>Saccharomyces cerevisiae</i> .....	29
3.9.1.4.	<i>Saccharomyces cerevisiae</i> competent cells .....	30
3.9.2.	Amplification of <i>QsHTH</i> .....	30
3.9.3.	Isolation of plasmid DNA .....	30
3.9.4.	DNA purification.....	31
3.9.4.1.	Phenol/Chloroform DNA extraction method.....	31
3.9.4.2.	Wizard SV Gel and PCR Clean-Up System.....	32
3.9.5.	Cloning procedures.....	32
3.9.5.1.	Cloning into pGEM-T.....	32
3.9.5.2.	Cloning into pGAD424 .....	32
3.9.5.3.	pGAD424 digestion reaction.....	32
3.9.5.4.	QsHTH digestion reaction .....	33
3.9.5.5.	Ligation reaction .....	33
3.9.6.	Bacterial/yeast transformation .....	33
3.9.6.1.	Transformation in <i>E. coli</i> .....	33
3.9.6.2.	Transformation in Yeast .....	34

<b>4. Results and Discussion .....</b>	<b>35</b>
<b>4.1. Phenological Observations .....</b>	<b>35</b>
<b>4.2. Identification of <i>Q. robur</i> homologs relevant to dormancy and flowering time regulation 38</b>	
<b>4.2.1. FT family.....</b>	<b>39</b>
<b>4.2.2. SPL family.....</b>	<b>42</b>
<b>4.2.3. SOC1 .....</b>	<b>44</b>
<b>4.2.4. LEAFY transcription factors .....</b>	<b>46</b>
<b>4.2.5. SVP family .....</b>	<b>47</b>
<b>4.2.6. FLC family.....</b>	<b>50</b>
<b>4.3. Expression analysis of flowering and dormancy regulator genes in <i>Q. robur</i> .....</b>	<b>51</b>
<b>4.4. Testing the interaction between <i>QsPI</i> promoter and <i>QsHTH</i> .....</b>	<b>58</b>
<b>4.4.1. Cloning <i>QsHTH</i> into pGAD424 .....</b>	<b>60</b>
<b>4.4.2. Integrating pAbai-F3p<i>QsPI</i> in Y1H Gold genome .....</b>	<b>64</b>
<b>5. Conclusion.....</b>	<b>66</b>
<b>6. Bibliography .....</b>	<b>69</b>
<b>7. Supplementary material.....</b>	<b>90</b>

## List of figures

**Figure 1. *Q. robur* vegetative and reproductive structures.** a)- *Q. robur* tree at *Universidade do Minho*. b)- *Q. robur* female flowers (pink arrow) developing at the tip of peduncled emerging from the axils of newly formed leaves. c)- *Q. robur* male flowers structured in linear catkins (blue arrow). a) and b) were taken at the campus of the University of Minho in Gualtar, Braga, while c) was adapted from <https://www.euforgen.org/species/quercus-robur/>.

**Figure 2.** Distribution map of *Quercus robur* (pedunculate oak). The native range of the species is represented in solid green ( ), while the green crosses ( ) refer to isolated populations and the orange triangles ( ) refer to introduced and naturalized populations. Adapted from (Caudullo et al., 2017).

**Figure 3.** Distribution map of *Quercus suber* (cork oak). The native range of the species is represented in solid green ( ), while the green crosses ( ) refer to isolated populations and the orange triangles ( ) refer to introduced and naturalized populations. Adapted from (Caudullo et al., 2017).

**Figure 4.** Representation of distinctive *Q. suber* features. a) Male catkins originating in the previous season branches; b) Female flowers developing in spikes, surging from the axils of newly formed leaves; adapted from (Sobral & Costa, 2017). c) *Q. suber* twig displaying both entire leaves and dentated leaves, adapted from <https://www.arbolapp.es/en/species/info/quercus-suber/>, n.d.). d) Cork oak bark, adapted from <https://www.euforgen.org/species/quercus-suber/>.

**Figure 5.** Schematic representation of the yearly growth and dormancy cycle of a perennial tree. As dormancy progressively releases and temperature increases (warm temperatures - ) the buds will swell, with bud burst occurring when favorable conditions are met, typically in spring. The warmer conditions and possibly coupled with longer days (  ) will lead to the newly formed structures, including meristems, growing throughout the summer months. As summer ends and autumn approaches the meristems will already have developed organ primordia and bud scales enclosing it. At this stage, in response to the decreasing day length (short days  ), bud development gradually decreases until growth cessation. Later in autumn as days get progressively shorter, and probably also in response to lower temperatures (  ), bud dormancy is established. During early winter, shortly after bud dormancy induction, the buds are in a deep dormant state maintained by endogenous mechanisms and impervious to growth promoting exogenous signals. As winter progresses, the accumulation of low temperatures will

gradually lead to dormancy release and the progressive resumption of growth, restarting the cycle. Adapted from (Singh et al., 2017).

**Figure 6. Representative model of flowering pathways in *A. thaliana*.** Flowering repressors are shown in blue; the flowering promoters are represented in green and floral meristem identity genes in orange. *FT* binds to *FD* to activate floral meristem identity genes. These in turn are up regulated by the inductive photoperiod pathway through *CO* accumulation. *FT* and *FD* complex also activates *SOC1* expression, and in turn, the floral meristem identity genes (*SEP3*, *FUL*, *API1* and *LFY*). Both *SOC1* and *LFY* are also up regulated by the GA pathway. *FLC* represses these floral integrator genes, and it is under the control of vernalization and autonomous pathways. *SVP*, another floral repressor, represses the expression of both floral integrator genes, *FT* and *SOC1* while also repressing floral meristem identity genes. *TFL1* represses flowering through competition for *FD* binding, that results in *LFY* and *API1* repression. Adapted from Kim et al. (2009).

**Figure 7. Representation of ABCDE model for flower organ identity in *A. thaliana*.** The formation of flower organs, sepals, petals, stamens and carpels (whorls) depends on the combination of several genes belonging to classes A to E. The class E genes (*SEP*) are required for interaction with all remaining classes of genes. A and E genes combine to specify for sepals; A, B and E to specify for petals; B, C and E for stamens, while female organ differentiation requires, in a first step, class C and E genes in carpel formation, and C, D and E (specifically *SHP*) to specify ovule formation. Adapted from (Theissen & Melzer, 2007).

**Figure 8. Adapted ABCDE model for *Q. suber* flower reproductive organ identity.** (A) The reported interaction between QsAG, QsAP1, QsSEP1 could be associated with a meristem's transition from vegetative to reproductive development; (B) QsSHP, QsAP3, QsSEP3, QsTM6 and QsPI are suggested to form a complex needed to promote the development of male flowers. The fact that QsPI was not expressed in female flowers may be indicative of enabling the interaction between QsSHP e QsSEP3, leading to carpel development promotion and blocking the initiation of stamen primordia. Adapted from (Sobral & Costa, 2017).

**Figure 9. Developmental bud stages of *Q. robur*.** a) - *Q. robur* twig with enclosed bud structures in the axils of leaves. b) - Early development male catkin inside an enclosed bud structure observed. c) - Dormant bud structure. d) - Bud swelling. e) - Bud burst with the flush of new leaves and already

developed male catkins. f), g) - Female flowers in early stages of maturation surging at the end of spikes originating at the axils of newly formed leaves. h) Recently flushed male catkins emerging along newly formed leaves. i) - Fully developed male catkins. j) - Pollinated female flowers maturing into acorns. k) - Case of summer flowering. a), c) and e) – the scale bar represents 1 cm; d), j) and k) – the scale bar represents 5 mm; i) – the scale represents 2 mm; b) – the scale bar represents 1 mm; f), g) and h) – the scale represents 500  $\mu\text{m}$ .

**Figure 10. Phylogenetic analysis of FT-like genes by Maximum Likelihood method.** The evolutionary history was inferred by using the Maximum Likelihood method and JTT matrix-based model (Jones et al., 1992). The tree with the highest log likelihood (-8333.29) is shown. The percentage of trees in which the associated taxa clustered together is shown next to the branches. Initial tree(s) for the heuristic search were obtained automatically by applying Neighbor-Join and BioNJ algorithms to a matrix of pairwise distances estimated using the JTT model, and then selecting the topology with superior log likelihood value. The tree is drawn to scale, with branch lengths measured in the number of substitutions per site. This analysis involved 83 amino acid sequences. There was a total of 225 positions in the final dataset. Evolutionary analyses were conducted in MEGA X (S. Kumar et al., 2018). *Q. robur* proteins are highlighted in red and *A. thaliana* proteins are highlighted in green.

**Figure 11. Phylogenetic analysis of SPL-like genes by Maximum Likelihood method.** The evolutionary history was inferred by using the Maximum Likelihood method and JTT matrix-based model (Jones et al., 1992). The tree with the highest log likelihood (-52512.44) is shown. The percentage of trees in which the associated taxa clustered together is shown next to the branches. Initial tree(s) for the heuristic search were obtained automatically by applying Neighbor-Join and BioNJ algorithms to a matrix of pairwise distances estimated using the JTT model, and then selecting the topology with superior log likelihood value. The tree is drawn to scale, with branch lengths measured in the number of substitutions per site. This analysis involved 92 amino acid sequences. There were a total of 1274 positions in the final dataset. Evolutionary analyses were conducted in MEGA X (S. Kumar et al., 2018). *Q. robur* proteins are highlighted in red and *A. thaliana* proteins are highlighted in green.

**Figure 12. Phylogenetic analysis of SOC1-like genes by Maximum Likelihood method.** The evolutionary history was inferred by using the Maximum Likelihood method and JTT matrix-based model (Jones et al., 1992). The tree with the highest log likelihood (-15071.71) is shown. The percentage of trees in which the associated taxa clustered together is shown next to the branches. Initial tree(s) for the

heuristic search were obtained automatically by applying Neighbor-Join and BioNJ algorithms to a matrix of pairwise distances estimated using the JTT model, and then selecting the topology with superior log likelihood value. The tree is drawn to scale, with branch lengths measured in the number of substitutions per site. This analysis involved 72 amino acid sequences. There was a total of 329 positions in the final dataset. Evolutionary analyses were conducted in MEGA X (S. Kumar et al., 2018). *Q. robur* proteins are highlighted in red and *A. thaliana* proteins are highlighted in green.

**Figure 13. Phylogenetic analysis of LFY-like genes by Maximum Likelihood method.** The evolutionary history was inferred by using the Maximum Likelihood method and JTT matrix-based model (Jones et al., 1992). The tree with the highest log likelihood (-7615.74) is shown. The percentage of trees in which the associated taxa clustered together is shown next to the branches. Initial tree(s) for the heuristic search were obtained automatically by applying Neighbor-Join and BioNJ algorithms to a matrix of pairwise distances estimated using the JTT model, and then selecting the topology with superior log likelihood value. The tree is drawn to scale, with branch lengths measured in the number of substitutions per site. This analysis involved 29 amino acid sequences. There was a total of 507 positions in the final dataset. Evolutionary analyses were conducted in MEGA X (S. Kumar et al., 2018). *Q. robur* proteins are highlighted in red and *A. thaliana* proteins are highlighted in green.

**Figure 14. Phylogenetic analysis of SVP-like genes by Maximum Likelihood method.** The evolutionary history was inferred by using the Maximum Likelihood method and JTT matrix-based model (Jones et al., 1992). The tree with the highest log likelihood (-10145.18) is shown. The percentage of trees in which the associated taxa clustered together is shown next to the branches. Initial tree(s) for the heuristic search were obtained automatically by applying Neighbor-Join and BioNJ algorithms to a matrix of pairwise distances estimated using the JTT model, and then selecting the topology with superior log likelihood value. The tree is drawn to scale, with branch lengths measured in the number of substitutions per site. This analysis involved 59 amino acid sequences. There was a total of 504 positions in the final dataset. Evolutionary analyses were conducted in MEGA X (S. Kumar et al., 2018). *Q. robur* proteins are highlighted in red and *A. thaliana* proteins are highlighted in green.

**Figure 15. Phylogenetic analysis of FLC-like genes by Maximum Likelihood method.** The evolutionary history was inferred by using the Maximum Likelihood method and JTT matrix-based model (Jones et al., 1992). The tree with the highest log likelihood (-5938.05) is shown. The percentage of trees in which the associated taxa clustered together is shown next to the branches. Initial tree(s) for the

heuristic search were obtained automatically by applying Neighbor-Join and BioNJ algorithms to a matrix of pairwise distances estimated using the JTT model, and then selecting the topology with superior log likelihood value. The tree is drawn to scale, with branch lengths measured in the number of substitutions per site. This analysis involved 27 amino acid sequences. There was a total of 298 positions in the final dataset. Evolutionary analyses were conducted in MEGA X (S. Kumar et al., 2018). *Q. robur* proteins are highlighted in red and *A. thaliana* proteins are highlighted in green.

**Figure 16. Analysis of the expression of potential dormancy and flowering regulator genes in *Q. robur*.** a) *QrFT* expression was analysed in leaf samples with *QrACTIN* as the normalizing gene. b) The expression of *QrSHP*, *QrSVP1*, *QrFLC*, *QrSOC1* and *QrSPL4* was analyzed in bud samples with *PP2A3* as the normalizing gene. PCR analysis of the expression of potential flower development and growth promoters (*QrFT*, *QrSOC1*, *QrSPL4*, *QrSHP*), and potential flowering repressors and dormancy promoter genes (*QrFLC* and *QrSVP1*) in *Q.robur* monthly cDNA samples during the year of 2021. Each lane corresponds to the respective month listed below, with the last lane being the negative control.

**Figure 17. Relative expression of potential flowering and bud dormancy regulator genes in *Q. robur* throughout 2021.** a)-d) Potential flower/bud development promoters. (a)- *QrFT* relative expression, with *QrACTIN* as the reference gene; b)- *QrSPL4* relative expression with *QrPP2A3* as the reference gene; c)- *QrSOC1* relative expression with *QrPP2A3* as the reference gene; d)- *QrSHP* relative expression with *QrPP2A3* as the reference gene.) e)-f) Potential flowering/dormancy release repressors. e)- *QrFLCb* relative expression with *QrPP2A3* as the reference gene; f)- *QrSVP* relative expression with *QrPP2A3* as the reference gene.) Relative expression levels were obtained by scanning the densitometry of the gel bands presented in Figure 12 using the ImageJ software.

**Figure 18. Maps of the pAbAi and the pGAD424 Vectors.** a)- pAbAi. pAbAi is a yeast reporter vector, designed for use with the Matchmaker Gold Yeast One-Hybrid Library Screening System and can be used in one-hybrid assays to identify and characterize DNA-binding proteins. The vector contains a multiple cloning site (MCS; lower panel), the AUR1-C gene, an antibiotic resistance gene that confers resistance to Aureobasidin A (AbA), and the URA3 gene. b)- pGAD424. pGAD242 regenerates a hybrid protein containing a target sequence fused to the GAL4 activation domain, for Yeast One-Hybrid assays. pGAD424 contains a *ADH1* promoter, a MCS (lower panel), the GAL4 AD, *ADH1* transcription terminator signal and two antibiotic resistant genes that confer resistance to leucine (*LEU2*) and ampicillin (*bla*). Adapted from (Clontech Laboratories, 2012).

**Figure 19. Schematic representation of the bait strain creation.** The inactive *ura3-52* locus of Y1HGold is repaired by homologous recombination with the wild type *URA3* gene present in the pBait-AbAi vector. Transformation of Y1HGold with a pBait-AbAi vector linearized with *Bst*BI or *Bbs*I, results in colonies that can grow in the absence of uracil on SD/-Ura agar plates. Adapted from (Clontech Laboratories, 2012).

**Figure 20. Representation of the strategy employed for cloning *QsHTH* into pGAD424.** The pGAD424 plasmid contains within its sequence the *ADH1* promoter, the *GAL4* activation domain, a multiple cloning site, and the *ADH1* terminator. Primers were designed to amplify the *QsHTH* coding sequence and to introduce the recognition sites for *Sma*I and *Sa*I restriction enzymes in the amplification products.

**Figure 21. PCR amplification of *QsHTH* open reading frame.** Amplification was carried out with the lower primer annealing temperature of 48°C. Electrophoresis run was performed with samples loaded into a 1.5 % agarose gel along with 1 kb Plus DNA Ladder (New England Biolabs) (L). The expected amplification product size of 1.744kbp is observed in lanes 1 in a) and lanes 1 to 5 in b).

**Figure 22. Colony PCR confirming *QsHTH* transformation into *E. coli* DH10B competent cells.** Amplification was carried out using the *QsHTH* forward and reverse primers, with 20 selected colonies (lanes 1-20) being used as template cDNA. The Electrophoresis run was performed with samples loaded into a 1.5 % agarose gel along with 1 kb Plus DNA Ladder (New England Biolabs) (L), and a negative control (-). Colonies 11 and 12 displayed the expected 1.744kbp amplification product.

**Figure 23. Colony PCR confirming pGAD424+*QsHTH* transformation into *E. coli* DH10B competent cells.** Amplification was carried out using the pGAD424 forward and reverse primers, with the 3 colonies (lanes 1-3) being used as template cDNA. The Electrophoresis run was performed with samples loaded into a 1.5 % agarose gel along with 1 kb Plus DNA Ladder (New England Biolabs) (L), and a negative control (-). Colonies 1 and 2 both displayed the expected 1.895kbp amplification product.

**Figure 24. Colony PCR confirming the integration of the pAbai+F3QsPI plasmid into Y1Hgold genome.** Amplification was carried out using the pAbai forward and reverse primers, with 26 selected colonies (lanes 1-26) being used as template cDNA. The Electrophoresis run was performed with samples loaded into a 1.5 % agarose gel along with 1 kb Plus DNA Ladder (New England Biolabs) (L), and a negative control (-). The yeast colonies represented in in lanes 14 and 15 both displayed the expected amplification product size of 879bp.

## List of tables

**Table 1.** Content of the mixture used for PCR amplification.

**Table 2.** Content of the mixture used for colony PCR amplification.

## List of Abbreviations

**ABA:** Abscisic acid

**AG:** *AGAMOUS*

**AGL24:** *AGAMOUS-like 24*

**AP:** *APETALA*

**BFT:** *BROTHER OF FT AND TFL1*

**BLAST:** Basic local alignment search tool

**b-ZIP:** Basic leucine zipper

**CBF:** *C-REPEAT BINDING FACTORS*

**cDNA:** complementary DNA

**CEN:** *CENTRORADIALIS*

**CO:** *CONSTANS*

**DAM:** *DORMANCY-ASSOCIATED MADS-box*

**DNA:** Deoxyribonucleic acid

**dNTPs:** Deoxynucleoside triphosphate

***EBB:*** EARLY BUD-BREAK

**EDTA:** ethylenediaminetetraacetic acid

***FD:*** FLOWERING LOCUS D

***FLC:*** FLOWERING LOCUS C

***FRI:*** FRIGIDA

***FT:*** FLOWERING LOCUS T

***FUL:*** FRUITFUL

**GA:** Gibberellic acid

**GAL4 AD:** GAL4 activation domain

**GTE:** Glucose-Tris-EDTA

***HTH:*** HOTHEAD

**IAA:** Isoamyl alcohol

**JTT:** Jones-Taylor Thornton

**LB:** Luria Broth medium

**LD:** Longer days

***LFY:*** LEAFY

**LT:** Low temperatures

***MFT:*** MOTHER OF FT

**NCBI:** National Center for Biotechnology Information

**PCR:** Polymerase chain reaction

**PEBP:** Phosphatidyl ethanolamine-binding protein

**PEG:** Polyethylene glycol

***PI:*** *PISTILLATA*

**RNA:** Ribonucleic acid

**ROS:** Reactive oxygen species

**SAM:** Shoot apical meristem

**SD:** Shorter days

***SEP:*** *SEPALLATA*

***SHP:*** *SHATTERPROOF*

***SOC1:*** *SUPPRESSOR OF CONSTANS1*

***SPL:*** *SQUAMOSA-PROMOTER BINDING PROTEIN-LIKE*

***STK:*** *SEEDSTICK*

***SVP:*** *SHORT VEGETATIVE PHASE*

**TE:** Tris-EDTA

***TFL1:*** *TERMINAL FLOWER 1*

**Tris:** tris(hydroxymethyl)aminomethane

***TSF:*** *TWIN SISTER OF FT*

**WT:** Warm temperatures

**Y1H:** Yeast One-Hybrid

**YPDA:** Yeast peptone dextrose adenine medium

## 1. Introduction

### 1.1. Fagaceae

Fagaceae is a large plant family, comprising more than 900 species, pivotal for the dynamics of forest ecosystems and important economic resources due to their fruits and timber (Kremer et al., 2012). Due to their importance, Fagaceae species have been widely studied (Cannon et al., 2018; M. G. Simpson, 2010).

In terms of distribution, Fagaceae trees are spread worldwide, being mostly characteristic of the temperate and subtropical zones of both hemispheres (M. G. Simpson, 2010; Van Benthem et al., 1984). Many Fagaceae species are large trees, such as *Quercus* (oak), and *Fagus* (beech), which dominate the deciduous and evergreen forests in which they are found. These trees' ample canopies provide habitats for countless species, and are vital for the ecosystems they inhabit, therefore having a crucial role in global ecosystem services (Cannon et al., 2018; Cavender-Bares et al., 2016; Marañón & Muñoz-Rojas, 2012; Van Benthem et al., 1984). This family also contains some of the world's most important trees regarding human culture and economics, including valuable lumber trees like the previously mentioned oak and beech, as well as chestnut (*Castanea*). Cork extracted from the outer bark of *Quercus suber*, as well as seeds and fruits of several species have been used as a source of food for humans and animals alike (Rogers, 2004; M. G. Simpson, 2010).

Species from the Fagaceae family are mainly of monoecious (rarely dioecious) trees or shrubs, meaning that female and male flowers are organized in separate structures within the same plant. (Cannon et al., 2018; M. G. Simpson, 2010). Monoecy has evolved from hermaphroditism, the still predominant form of sexual reproduction in angiosperms. The spatial, sometimes coupled with temporal separation of female and male flowers may offer the advantage of higher outcrossing, while mitigating self-pollination (Bertin, 1993; Harder et al., 2000; Kawagoe & Suzuki, 2005).

The great economic and ecologic importance of the Fagaceae family, coupled with the fact that some Fagaceae trees have been comprehensively studied makes them a promising model lineage for the advance in tree science. Now more than ever, with the current rapid climate change and emergence of new diseases threatening long-lived forest trees, studying the molecular mechanisms underlying oaks, beeches and chestnuts reproductive life cycle can be fundamental not only to understand their adaptation

and response to these new conditions, as well as to create a comparative framework that can facilitate the study of other tree species adaptations and responses to global environmental changes (Meetings, 2012).

### **1.1.1. *Quercus robur***

*Quercus robur* L., commonly referred to as pedunculate oak, is a large, usually deciduous, tree species belonging to the *Quercus* genus of the Fagaceae family. *Q. robur* trunks commonly grow to a height of about 30 m and width of 1 m, with some individuals growing up to 40 m tall and reaching widths of 3 to 4 m, while having a large canopy of a round shape supporting hairless and round lobed leaves (Fig 1). These large trees are also known to have a remarkable life-span with some specimens living over 1000 years (do Amaral Franco & da Luz da Rocha Afonso, 1994; Eaton et al., 2016; Sande Silva, 2007).

*Q. robur* trees are monoecious and bear unisexual flowers. Male flowers are arranged in linear catkins that appear in the axils of newly formed leaves (Fig 1), and female flowers are aggregated in groups of 1 to 5 on a peduncle. Flowering usually takes place between April and May, and there is a timelapse between male and female flowering, with female flowering usually occurring approximately one week after male flowering (Bacilieri et al., 1994). These trees are anemophilous (wind pollinated), and the fruit is an acorn (do Amaral Franco & da Luz da Rocha Afonso, 1994; Sande Silva, 2007).

Oak trees importance to humans in Europe dates back millennia as several cultures relied on its wood for fuel and construction while the acorns were used to feed the livestock. The relevance of these trees throughout history is highlighted by the fact that multiple cultures such as the Celts and Greeks revered the oak tree as sacred (Eaton et al., 2016). Nowadays, *Q. robur* trees are amongst the most economically valuable forest trees, largely due to the desirability of its timber in several different industries. The quality of the timber produced by oak trees has led to their use for a multitude of purposes such as house frames, furniture, paneling and barrels for aging wine and spirits.



**Figure 1. *Q. robur* vegetative and reproductive structures.** a)- *Q. robur* tree at *Universidade do Minho*. b)- *Q. robur* female flowers (pink arrow) developing at the tip of peduncled emerging from the axils of newly formed leaves. c)- *Q. robur* male flowers structured in linear catkins (blue arrow). a) and b) were taken at the campus of the University of Minho in Gualtar, Braga, while c) was adapted from <https://www.euforgen.org/species/quercus-robur/>.

*Q. robur* is native to Europe, where it is widely distributed, being found as far north as the Norwegian coast and the north of Scotland, as far south as the Mediterranean regions of Greece, Italy and Portugal and as far eastwards as the Ural Mountains (Eaton et al., 2016) (Fig 2).

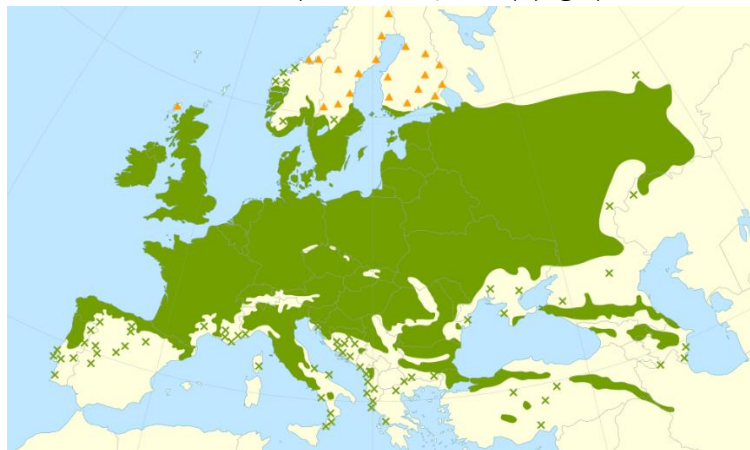


**Figure 2.** Distribution map of *Quercus robur* (pedunculate oak). The native range of the species is represented in solid green (■), while the green crosses (×) refer to isolated populations and the orange triangles (▲) refer to introduced and naturalized populations. Adapted from (Caudullo et al., 2017).

This species of oak thrives in humid and fertile soil such as wet lowlands and near water streams, although it can survive in an ample range of environmental and ecological conditions. *Q. robur* trees require plenty of light exposure (do Amaral Franco & da Luz da Rocha Afonso, 1994; Eaton et al., 2016; Sande Silva, 2007). Despite the large size of their broad-leafed canopy, it still allows for enough light to pass through to provide the undergrowth with conditions to thrive, promoting the growth of other plant species and the overall diversity of the forests these trees inhabit. The ecological value of *Q. robur* is immeasurable, as these trees play a central role in maintaining the food webs of temperate forests (Böhm et al., 2011; Eaton et al., 2016; Richard Southwood et al., 2004).

*Q. robur* trees support a vast array of species including epiphytic lichens that use the trees bark as substrate, vertebrates like birds and bats and the herbivorous invertebrates they prey upon (Böhm et al., 2011; Böhm & Kalko, 2009; Richard Southwood et al., 2004; Westerberg et al., 2017). In fact, in the temperate ecosystems that they are present, *Q. robur* trees are specially targeted by birds as their favored foraging substrate, indicating the abundance of herbivorous arthropods supported by these trees vast canopy (Böhm & Kalko, 2009). In the other hand, these associations also provide advantages to the tree, for example, communities of birds and bats help to contain herbivore population and reduce the foliage damage caused by these invertebrates (Böhm et al., 2011).

### **1.1.2. *Quercus suber***

*Quercus suber*, also known as cork oak, is an evergreen tree species belonging to the *Quercus* genus of the Fagaceae family. The leaves can be either simple, with a whole margin, or punctuated by small acute teeth (Fig 4 – c)). These trees, while not as longevous as *Q. robur* are still able to live between 150–250 years (Gil & Varela, 2008a). *Q. suber* trunks are relatively short, usually not reaching heights greater than 15–20 m, yet the trees crown is considerably large, making *Q. suber* trees, similarly to *Q. robur*, vital for the support of many different species and the ecosystems they inhabit. Their highly distinguishable corrugated and porous bark grows to 20 cm thick. This thick dermal system not only offers protection against some pathogens and makes *Q. suber* trees more fire resilient but is also the

source of our primary use for these species, cork (Fig 4 – d)). For more than three centuries, cork has been extensively used for the production of bottle stoppers, while the properties of cork also make this material valuable for different types of industry such as thermal and acoustic insulation, furniture, clothing, and footwear (Gil & Varela, 2008a, 2008b; Rives et al., 2013). Due to the regenerative way bark is obtained, cork extraction has actually been a driving force on the sustainable management of *Q. suber* forests (Gil & Varela, 2008a, 2008b).

In contrast to *Q. robur*, cork oak trees thrive in warm conditions and less productive soils, being adapted to survive to hot and dry summers. Their distribution is concentrated in the western Mediterranean regions of Europe and Africa, as far eastward as the Adriatic Sea and southern Italy and the vastest forests located in the Atlantic coast of the Iberian Peninsula, where *Q. suber* trees are regularly grown in agroforestry systems, named the *montado* in Portugal and *dehesa* in Spain (Fig 3) (Gil & Varela, 2008a; Natividade, 1950; Rives et al., 2013).



**Figure 3.** Distribution map of *Quercus suber* (cork oak). The native range of the species is represented in solid green ( ), while the green crosses ( ) refer to isolated populations and the orange triangles ( ) refer to introduced and naturalized populations. Adapted from (Caudullo et al., 2017).

*Q. suber* trees are monoecious, with 1 to 12 female flowers being gathered in spikes forming at the axils of newly formed leaves on new growth, while male flowers originate in the previous season branches and are arranged in long dropping catkins (Fig 4 - a) and b)). Male flowering usually occurs during March and April, with female flowering commonly taking place four to eight weeks later, meaning that *Q. suber*

trees are dichogamous, more specifically protandrous. This spatial and temporal separation of female and male flowering and flower maturation contributes to preventing self-pollination. Female flowers are wind pollinated, developing into an acorn (M. C. Varela & Valdivieso, 1996). A particularity of *Q. suber* is that it is unisexual by inception, meaning that female and male flowers show no prove of opposite reproductive organ abortion during each flowers developmental phase (Boavida et al., 2001; M. Varela et al., 2016; M. C. Varela & Valdivieso, 1996). This, coupled with the fact that *Q. suber* flowers display spatial and temporal separation, makes them a valuable target species for studies uncovering the mechanisms controlling flower development and the specification of flower organ identity in unisexual species (Rocheta et al., 2014; Sobral et al., 2020; Sobral & Costa, 2017).



**Figure 4.** Representation of distinctive *Q. suber* features. a) Male catkins originating in the previous season branches; b) Female flowers developing in spikes, surging from the axils of newly formed leaves; adapted from (Sobral & Costa, 2017). c) *Q. suber* twig displaying both entire leaves and dentated leaves, adapted from <https://www.arbolapp.es/en/species/info/quercus-suber/>, n.d.). d) Cork oak bark, adapted from <https://www.euforgen.org/species/quercus-suber/>.

## **1.2. Bud dormancy and growth cycle**

In temperate climate regions, characterized by the seasonal variation of environmental conditions, winter dormancy is an essential process for the survival, development and reproduction of the plants that inhabit them, since this process protects the meristems and organ primordia from unfavorable conditions by enclosing them in a dormant bud structure. Perennial trees, that must coordinate multiple reproductive events during their lifespan, have developed mechanisms that allow them to establish an annual cycle of development with the buds alternating between active growth and dormancy phases. In temperate perennials bud growth usually starts in Summer when cells from the peripheral zone of the shoot apical meristem SAM start differentiating into bud scale primordia. Then in Autumn the trees detect the arrival of winter, largely due to the decreasing photoperiod, and gradually dormancy is established (Fig 5). Ultimately, organ primordia growth ceases and these structures become enclosed in a dormant bud structure. In short, trees grow during seasons with favorable conditions and progressively cease their development until establishing dormancy, allowing the structures enclosed inside the bud to survive the seasons with least favorable conditions. During late winter and early spring, primarily in response to rising temperatures, bud dormancy is progressively released, meristematic cell growth gradually resumes, and the buds start to swell, culminating in bud burst (Fig 5). This morphological plasticity facing different seasons is only possible due to the plants mechanisms of environmental perception and the signalling pathways integrated in their developmental process (Cooke et al., 2012; Fadón et al., 2020; Lloret et al., 2018a; Rohde & Bhalerao, 2007; Singh et al., 2017, 2021).

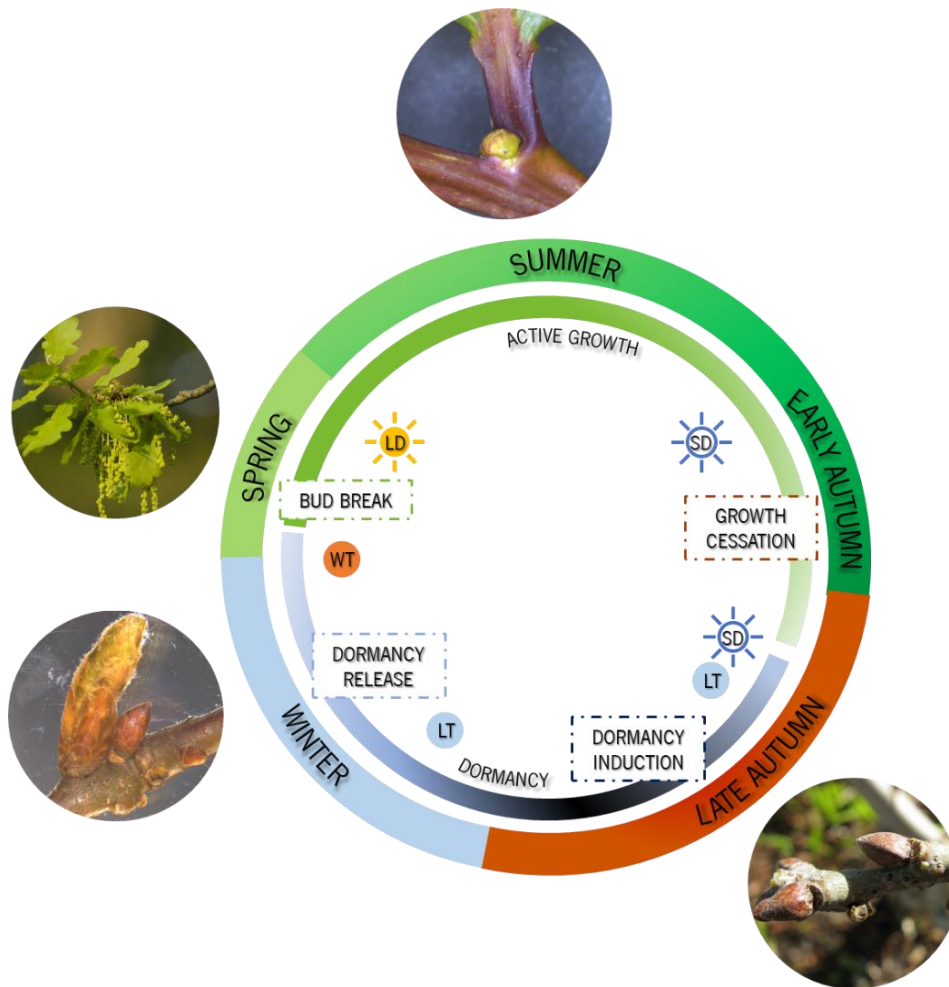


**Figure 5.** Schematic representation of the yearly growth and dormancy cycle of a perennial tree. As dormancy progressively releases and temperature increases (warm temperatures - **WT**) the buds will swell, with bud burst occurring when favorable conditions are met, typically in spring. The warmer conditions and possibly coupled with longer days ( **LD** ) will lead to the newly formed structures, including meristems, growing throughout the summer months. As summer ends and autumn approaches the meristems will already have developed organ primordia and bud scales enclosing it. At this stage, in response to the decreasing day length (short days **SD** ), bud development gradually decreases until growth cessation. Later in autumn as days get progressively shorter, and probably also in response to lower temperatures ( **LT** ), bud dormancy is established. During early winter, shortly after bud dormancy induction, the buds are in a deep dormant state maintained by endogenous mechanisms and impervious to growth promoting exogenous signals. As winter progresses, the accumulation of low temperatures will gradually lead to dormancy release and the progressive resumption of growth, restarting the cycle. Adapted from (Singh et al., 2017).

### **1.2.1. Dormancy stages**

Dormancy is a result of multiple processes that are themselves regulated by a multitude of environmental factors and complex molecular mechanisms that are interconnected. Therefore, characterizing and categorizing the different phases of dormancy has been a difficult task. However, the classification system proposed in Lang et al. (1987) presents a definition that simplifies the comprehension of the processes of dormancy. In this system dormancy is characterized in three stages: Paradormancy, Endodormancy, and Ecodormancy.

Paradormancy is defined by the suppression of axillary bud growth imposed by signals preventive from other parts of the plant. Apical dominance is one commonly cited example of the multiple factors related with paradormancy (Cline & Deppong, 1999; Lang, 1987; Lang et al., 1987). This dormancy type is also thought to be the evolutionary predecessor of the annual cyclic dormancy of temperate perennial trees (Rohde & Bhalerao, 2007).

Endodormancy refers to state of which buds cannot release dormancy even if favorable environmental conditions are met, only being possible after cold accumulation (Lang, 1987; Lang et al., 1987). In autumn, when perennial trees perceive the approaching winter, the buds cease their growth and enter an endodormant state until enough exposure to cold temperatures fulfills the trees specific chilling requirements (Rohde & Bhalerao, 2007; Fadón et al., 2020; Singh et al., 2017). However, bud burst does not occur immediately after prolonged exposure to cold, as endodormancy corresponds to the first phase of the annual dormancy cycle of temperate perennial trees. After endodormancy, buds remain dormant until favorable environmental conditions are met to flush – this dormancy state is called Ecodormancy, also referred as quiescence (Lang, 1987; Lang et al., 1987).

Despite the utility that Lang's definitions had in comprehending and categorizing the processes involved in dormancy, it is important to highlight that they do not seem to align with the current understanding of the molecular mechanisms involved in it. Bud dormancy in perennial trees is now thought to be a gradual and dynamic phenomenon akin to the dormancy continuum of seeds, rather than being an absolute state. Buds display a continuous range of dormancy states determined by internal and environmental signals, with the meristematic cells being capable of fluctuating between different depths of dormancy during the rest cycle (Baskin & Baskin, 2004; Cooke et al., 2012; Lundell et al., 2020). Thus, multiple authors have recently proposed the revision and redefinition of the dormancy system proposed

by Lang et al. (1987) or the adoption of an entirely novel set of terminologies to define bud dormancy, based more on the molecular processes and genetic pathways at the cell level that recent developments in technology have allowed to characterize. (Considine & Considine, 2016; Cooke et al., 2012; Lundell et al., 2020; Singh et al., 2017).

### **1.3. Dormancy and flower induction regulation**

With the end of dormancy, that results in bud burst, new branches emerge from the bud, bearing structures, such as new leaves and flowers (or flower primordia) that will develop into mature flowers. During the winter months, as chilling accumulation slowly releases dormancy, it will also drive floral development ultimately leading to flowering in spring. This process also draws parallelism with the cold requirements for flowering in herbaceous plants (vernalization)(Brunner et al., 2014). Thus, it has long been suggested that the molecular mechanisms involved in maintaining and releasing dormancy are also responsible for kickstarting the floral development pathway in perennial trees. (D. Horvath, 2009; Z. Liu et al., 2015).

Previous studies have outlined that dormancy and, consequentially, flowering are controlled by a set of complex interactions between external stimuli, such as changes in light and temperature, and multiple physiological processes that occur in different parts of the plant such as meristems, buds, twigs, and vascular tissues. These processes can be grouped into 4 main factors regulating dormancy and flowering: transport of carbohydrates and signaling compounds, phytohormones, genetic and epigenetic regulation, and the metabolism of carbohydrates (Fadón et al., 2020).

#### **1.3.1. Transport in perennial trees**

In all higher plants, transport between organs is assured by the xylem and phloem, which together form the plants vascular system. While the xylem is responsible for the transport of water and minerals from the roots to the structures aboveground, the phloem is responsible for the long-distance transport of photosynthates as well as supporting the signaling pathway. Transport in the xylem is passive and facilitated by the negative pressure formed in the leaves and caused by evaporation. Thus, in spring and summer the xylem is able to supply enough water for leaves and flowers to develop and expand. On the

other hand, as temperatures drop reducing evaporation, and in the case of deciduous trees the foliage shedding, transport of water and solutes is halted or drastically decreased during dormancy. Transport in the phloem, contrary to the xylem, is active and requires symplastic transport through cellular membranes (De Schepper et al., 2013; Delpierre et al., 2016; Foster, 2003). Plasmodesmata located in the SAM are obstructed by the deposition of callose promoted by dormancy inducing cues, thus blocking the passage of growth inducing signals (Tylewicz et al., 2018; S.-W. Wu et al., 2018). These structures, which are membranous channels perforating the walls of neighboring cells allowing for cell-to-cell communication, are therefore thought to play a major role in facilitating the transport of dormancy regulating molecular signals to the SAM and in the management of plant growth and development (Fadón et al., 2020; Foster, 2003).

### **1.3.2. Metabolism of carbohydrates**

The significant fluctuations in the synthesis and degradation of sugars, such as glucose and fructose, and starch observed in the different phases of dormancy and development of temperate perennial trees has led researchers to consider the dynamics of non-structural carbohydrates as likely to be involved in dormancy regulation (Fadón et al., 2018; Fernandez et al., 2019). Plants also capitalize on the reactive oxygen species (ROS) formed as by-products of metabolic pathways, to act as signals that mediate several important processes in plants such as signalling in response to external cues and in this case dormancy regulation (Fadón et al., 2020; Mhamdi & Van Breusegem, 2018). For instance, a study in *Vitis vinifera* suggested that ROS generated in gluconeogenesis and oxidative phosphorylation might be leading to dormancy release in response to winter cold accumulation (Pérez et al., 2009).

### **1.3.3. Phytohormones**

. Since dormancy progression is extensively tied to the perception of environmental cues, such as temperature, that contribute to determine whether the meristems divide or enter a dormant state, there is a strong suggestion for the involvement of hormones as integrators of these environmental signals, acting in pathways that control cell cycle and expansion (Cooke et al., 2012; Lloret et al., 2018a). Phytohormones are compounds effective in low concentrations produced by the plant that mediate long and short distance signaling. Yearly concentration patterns of certain hormones indicate a major role in

the perception of season variability, with multiple phytohormones, namely auxin, gibberellic acid (GA), abscisic acid (ABA) and cytokinins, reported to be involved in the regulation of various processes and phases of dormancy (Fadón et al., 2020; D. P. Horvath et al., 2003).

Several studies have distinctively associated ABA and GA with dormancy-growth regulation, with ABA being linked to dormancy maintenance and GA associated with cell growth (Lloret et al., 2018a). ABA is a well-known growth inhibitor and has been associated with dormancy, with multiple studies in temperate perennials having observed that the ABA content peaked around dormancy induction and decreased along dormancy release (J. Li et al., 2018; Tuan et al., 2017; D. Wang et al., 2016; Zheng et al., 2015). ABA has also been implicated to be interacting with the photoperiodic pathway in the regulation of bud growth, with studies on poplar observing bud development altering in response to short days on ABA signaling mutants (Lloret et al., 2018a; Rohde et al., 2002; Singh et al., 2017; Tylewicz et al., 2015). Furthermore, in hybrid aspen with reduced ABA signaling, growth halting and the enclosure in a bud structure were observed under short day photoperiod, however the buds failed to enter a dormant state, pointing to ABA acting particularly in dormancy induction (Tylewicz et al., 2018). Moreover, ABA has been presumed to regulate bud dormancy by controlling the expression of cell cycle genes in grapevine (Vergara et al., 2017). By contrast, several studies in different perennial trees, such as poplar (Rinne et al., 2011a; Zawaski et al., 2011; Zawaski & Busov, 2014; Zheng et al., 2018a), aspen (Eriksson et al., 2015), grapevine (Zheng et al., 2018b), bay willow (Junttila & Jensen, 1988) and Japanese apricot (Wen et al., 2016; Zhuang et al., 2013), have reported GA as bud dormancy release and growth promoter.

#### **1.3.4. Epigenetic regulation**

Recent evidence has also demonstrated that epigenetics play an important role in the regulatory mechanisms of dormancy in perennial trees (Anh Tuan et al., 2016; Conde, Le Gac, et al., 2017; de la Fuente et al., 2015; M. Santamaría et al., 2009; M. E. Santamaría et al., 2011; H. G. Silva et al., 2020). Epigenetic regulation consists in the altering of expression patterns of certain genes through structural changes in the DNA or the surrounding structural proteins (histones). The levels of histone acetylation and DNA methylation and the expression patterns of genes associated with epigenetic marking have been found to fluctuate in relation to dormancy establishment and progression in several temperate perennial trees such as peach (*Prunus persica*) (de la Fuente et al., 2015), Japanese pear (*Pyrus pyrifolia*) (Anh Tuan et al., 2016; Saito et al., 2013), and poplar (*Populus sp.*) (Conde, Le Gac, et al., 2017; Conde,

Moreno-Cortés, et al., 2017), including Fagaceae, namely sweet chestnut (*Castanea sativa*) (M. Santamaría et al., 2009; M. E. Santamaría et al., 2011) and cork oak tree (*Q. suber*) (H. G. Silva et al., 2020).

### 1.3.5. Genetic regulation

There are numerous genes reported to be involved in the dormancy regulation of temperate perennial trees, with *DORMANCY-ASSOCIATED MADS-box (DAM)*, *SHORT VEGETATIVE PHASE (SVP)* and *FLOWERING LOCUS T (FT)* and *FT-like* genes amongst the more extensively studied genes postulated to regulate bud dormancy (Falavigna et al., 2019; D. Horvath, 2009; D. P. Horvath et al., 2003; Z.-M. Li et al., 2010; Z. Liu et al., 2015; Rinne et al., 2011b; Rohde & Bhalerao, 2007; Singh et al., 2017; R. Wu et al., 2014; R. Wu, Tomes, et al., 2017; R. Wu, Wang, et al., 2017; R.-M. Wu et al., 2012; F. Xu et al., 2012; T. Zhao et al., 2021). The study of dormancy related genes in fruit trees began with the study of the peach (*P. persica*) *evergrowing (evg)* mutant tree, which displays continuous growth throughout the year. This led to the identification of a highly conserved group of six tandemly repeated *MADS-box* genes, whose deletion was responsible for the *evg* phenotype, and named in accordance with their involvement in bud dormancy, *DAM* genes (*DAM1-6*) (Bielenberg et al., 2004, 2008; Rodriguez-A. et al., 1994). Since then homolog *DAM* genes have been described to have a prominent role in dormancy regulation of several other species, mainly belonging to the Rosaceae family, such as Japanese apricot (*Prunus mume*) (Kitamura et al., 2016; Sasaki et al., 2011), sweet cherry (*Prunus avium*) (Castède et al., 2015), apple (*Malus x domestica*) (Allard et al., 2016; Celton et al., 2011; van Dyk et al., 2010) and pear (*Pyrus communis* L.) (Gabay et al., 2017). *DAM* genes are closely related to a known floral repressor in *A. thaliana*, *SVP*, both belonging to the StMADS11 subfamily of MADS-box transcription factors (Jiménez et al., 2009). Despite the roles of *AtSVP* differing from that of *DAM* genes found in Rosaceae, with the former suppressing flower induction in the meristem and the later maintaining bud dormancy, other *SVP*-like genes from perennial trees have also been observed to play a role in dormancy regulation. *SVP-like* genes have been particularly associated with bud break regulation, functioning as growth inhibitors that halt premature growth during the late dormant stages before bud break in apple (R. Wu, Tomes, et al., 2017), and kiwifruit (*Actinidia deliciosa*) (R. Wu, Wang, et al., 2017; R.-M. Wu et al., 2012). In fact, in species which contain both *DAM* and *SVP*-like genes, evidence shows distinct functions within the buds dormancy/growth cycle, with *SVP* and *DAM*

genes being able to act in distinct phases (R. Wu, Tomes, et al., 2017).

Several studies have in fact reported the functional specification within the STMADS-11 family regarding the repression of dormancy release and flower development, in Rosaceae species (Jiménez et al., 2009; J. Liu et al., 2020; Xiang et al., 2016). In a review, Falavigna et al. (2019) upon analyzing the several *SVP* and *DAM*-functional characterization studies in perennial trees, denoted that the majority of *DAM* and *SVP*-like genes are suggested to be involved in the maintenance of dormancy instead of dormancy induction, except for peach and Japanese apricot *DAM6*. *SVP* was firstly studied in *A. thaliana* where it was described to suppress floral induction, partly by repressing *FT* expression (Hartmann et al., 2000; D. Li et al., 2008). *FT* has been the most extensively studied and widely acknowledged as an effective flowering promoter gene in flowering plants (F. Xu et al., 2012). *FT* is described in *A. thaliana* as the main output of the photoperiod pathway, while also integrating signals from the autonomous, and vernalization pathways that will eventually lead to flowering (Kardailsky et al., 1999; Kobayashi & Weigel, 2007; F. Xu et al., 2012). *FT* together with *CONSTANS (CO)* constitute a regulatory module that will function as a sensor that responds to the phytochromes present in the plants leaves, detecting variations in levels of red and far-red light. This mechanism has been extensively documented in *A. thaliana*, however, *FT* homologs were also suggested in numerous perennial species to not only promote flowering but also as regulators of other processes, namely dormancy (Rinne et al., 2011b; Singh et al., 2017). Shorter days result in stability loss in the CO protein which will lead to a decline in *FT* expression and GA synthesis, conditions favorable for bud formation (Fadón et al., 2020; Horvath, 2009). In poplar, multiple homologs of *FT* were observed to be involved in the control of dormancy establishment through the short-day photoperiod pathway (Bohlenius et al., 2006). Despite the observed relevance of photoperiod and *FT* as the main regulator of bud dormancy induction in several perennials, in other species such as apples and leafy spurge (*Euphorbia esula*) cold temperatures were reported as the primary signal regulating dormancy induction (Foley et al., 2009; Heide & Prestrud, 2005). Recent studies have highlighted *C-REPEAT BINDING FACTORS (CBF)*, a gene induced in response to temperature decrease, as a likely candidate for temperature regulation of dormancy and possibly dormancy induction (BENEDICT et al., 2006; Dođramacı et al., 2010).

The proteins encoded by *CBF* genes were observed to bind to the promoter region of *DAM* genes in some perennial species such as the above-mentioned apple tree (Wisniewski et al., 2015) and leafy

spurge (D. P. Horvath et al., 2008) but also in Japanese pear (Niu et al., 2016) and Japanese apricot (K. Zhao et al., 2018). By contrast, in poplar, a species in which temperature seems not to have a determinant effect on dormancy induction, no promoter regions of genes were found to contain CBF binding sites. This further supports *DAM* gene regulation by CBFs as a temperature-controlled dormancy induction mechanism in these species (D. Horvath, 2009). Yet, it is important to point out that the mechanisms underlying temperature sensing and regulation are considerably less well known than the ones involved in photoperiod pathway (Cooke et al., 2012). There are also strong suggestions that temperature and photoperiod signals involved in dormancy regulation are interconnected and converge on the light sensing/circadian clock pathway (Cooke et al., 2012; D. Horvath, 2009). For instance, in sweet cherry circadian clock oscillator genes upstream of *FT* during dormancy were observed to be disrupted in response to cold temperatures and resumed normal activity when returned to 22 °C (Ramos et al., 2005). *DAM* expression, which is induced by cold temperatures, was also observed to be higher in long-day (LD) conditions in leafy spurge, implying interaction with the mechanisms regulating the circadian clock (Foley et al., 2009).

Contrary to dormancy induction, both dormancy release and bud burst are primarily regulated by temperature. *FT* is also presumed to be a determinant factor controlling the release of dormancy. For instance, in poplar there are two *FT* homologs, *PtFT1* and *PtFT2*, and while *FT2* was observed to be up-regulated in response to flower inducing conditions during the growing season, suggesting involvement in flowering induction, *FT1* was observed to be up-regulated in response to seasonal cold, indicating an involvement in dormancy release. (Hsu et al., 2011; Lloret et al., 2018a; Rinne et al., 2011). Further supporting the above-mentioned, GA, which is also up-regulated in response to chilling, promotes the expression of genes involved in the reopening of plasmodesmata, allowing for cell-to-cell communication in the meristems to resume. Therefore peptides, such as the product of *FT*, which is primarily expressed in leaf tissues and transported to the meristems where it will act, are likely candidates for the control of growth resumption during this dormancy release phase (Lin et al., 2007; Lloret et al., 2018a; Rinne et al., 2011b; Tylewicz et al., 2018). Another mobile peptide that has also been linked with dormancy release in perennials is CENTRORADIALIS (CEN). Studies in poplar and kiwifruit have suggested that CEN offsets the FT flower promoting action, and that the ratio of these peptides might determine bud dormancy release in perennials (Brunner et al., 2014; Mohamed et al., 2010). *CENTRORADIALIS-like* (*CENL1*), a poplar *CEN* homolog, is closely related to *FT*, belonging to the same gene family, however, unlike *FT*, *CENL1* was observed to negatively regulate dormancy release. (Mohamed et al., 2010).

Another gene named *EARLY BUD-BREAK (EBB)*, has been suggested to be particularly involved in bud break of different perennial trees. In a study in poplar mutants, overexpression of *EBB* resulted in early bud break whilst *EBB* down-regulation resulted in late bud break (Yordanov et al., 2014). Moreover, the variations in *EBB* expression levels were observed to modify the expression of multiple genes linked with important processes for bud development such as meristem growth (Yordanov et al., 2014). Comparative analysis has also showed *EBB* sequence and expression pattern to be conserved amongst several different tree species, which points to a conservation of *EBB* function in promoting bud break across the broad spectrum of perennial trees (Busov et al., 2016). Expression analysis in trees overexpressing poplar *EBB1* has revealed certain *DAM* and *SVP-like* genes associated with dormancy maintenance to be downregulated, pointing to *EBB1* repression of these genes as a possible mechanism for bud break induction (Singh et al., 2021; Yordanov et al., 2014).

#### **1.4. Flowering**

As mentioned before, since seasonal dormancy in temperate perennials interjects flowering events, the processes regulating dormancy, chilling/vernalization, and flowering are interconnected and interdependent.

As bud dormancy is progressively released, multiple genetic pathways are thought to integrate environmental and endogenous signals starting and regulating the flowering transition in the SAM. Like many molecular processes in plants, these pathways and genetic mechanisms regulating flowering have been widely studied in *A. thaliana* (Fig 6). Despite clear phenological differences between flowering in perennial and herbaceous species, the pathways and genes that regulate it were observed to be broadly conserved among perennial and herbaceous species (Kurokura et al., 2013; Lloret et al., 2018b).

In *A. thaliana*, as is postulated to occur similarly in perennials, these genetic networks regulate flowering in response to environmental cues, such as the vernalization and photoperiod pathways that are influenced by temperature and light respectively, and the autonomous and GA dependent pathways which respond to endogenous signals. These pathways can operate separately to promote flowering, however, all are presumed to converge on a few downstream target genes named floral integrators, specifically *FLOWERING LOCUS D (FD)*, *FT*, *SUPPRESSOR OF CONSTANS1 (SOC1)* and *LEAFY (LFY)* (Moon et al., 2005; G. G. Simpson & Dean, 2002).

In *A. thaliana*, photoperiod influences flowering through the circadian clock *FT/CO* regulatory module, as mentioned before regarding photoperiod control of dormancy induction. Contrary to SD conditions, in long day (LD) conditions the CO protein is less destabilized resulting in CO accumulation, leading to *FT* expression activation, and ultimately flowering (Valverde et al., 2004). As the product of *FT* arrives in the SAM it will interact with FD, a transcription factor of the basic leucine zipper (bZIP) family, forming a flower induction complex that will act through *APETALA1 (AP1)*, *APETALA3 (AP3)*, *FRUITFUL (FUL)* and *LFY*, the floral meristem identity genes that specify differentiation of the meristem into a floral meristem (Abe et al., 2005; Wigge et al., 2005). *LFY* is considered both a key meristem identity gene and a floral integrator since it is a direct output of GAs pathway (Blázquez et al., 1998).

Regarding temperature control of flowering and vernalization, a gene named *FLOWERING LOCUS C (FLC)* is described to be central in vernalization regulated flowering repression. *FLC* is a MADS-box gene, and its product combines with *SVP*, another known flowering repressor, forming a complex that binds to the sequence of flowering promoter genes namely *FT*, *SOC1* and *FD*, repressing them (Kurokura et al., 2013; D. Li et al., 2008; Michaels & Amasino, 1999; Searle et al., 2006). *FLC* binding is, therefore, suggested to undermine the capacity of the photoperiod pathway to activate these flowering promoter genes. *FLC* is positively regulated by another gene named *FRIGIDA (FRI)* and downregulated by winter chilling temperatures, being the primary control of vernalization (Kim et al., 2009; Kurokura et al., 2013; Shindo et al., 2005). *FLC* is also repressed by the autonomous pathway, responsible for flowering, disregarding environmental conditions. Warm temperatures also affect flowering through control of *FT* expression levels. *SVP*, which represses *FT* and *SOC* is dependent of cooler temperatures to be activated, thus, warmer temperatures result in *SVP* expression decrease and flowering promotion (J. H. Lee et al., 2007; Samach & Wigge, 2005). *SVP* also represses the floral meristem identity gene *AP3* (C. Liu et al., 2009). More recently, epigenetic regulation has also been postulated to activate *FT* transcription in response to warm temperatures (S. V. Kumar et al., 2012; S. V. Kumar & Wigge, 2010).

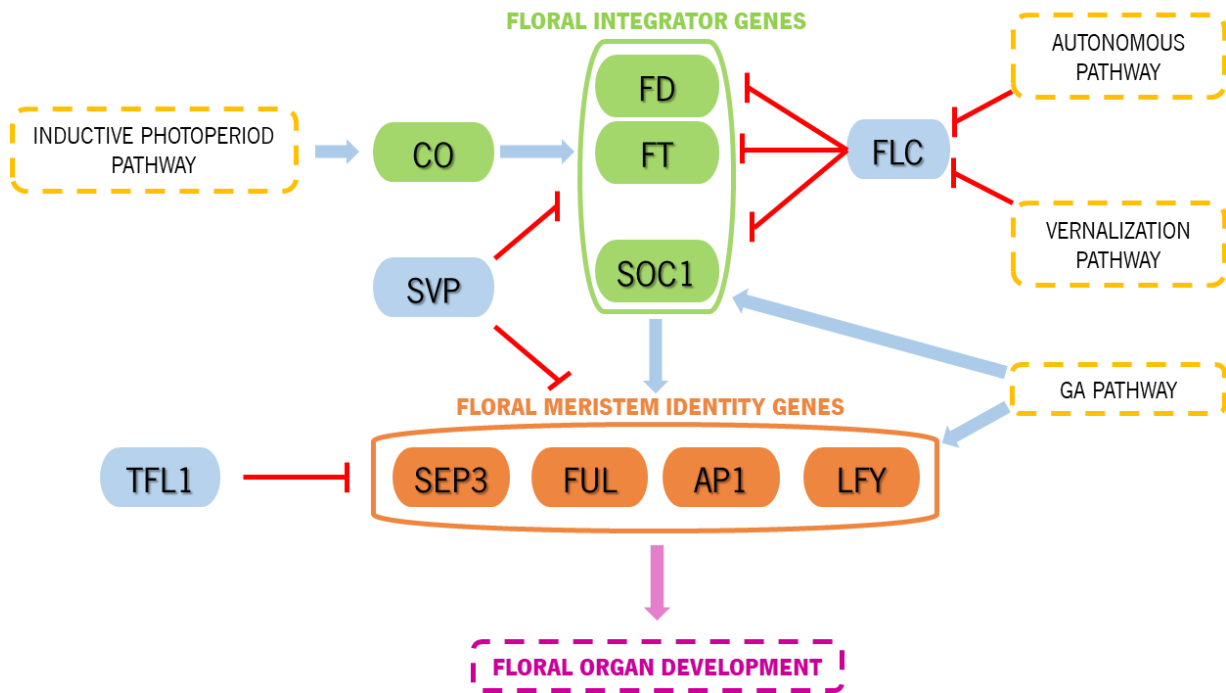


**Figure 6. Representative model of flowering pathways in *A. thaliana*.** Flowering repressors are shown in blue; the flowering promoters are represented in green and floral meristem identity genes in orange. *FT* binds to *FD* to activate floral meristem identity genes. These in turn are up regulated by the inductive photoperiod pathway through *CO* accumulation. *FT* and *FD* complex also activates *SOC1* expression, and in turn, the floral meristem identity genes (*SEP3*, *FUL*, *AP1* and *LFY*). Both *SOC1* and *LFY* are also up regulated by the GA pathway. *FLC* represses these floral integrator genes, and it is under the control of vernalization and autonomous pathways. *SVP*, another floral repressor, represses the expression of both floral integrator genes, *FT* and *SOC1* while also repressing floral meristem identity genes. *TFL1* represses flowering through competition for *FD* binding, that results in *LFY* and *AP1* repression. Adapted from Kim et al. (2009).

*SOC1* is activated in the meristem by the FT/FD floral complex, while being regulated by the vernalization pathway through *FLC* and through *FLC* repression of *FT*, while also being indirectly up regulated by *CO*. Thus, as *FT*, *SOC1* is part of both the photoperiod, vernalization and autonomous pathways, however unlike *FT*, *SOC1* is also regulated by the GA pathway (H. Lee et al., 2000; Moon et al., 2003; Samach et al., 2000). *SOC1* has the particularity of also being considered a meristem-identity gene since it works along *FUL* in the floral state maintenance of the meristem (Melzer et al., 2008). *SOC1* and *AGAMOUS-like 24 (AGL24)*, a closely related gene of *SVP*, have been observed to promote each other

expression, with SOC1 reported to interact with AGL24 to activate *LFY* (C. Liu et al., 2008; Michaels et al., 2005).

In addition to *SVP*, a gene named *TERMINAL FLOWER 1 (TFL1)*, has also been suggested pivotal role in repressing flowering. *TFL1* encodes for a protein that belongs to the phosphatidyl ethanolamine-binding protein (PEBP) family similarly to FT, being also capable of forming a complex with FD, leading to competition between these transcription factors for binding with FD. However, contrary to FT, TFL represses *LFY* and *AP1*, promoting in turn the maintenance of an indetermined meristem (Hanano & Goto, 2011; Karlgren et al., 2011a; Kobayashi et al., 1999; Liljegren et al., 1999). On the other hand, expression of *LFY*, in tandem with *AP1*, will trigger the activation of the floral organ identity genes (Irish & Sussex, 1990; Ng & Yanofsky, 2001; Pelaz et al., 2000; Weigel et al., 1992).

Extensive studies on the genetic mechanisms controlling the flower organogenesis, particularly in hermaphrodite flowers where these mechanisms are more easily identified, has led to the identification of the floral organ identity genes and their orchestration of flower organ development being detailed in the ABCDE model (Fig 7) (Becker, 2003). The ABCDE model identifies 5 classes of homeotic genes, (A, B, C, D, and E) with genes from each class being recruited by the floral meristem in different combinations to specify the development of reproductive – (carpels, stamen and ovules), and non-reproductive (petals and sepals) structures (Bowman et al., 1989, 1993; Coen & Meyerowitz, 1991; Flanagan et al., 1996; Liljegren et al., 2000; Pelaz et al., 2000).

To specify, the ABCDE model postulates that in *A. thaliana* A class genes (*AP1* and *AP2*) combine with E class genes (*SEPALLATA 1* to *4(SEP1-4)*) to specify sepal identity, while these classes together with B class genes (*AP3* and *PISTILLATA (PI)*) specify petal identity. Regarding the reproductive structures, B class genes in combination with E and C (*AGAMOUS (AG)*) specify stamen development, C and E class genes specify carpel identity, whereas D class genes (*SEEDSTICK(STK)* and *SHATTERPROOF 1* and *2 (SHP1/2)*) are also required along classes C and E for definition of ovule identity (Bowman et al., 1989; Coen & Meyerowitz, 1991; Flanagan et al., 1996; Liljegren et al., 2000; Pelaz et al., 2000; Pinyopich et al., 2003).

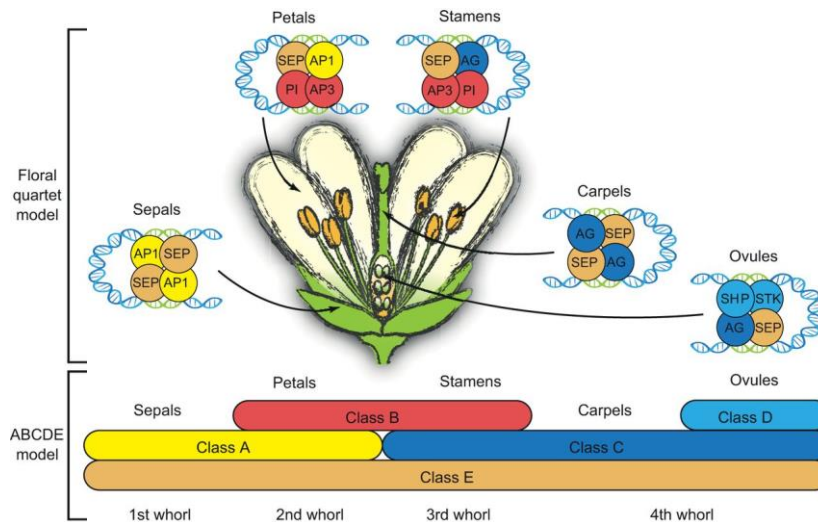


**Figure 7. Representation of ABCDE model for flower organ identity in *A. thaliana*.** The formation of flower organs, sepals, petals, stamens and carpels (whorls) depends on the combination of several genes belonging to classes A to E. The class E genes (*SEP*) are required for interaction with all remaining classes of genes. A and E genes combine to specify for sepals; A, B and E to specify for petals; B, C and E for stamens, while female organ differentiation requires, in a first step, class C and E genes in carpel formation, and C, D and E (specifically *SHP*) to specify ovule formation. Adapted from (Theissen & Melzer, 2007).

### 1.5. Previous studies in *Q. suber* and its particular case of unisexuality and flower organ determination.

As mentioned before, *Q. suber* flowers are theorized to be unisexual by inception (Boavida et al., 2001; M. Varela et al., 2016; M. C. Varela & Valdivieso, 1996). Recent comparative transcriptomic studies in *Q. suber* have reported the B class genes to be differentially more expressed in male flowers, with *QsPISTILLATA* expression being absent in female flower samples, while *QsSHATTERPROOF*, the C-class gene, was observed to not be differentially expressed in female and male samples. Therefore, these results are suggestive that B class genes downregulation might underlie the regulatory mechanism for the absence of stamens in the early development of the female pistillate flower, with *QsPI* potentially playing a central role in the specification of sexual identity of *Q. suber* flowers (Fig 8) (Rocheta et al., 2014; Sobral & Costa, 2017). This makes uncovering the mechanisms controlling *QsPI* expression an important front to expand the knowledge of flowering and flower organ determination.

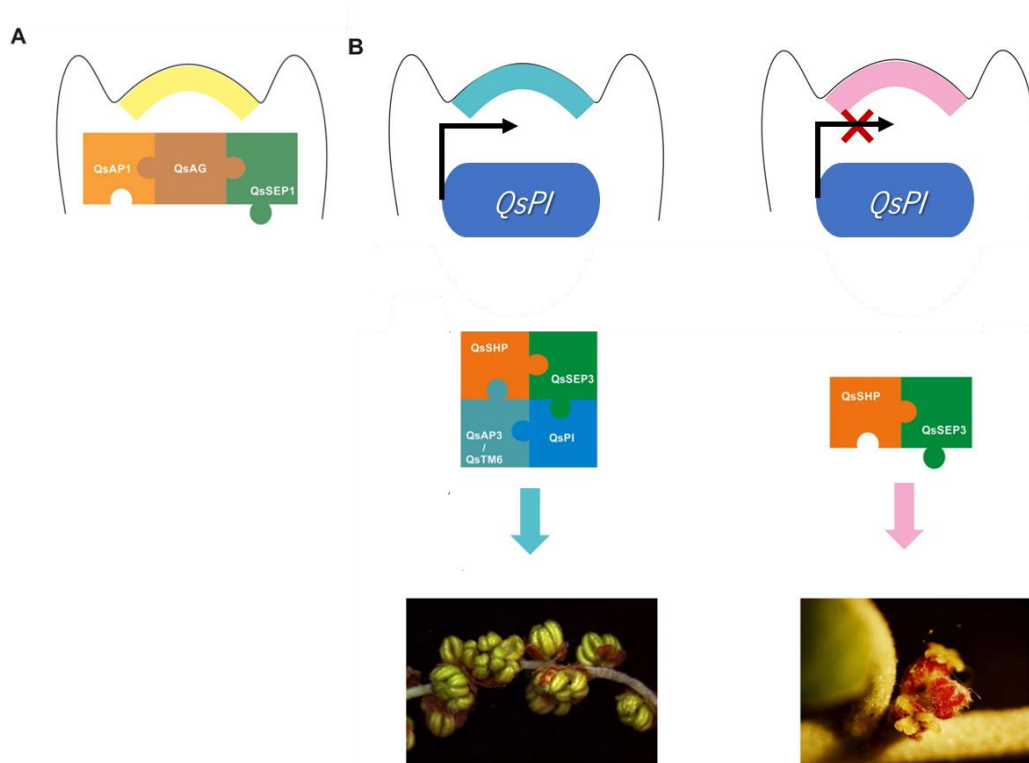


**Figure 8. Adapted ABCDE model for *Q. suber* flower reproductive organ identity.** (A) The reported interaction between QsAG, QsAP1, QsSEP1 could be associated with a meristem's transition from vegetative to reproductive development; (B) QsSHP, QsAP3, QsSEP3, QsTM6 and QsPI are suggested to form a complex needed to promote the development of male flowers. The fact that QsPI was not expressed in female flowers may be indicative of enabling the interaction between QsSHP e QsSEP3, leading to carpel development promotion and blocking the initiation of stamen primordia. Adapted from (Sobral & Costa, 2017).

In H. Silva (2018), a library of possible protein targets for *QsPI* promoter interaction was obtained by Yeast One-Hybrid (Y1H) screening. One of the targets, QsHOTHEAD (QsHTH), was identified as a homolog of the protein encoded by the gene *HOTHEAD (HTH)*, described in Arabidopsis to limit interactions among conjoint epidermal cells during flower development (Krolkowski et al., 2003). Several *HTH* homologs have also been recently identified in rice (*Oryza sativa*) (Akiba et al., 2014; Fang et al., 2015; Y. Xu et al., 2017), including *OsHTH1* that was suggested to be required for the development of anthers and pollen fertility in rice flowers (Y. Xu et al., 2017). Therefore, QsHTH might be a promising target for regulation of *QsPI* and the flower reproductive organ determination in *Q. suber*, and thus requiring further analysis and confirmation of the interaction between QsHTH and the promoter region of *QsPI*.

More recently, identification, functional and expression analysis of multiple *Q. suber* flowering and dormancy regulator homologs was conducted in Sobral et al (2020). In this study a homolog of *A. thaliana* *FT*, *QsFT*, was reported to have two expression peaks in adult trees, one during the buds swelling phase in March and other in August, before bud growth halting, suggesting two flower induction events. This was further supported by expression analysis of the floral meristem identity homolog gene *QsLFY*, which was also observed to be highly expressed before growth cessation and during bud swelling. Thus, it was suggested that these two reported flower induction events might, considering the particular unisexual and dichogamous nature of *Q. suber*, constitute a total separation of male and female flower development occurring in these distinct phases. The expression of *Q. suber* genes homolog to both *A. thaliana* known floral repressors, and perennials dormancy promoters, was also analyzed, namely with *QsSVP1* and *QsSVP4* observed to be highly expressed during bud growth halting which suggested a conservation for the role of *SVP*-like genes in dormancy induction of perennial trees (Sobral et al, 2020). Moreover, functional analysis in *A. thaliana* mutants overexpressing *Q. suber* flowering genes has also pointed to the function of some of these genes, such as *QsFT* *QsSVP1* *QsSVP4* and *QsSPL4* being conserved in *A. thaliana*.

The above-mentioned studies in *Q. suber* have set an important basis for understanding the genetic processes regulating dormancy and flowering in Oak trees and generally in the Fagaceae family. Therefore, this thesis aimed to examine if, and to what extent, are these mechanisms conserved across Fagaceae trees, by analyzing the genetic regulation of dormancy and flowering in the closely related species, *Q. robur*.

## 2. Objectives

This thesis had the objective of further uncovering the genetic mechanisms regulating dormancy and flowering in Fagaceae trees, specifically *Q. robur* and *Q. suber*. To achieve that, this study aimed to:

- Catalog different bud and flower developmental stages in *Q. robur* throughout an annual growth/dormancy cycle.
- Identify potential dormancy and flowering regulators in *Q. robur* through comparative phylogenetic analysis with known floral regulators of *A. thaliana* as well as genes suggested to be involved in dormancy control of perennial species.
- Analyze the expression of potential floral and dormancy regulator genes in a *Q. robur* tree bud and leaf samples throughout one growing season.
- Further uncover the regulation of flower reproductive organ development in *Q. suber*, through testing of potential interaction between QsHTH and the promoter region of *QsPI*. To achieve that, QsHTH coding sequence was cloned into a vector compatible with a Yeast-1 Hybrid assay.

### **3. Materials and Methods**

#### **3.1. Plant material**

The samples used in this project were axillary buds and leaves, monthly collected during 2 annual cycles, beginning at January of 2020 until December of 2021, from a *Q. robur* adult tree (robur A1) located at the UMINHO campus (<https://www.icampi.uminho.pt/pt/ambiente/green/>). The samples were collected randomly within the branch. However, a determined region from the bottom of the tree crown was selected. Thus, diminishing the effect that light exposure variances might have on genetic the targeted genes expression. All monthly samples were collected between 9:00 a.m. and 11:00 a.m. using a pruning shear, catalogued, and then frozen in liquid nitrogen and stored at – 80 °C. Samples from the 2022 annual cycle were also collected, with the addition of four *Q. robur* adult trees one *Q. robur* juvenile tree (robur J2), two adult *Q. suber* tree (suber A1, A5) and one *Q. suber* juvenile tree (suber chaparro). Four new *Q. robur* adult trees (robur A2, A3, A4, A5), and stored as mentioned above. These samples were photographed for the purpose of analysing the phenotype variations and growth cycle stages of the different trees, including the robur A1 images presented in the results.

#### **3.2. Phylogenetic analysis**

A Basic Local Alignment Search Tool (BLAST) was performed in the Oak database (<https://Urgi.Versailles.Inra.Fr/Blast/>) and National Center for Biotechnology Information (NCBI) (<https://www.ncbi.nlm.nih.gov/>) to obtain the *Q. robur* protein sequences, using the *A. thaliana* and *Q. suber* genes, (listed on table 2 of the supplementary material), as query. The homologous proteins from other plant species were obtained by carrying-out a PSI-BLAST at the NCBI database. The sequences were aligned with the MUSCLE algorithm (Edgar, 2004), and the maximum likelihood trees were constructed using MEGA 11 software package, with distances estimated by applying the Jones–Taylor Thornton (JTT) model of evolution. The trees were rooted in the outgroup, and to render statistical backing to the nodes, each consensus tree was generated from 1000 bootstrap data sets.

### 3.3. RNA extraction

The RNA samples were extracted using the CTAB/LiCl method for total RNA extraction (Chang et al. 1993) with modifications (Le Provost et al., 2007; Serrazina et al., 2015). The frozen plant material was grinded to dust in a mortar with liquid nitrogen poured in and transferred to a 2 mL Eppendorf® tube along with 900 µL a Cetyltrimethyl ammonium bromide (CTAB) solution (20 g L<sup>-1</sup> CTAB; 30 mM EDTA; 2 M NaCl; 0,1 M Tris-HCl; 20 g L<sup>-1</sup> PVP) mixed with 2 % (w/v) dichlorodiphenyltrichloroethane (DDT). After vortexing, the samples were incubated at 65°C for 15 minutes while vortexing every 5 minutes. 900 µL of Chloroform:Isoamyl alcohol (IAA) 24:1 solution was added following the incubation and the samples thoroughly agitated in vortex until the content in the tube is homogeneously mixed. Samples were then centrifuged at 17.530 g for 15 minutes at 4 °C and the supernatant collected to a new tube. A solution of 900 µL of Chloroform:Isoamyl alcohol 24:1 solution was added, the sample vortexed and the previous centrifugation step repeated with the supernatant added to a new tube. The collected supernatants volume (¼) was added to 8 M LiCl solution, and the samples incubated overnight at 4 °C. The samples were then centrifuged at 13.000 g for 30 minutes at 4 °C, the supernatant discarded, the pellet resuspended with 300 µL of Sodium Chloride-Tris-EDTA (STE) buffer (pre-heated to 65 °C) and 450 µL of Chloroform:Isoamyl alcohol 24:1 solution was added. Samples were mixed by inverting the tubes and centrifuged at 9000 g for 15 minutes at 4 °C. The supernatant was collected to a new tube and stored in ice while 150 µL of STE buffer was added to the remaining organic phase. The centrifugation step was repeated, and the supernatant added to the previously collected supernatant. 60 µL of 3 M NaAc solution (pH = 5.6) and 750 µL of Ethanol 100 % were added to the tubes and the samples incubated at – 80 °C for 1 hour. The samples were then centrifuged at 12.000 g for 30 minutes at 4 °C, the supernatant discarded, and the pellet washed with 400 µL Ethanol 70 % (v/v). Following two centrifugation steps at 12.000 g for 5 and 1 minute respectively, discarding the supernatant between centrifugations to remove the ethanol, the pellet was left to dry and finally resuspended in 20 µL of Diethyl Pyrocarbonate (DEPC) H<sub>2</sub>O. RNA concentration was evaluated in a nanodrop, and its integrity was visualized after electrophoresis run in a 0.8 % (w/v) agarose gel using GreenSafe Premium nucleic acid stain (nyzTech).

All materials used in RNA extraction were autoclaved 3 times over and samples were always kept on ice between steps to minimize the presence and activity of RNAses and the RNA degradation they cause.

### **3.4. DNase treatment**

RNA samples were then treated with DNase (DNase I set (Grisp)) according to the manufacturer's instructions, and RNA concentration and integrity measured as mentioned above in 3.3

### **3.5. cDNA synthesis**

cDNA was amplified using 500 ng of each previously purified RNA. cDNA synthesis was done using with SuperScript™ IV Reverse Transcriptase by ThermoFischer® and performed according to the manufacturer's instruction.

### **3.6. Polymerase chain reaction (PCR)**

cDNA samples were amplified using the mix represented in Table 1 and 0.5 μL of each gene specific forward and reverse primers (Table 1 of supplementary material). The reactions were carried out in a BIO-RAD T100™ Thermal cycler with an initial denaturation incubation at 95 °C for 3 minutes followed by 35 cycles of PCR at 95 °C for 30 seconds then, for 30 seconds, at an annealing temperature adjusted for each primers pair (3-5 °C lower than the lowest primer melting temperature), and 1 minute at 72 °C (for DNA polymerase to extend the primers sequences from 3' to the end of the amplicon), and followed by an additional extension at 72 °C for 5 minutes. An electrophoresis run was performed with samples loaded into a 1.5 % agarose gel along with 1 kb Plus DNA Ladder (New England Biolabs) and visualized using the GreenSafe Premium nucleic acid stain (nyzTech).

**Table 1.** Content of the mixture used for PCR amplification.

<b>PCR Mix (for each 25 <math>\mu</math>L reaction)</b>	
cDNA template	0.5 $\mu$ L
Primers (0.5 $\mu$ M)	0.5 $\mu$ L
dNTPs (100 $\mu$ M)	0.5 $\mu$ L
Taq polymerase (homemade)	0.5 $\mu$ L
MgCl <sub>2</sub> (25 mM)	2.5 $\mu$ L
Promega 5X Green GoTaq™ Flexi Buffer	5 $\mu$ L
dH <sub>2</sub> O	15 $\mu$ L

### **3.7. Colony PCRs**

Colony PCR amplification was applied to confirm the insertion of plasmids in transformed cell colonies as follows: A portion of each bacterial/yeast colonies was scraped and dissolved in 5  $\mu$ L of dH<sub>2</sub>O to be used as DNA template, which was amplified using 0.5  $\mu$ L of each forward and reverse primers (Table 3, Supplementary materials) and the mix represented in Table 2. The reactions were carried out in a BIO-RAD T100™ Thermal cycler with an initial denaturation incubation at 95 °C for 10 minutes followed by 35 cycles of PCR at 95 °C for 30 seconds then, for 30 seconds, at an annealing temperature adjusted for each primer's pair (3-5 °C lower than the lowest primer melting temperature), and 1 min and 30 sec at 72 °C, and followed by an additional extension at 72 °C for 5 minutes. An electrophoresis run was performed with samples loaded into a 1.5 % agarose gel along with 1 kb Plus DNA Ladder (New England Biolabs) and visualized using the GreenSafe Premium nucleic acid stain (nyzTech).

**Table 2.** Content of the mixture used for colony PCR amplification.

<b>PCR Mix (for each 25 <math>\mu\text{L}</math> reaction)</b>	
Template	5 $\mu\text{L}$
Primers (0.5 $\mu\text{M}$ )	0.5 $\mu\text{L}$
dNTPs (100 $\mu\text{M}$ )	0.5 $\mu\text{L}$
Taq polymerase (homemade)	0.5 $\mu\text{L}$
MgCl <sub>2</sub> (25 mM)	2.5 $\mu\text{L}$
Promega 5X Green GoTaq™ Flexi Buffer	5 $\mu\text{L}$
dH <sub>2</sub> O	11 $\mu\text{L}$

### 3.8. Scanning densitometry

The analysis of PCR results was performed by scanning densitometry using the ImageJ software (Gassmann et al., 2009; Schneider et al., 2012). The optical density of each band was determined by calculating the area of the associated absorbance peaks. The percentage of each peak area was then calculated in relation to the total measured peak area for each respective gene. These calculations were also applied to both housekeeping genes. The relative expression quantification was finally obtained by dividing each peak's area percentage by the respective peak area percentage measured in the constitutive gene (*ACTIN* or *PP2A3*). The optical density graphs are represented in Fig. 1 and the relative expression levels displayed in Table 3 of the supplementary materials.

### **3.9. Molecular assays**

#### **3.9.1. Bacterial/yeast material**

##### **3.9.1.1. *Escherichia coli***

The *E. coli* strain DH10B (F- *mcrA*  $\Delta$ (*mrr-hsdRMS-mcrBC*)  $\phi$ 80/*lacZ* $\Delta$ M15  $\Delta$ *lacX74* *recA1* *endA1* *araD139*  $\Delta$  (*ara-leu*)7697 *galU* *galk*  $\lambda$ - *rpsL*(Str<sup>r</sup>) *nupG*) was used for the propagation and storage of plasmid DNA and cloning procedures, except for the *pAbai-F3pQsPi* plasmid that was extracted from *E. coli* XL1-Blue strain ((*recA1* *endA1* *gyrA96* (*nalR*) *thi-1* *hsdR17* *supE44* *relA1* *lac* *glnV44* F'[*proAB+* *lacI* q  $\Delta$ M15 Tn10] where it had been previously transformed.

##### **3.9.1.2. *E. coli* competent cells**

*E. coli* DH10B cells were made competent for transformation according to the following procedure: An *E. coli* DH10B colony was inoculated in 10 mL of Luria-Bertani (LB) medium (10 g L<sup>-1</sup> Tryptone; 5 g L<sup>-1</sup> Yeast extract and 10g L<sup>-1</sup> NaCl) complemented with 10  $\mu$ L of streptomycin (50 mg L<sup>-1</sup>) and grown overnight at 37 °C with vigorous shaking. 100  $\mu$ L of the overnight culture was then incubated in 4.9 mL of fresh LB medium for 2 hours at 37 °C with vigorous shaking. The culture was centrifuged at 4000 g for 1 minute, the supernatant decanted, the pelleted cells resuspended in 2 mL of a 0.1 M CaCl solution and then centrifuged at 4000 g for 1 minute. After discarding the supernatant, the pelleted cells were resuspended in 500  $\mu$ L of 0.1 M CaCl solution and stored in ice until transformation.

##### **3.9.1.3. *Saccharomyces cerevisiae***

The *Saccharomyces cerevisiae* Y1HGold strain (*MAT $\alpha$* , *ura3-52*, *his3-200*, *ade2-101*, *trp1-901*, *leu2-3*, *112*, *gal4 $\Delta$* , *gal80 $\Delta$* , *met-*, *MEL1*) was used in the yeast-one hybrid assay and inoculated in yeast peptone dextrose adenine (YPDA) medium (20 g L<sup>-1</sup> Tryptone; 5 g L<sup>-1</sup> yeast extract; 20 g L<sup>-1</sup> D-glucose; 10  $\mu$ g L<sup>-1</sup> adenine) before transformation.

#### **3.9.1.4. *Saccharomyces cerevisiae* competent cells**

Y1H-GOLD *Saccharomyces cerevisiae* cells were made competent for transformation according to the following procedure: A Y1H-GOLD colony was inoculated in 10 mL of YPDA medium and grown overnight at 30°C with vigorous shaking. 250 µL of the starter culture was then re-inoculated in 10 mL of fresh YPDA medium and grown 2 hours at 30 °C with vigorous shaking. The culture was then centrifuged at 4000 g for 45 seconds, the supernatant decanted, the pelleted cells resuspended in 1 mL of ultrapure H<sub>2</sub>O and then centrifuged again at 4000 g for 45 seconds. The supernatant was then discarded, and the pelleted cells resuspended in 1mL of a 1 M LiAc in TE solution. The cells were transferred to an eppendorf® tube, centrifuged at 4000 g for 45 seconds and, after decanting the supernatant, resuspended in 200 µL of 1 M LiAc in TE solution. The competent Y1H-GOLD *S. cerevisiae* cells were kept on ice until transformation.

#### **3.9.2. Amplification of *QsHTH***

The *QsHTH* protein coding sequence was amplified from cDNA samples of *Q. suber* male and female flowers. RNA extraction, treatment and cDNA synthesis was performed as explained in sections 3.3 - 3.5. Amplification reaction components consisted in 1 µL of each primers *QsHTH Fw* and *QsHTH Rev*, listed on table 1 of the supplementary materials, 12.5µL of NZYtaq II 2× Green Master Mix and 10.5 µL of dH<sub>2</sub>O. PCR was carried out in a BIO-RAD T100™ Thermal cycler with an initial incubation at 95 °C for 3 minutes followed by 35 cycles of PCR at 95 °C for 30 seconds then, for 30 seconds at 48 °C, and 1 minute at 72 °C, followed by an additional extension at 72 °C for 5 minutes. Primers *QsHTH Fw* and *QsHTH Rev* were designed to also insert the restriction enzymes *Sma*I (5') and *Sall* (3') recognition sites.

#### **3.9.3. Isolation of plasmid DNA**

Plasmid DNA was extracted from *E. coli* DH10β and XL1-Blue cells using a Miniprep method based on Sambrook and Russells 2006 alkaline lysis protocol. A bacterial colony was inoculated in 10 mL of LB medium complemented with the appropriate antibiotics and grown overnight at 37°C with vigorous shaking. 1 mL of the overnight culture was transferred to a tube and centrifuged at maximum speed for 1 minute with the supernatant being discarded. This step was repeated 3 times. Then it was added to

the pellet 100  $\mu$ L of GTE I solution (50 mM Glucose; 10 mM EDTA; 25 mM Tri-HCL pH 8.0) and the sample vortexed until pellet was dissolved. 200  $\mu$ L of GTE II solution (0.1 M NaOH; 1 % SDS) was then added and the sample mixed by inversion. 150  $\mu$ L of GTE III solution (3 M Potassium Acetate; 5 M Acetic Acid glacial) was added and the sample incubated for 15 minutes in ice. Following the incubation, the sample was centrifuged at maximum speed for 15 minutes and the supernatant collected to a new tube. This step was repeated once, then 1 ml of ice-cold 100 % Ethanol was added to the supernatant and the sample centrifuged at max speed for 15 minutes at 4 °C. The supernatant was discarded, 50  $\mu$ L of a TE:RNase 1000:1 mixture (1 mL 1x TE; 1  $\mu$ L 10mg mL<sup>-1</sup> RNase) was then added to the pellet and the samples incubated at 37 °C for 5 minutes. The sample was then vortexed to dissolve the pellet and incubated once again at 37 °C for 15 minutes. 30  $\mu$ L of a PEG-NaCl solution (20 % PEG (w/v); 2.5 M NaCl) was added to the sample following incubation, and the sample vortexed and incubated on ice for 1 to 5 hours. The sample was then centrifuged at max speed for 15 minutes at 4 °C, the supernatant discarded, and the pellet washed with 500  $\mu$ L of 70 % ethanol solution. Following another centrifugation at max speed for 15 minutes at 4 °C the supernatant was discarded, and the pellet left to dry until the ethanol evaporates. At last, the pellet was resuspended in 30  $\mu$ L of TE.

### **3.9.4. DNA purification**

#### **3.9.4.1. Phenol/Chloroform DNA extraction method**

A Phenol/Chloroform DNA purification method was applied to extract and purify DNA from PCR products and plasmids/fragments from digestion reactions. To the DNA samples was added an equal volume of Phenol:Chloroform:IAA (25:24:1) mixture and then agitated in vortex. The samples were centrifuged for 5 minutes at 16.000 g, the supernatant collected to a new tube and an equal volume to the supernatant was pipetted of Isopropanol along with 10  $\mu$ L of a 3 M sodium acetate solution. The samples were then mixed by inverting the tubes and incubated at – 80 °C for 20 minutes. Following the incubation, samples were centrifuged at 16.000 g for 15 minutes at 4 °C, the supernatant discarded, and the pellet washed with 200  $\mu$ L of a 70 % (v/v) ethanol solution. The samples were then twice centrifuged at 16.000 g for 2 and 1 minutes respectively, at 4 °C, discarding the supernatant after each centrifugation to thoroughly remove the ethanol. The pellet was then air dried for 2 minutes and resuspended in 40  $\mu$ L of ultrapure H<sub>2</sub>O.

### **3.9.4.2. Wizard SV Gel and PCR Clean-Up System**

The Wizard SV Gel and PCR Clean-Up System (Promega) was performed to extract and purify DNA from agarose gels and was applied following the manufacturer's instructions.

## **3.9.5. Cloning procedures**

### **3.9.5.1. Cloning into pGEM-T**

The pGEM-T Easy (Promega) vector was used for a quick cloning of the PCR product resultant of the amplification of QsHTH open reading frame, to safeguard the sequence in a glycerol stock. Because pGEM-T Easy is a pre-linearized vector designed for easy cloning of PCR products with 3' T overhangs and since thermostable polymerases often add a single deoxyadenosine to the 3' of the amplified fragments, no digestion reaction with endonucleases for both vector and PCR product was required.

### **3.9.5.2. Cloning into pGAD424**

For high level expression in the yeast host cells of the fusion protein containing the targeted fragment QsHTH fused to the GAL4 AD, the QsHTH open reading frame was cloned into the vector pGAD424 (clontech) by amplification, as described in 3.9.2, digestion with restriction enzymes, and ligation into the pGAD424 vector.

### **3.9.5.3. pGAD424 digestion reaction**

The SmaI digestion reaction was carried out first (since the required buffer contains the lowest salt concentration) as follows: 10  $\mu$ L of plasmid DNA was incubated along with 1  $\mu$ L of SmaI restriction enzyme, 2  $\mu$ L of CutSmart buffer (New England Biolabs) and 7  $\mu$ L of deionized H<sub>2</sub>O at 37 °C for 2 hours. After the first digestion with SmaI the digested plasmid was purified as explained in section 3.9.4.1. For the Sall digestion reaction, 10  $\mu$ L of the purified digested plasmid were incubated along with 1  $\mu$ L of Sall restriction enzyme, 2  $\mu$ L of NEBuffer 3.1 (New England Biolabs) and 7  $\mu$ L of deionized H<sub>2</sub>O at 37 °C for

2 hours. The digested plasmid was loaded into an 1 % agarose gel and purified as referred in section 3.9.4.2.

#### **3.9.5.4. *QsHTH* digestion reaction**

For the *Sma*I digestion reaction, 10  $\mu$ L of purified PCR product was incubated along with 1  $\mu$ L of *Sma*I restriction enzyme, 2  $\mu$ L of CutSmart buffer (New England Biolabs) and 7  $\mu$ L of deionized H<sub>2</sub>O at 37 °C for 1 hour. 1  $\mu$ L of *Sal*I restriction enzyme was added to the reaction product along with 0.4  $\mu$ L of 5 M NaCl solution to match the required NaCl concentration for the *Sal*I reaction. The sample was then incubated at 37 °C for 1 hour.

#### **3.9.5.5. Ligation reaction**

The ligation reaction between the *QsHTH* insert and the pGAD424 linearized plasmid was preformed using a molar ratio of 3:1 (insert : plasmid). The formula  $\text{insert (ng)} = \text{vector (ng)} \times \text{insert size (Kb)} \times 3 / \text{vector size (Kb)}$  was used to calculate the quantity of insert and vector in the reaction and consequentially the adequate volume of each component to add to the reaction mixture. The ligation reaction mixture was prepared with 1  $\mu$ L of 10x T4 DNA ligase buffer (60 mM Tris-HCl, 50 mM MgCl<sub>2</sub>, 10 mM DTT, 10 mM ATP, pH 7.5) being added along with the appropriate volumes of both insert and vector, 0.5  $\mu$ L of T4 DNA ligase and dH<sub>2</sub>O until a total volume of 10  $\mu$ L. Two control reactions were also prepared consisting of the same reaction mixture with control reaction 1 lacking the insert and control reaction 2 lacking both the insert and the T4 DNA ligase. The reactions were incubated overnight at RT, transformed into *E. coli* DH10 $\beta$  competent cells and plated in selective medium containing ampicillin (100  $\mu$ g mL<sup>-1</sup>).

### **3.9.6. Bacterial/yeast transformation**

#### **3.9.6.1. Transformation in *E. coli***

For vector transformation in *E. coli* 5  $\mu$ L of ligation product were added to 500  $\mu$ L of *E. coli* DH10 $\beta$  competent cells and incubated on ice for 30 minutes, followed by a 45 second incubation at 42 °C and

then incubated on ice for 2 minutes. 900  $\mu\text{L}$  of LB medium were then added and the tubes incubated at 37  $^{\circ}\text{C}$  for 1 hour with agitation (200 rpm). The tubes were then centrifuged at 4000 g for 15 seconds, the supernatant discarded and the pelleted cells resuspended in 100  $\mu\text{L}$  of LB medium and plated onto LB-agar plates [LB medium, 1.5 % (w/v) agar] supplemented with the specific selection antibiotics. The plates were then incubated overnight at 37  $^{\circ}\text{C}$ .

### **3.9.6.2. Transformation in Yeast**

For vector introduction into Y1H-GOLD *Saccharomyces cerevisiae* cells a LiAc method was applied as follows: 10  $\mu\text{L}$  of plasmid DNA and 5  $\mu\text{L}$  of ssDNA were mixed then added to a tube containing 50  $\mu\text{L}$  of Y1H-GOLD competent cells. 300  $\mu\text{L}$  of a 1x PEG/LiAc/TE mixture (240  $\mu\text{L}$  50 % (w/v) PEG 3500; 30  $\mu\text{L}$  1M LiAc; 30  $\mu\text{L}$  1x TE) was added and the tube incubated at 30  $^{\circ}\text{C}$  for 30 minutes with agitation (200 rpm). 10  $\mu\text{L}$  of dimethyl sulfoxide (DMSO) was added and the mixture incubated at 42  $^{\circ}\text{C}$  for 15 minutes with agitation (200 rpm). Following the incubation, the tube was centrifuged at 4000 g for 15 seconds, the supernatant was discarded, the pelleted cells resuspended in 100  $\mu\text{L}$  of  $\text{dH}_2\text{O}$  and plated in synthetically defined (SD) medium lacking uracil.

## 4. Results and Discussion

### 4.1. Phenological Observations

*Q. robur* is a wind-pollinated monoecious species that displays an annual cyclic development typical of temperate perennial trees. During late summer and the autumn months, and probably in relation to the lowering temperatures and shorter photoperiod, the shoot meristems cease their activity and become dormant and enclosed in a bud structure (Fig. 9 - a) and c)). Once dormancy is established the buds will remain dormant until cold accumulation releases dormancy. At this stage, usually at the end of winter/beginning of spring, meristems, start resuming their activity, causing bud swelling (Fig. 9 - d)) when temperatures are favorable for growth, ultimately culminating in bud burst (Fig. 9 - e)).

In *Q. robur* bud burst usually occurs between April and May with the flushing of new leaves accompanied by the appearance of the first male flowers, which are linear catkins, with well-defined anthers emerging from the swelling axillary buds (Fig. 9 - e), h) and i)). Approximately one week later, the female flowers emerge (7.5 days, according to Bacilieri et al., 1994), with 1 to 5 flowers forming at the tip of a peduncle, originating from the axils of newly formed leaves (Fig. 9 - f) and g)). However, in the observed *Q. robur* tree, these developmental stages were observed to occur much earlier than expected in 2022.

The plant continues its growth throughout the rest of the spring and summer months, with male flower primordia already being observed inside the new buds before dormancy induction (Fig. 9 - a)), and with summer flowering sometimes occurring as observed in (Fig. 9 - k)). During late summer/early autumn, changes in photoperiod and temperature presumably trigger the molecular mechanisms responsible for bud dormancy induction. However, as discussed in the introduction, *Q. robur* is a species with a wide geographic distribution and a high frequency of interspecific hybridization leading to a vast range of phenotypes with differences in the physiology, morphology, and scheduling regarding the plant's development cycle. While *Q. robur* trees are usually described as deciduous species, the one selected for expression analysis in this study (robur A1) was observed to maintain the majority of its foliage alive during winter. Whether this is a result of the natural wide range of phenotypes in *Q. robur*, or a response to external factors such as climatic conditions, light exposure, nutrient availability, biotic stress, was not ascertained. However, a recent study has classified new semideciduous and/or evergreen *Quercus* species that closely related and recently specified from *Q. robur*, *Q. orocantabrica* and *Q.*

*estremadurensis*. (Vila-Viçosa et al., 2022). These species are found in Continental Portugal and could fit the description of some of the surveyed trees. Still, it might be an important factor to take into consideration in future analysis of the mechanisms responsible for the growth/dormancy cycle in these trees when interpreting possible differences in gene expression and bud burst/dormancy set and flowering time.

Regarding the timing of bud burst and flowering, it was observed that these events occurred much earlier than expected. In figure 9 – e), which were captured in early February 2022, bud burst can already be clearly observed along with the emergence of new shoots containing young leaves, as well as the appearance of male flowers and female flowers in an early developmental stage (Fig. 9 – e)). The early budburst observed might be related to a particularly warm winter, especially in the months of January and February. Several phenological studies have correlated the anticipation of bud burst in ligneous plants to climate warming either by long-term phenological observations backed by climacteric data records (Menzel et al., 2006; Parmesan, 2007; Wilkinson et al., 2017) or artificial warming experiments (Fu et al., 2014; Morin et al., 2010).

In Wilkinson et al., (2017) several different provenances of *Q. robur* trees were observed to have an earlier budburst date in relation to higher mean temperatures during the spring warming period. In Fu et al., (2014), *Q. robur* saplings exposed to warmer winter and early spring artificially set temperatures experienced an earlier leaf flushing date in comparison to saplings grown at ambient temperature. Fu et al., (2014) also hypothesized that the increased winter and early spring temperatures might have led buds to an earlier dormancy set in the fall, allowing for an earlier start of chilling accumulation and earlier achievement of the chilling requirement. Thus, the sensitivity of the bud to forcing temperatures is anticipated, resulting in an earlier bud burst in the following spring. However, there are other factors at play in the establishment of dormancy, such as endogenous signals and namely photoperiod, which is reported to play a central role in bud dormancy set of temperate perennial trees. It still remains unclear the full extent to which temperature influences bud set, as studies have observed that the responsiveness to temperature and photoperiod in dormancy establishment was highly varied between different species, and that these factors were often interconnected (Tanino et al., 2010). Although no temperature measurements were made at site in this study, daily climactic records from Rede DRAPN (available at <https://drapnsiapd.utad.pt/sia/Meteorologia/Leituras>) show untypically high maximum daily temperatures during the winter months of January and February 2022, with temperatures being observed

to reach or pass 18 °C in 15 days and a mean maximum daily temperature of 16°C during that period in Braga. In the monthly climacteric report from *Instituto Português do Mar e da Atmosfera* (IPMA), the medium temperature and especially the medium maximum temperature in Portugal were reported to be amongst the highest in the last century. In fact, January and February registered the highest and second highest mean maximum temperatures relative to those months since 1931, respectively (Instituto Português do Mar e da Atmosfera, 2022).



**Figure 9. Developmental bud stages of *Q. robur*.** a) - *Q. robur* twig with enclosed bud structures in the axils of leaves. b) - Early development male catkin inside an enclosed bud structure observed. c) - Dormant bud structure. d) - Bud swelling. e) - Bud burst with the flush of new leaves and already developed male catkins (old leaves removed). f), g) - Female flowers in early stages of maturation surging at the end of spikes originating at the axils of newly formed leaves. h) Recently flushed male catkins emerging along newly formed leaves. i) - Fully developed male catkins. j) - Pollinated female flowers maturing into acorns. k) - Case of summer flowering. a), c) and e) – the scale bar represents 1 cm; d), j) and k) – the scale bar represents 5 mm; i) – the scale represents 2 mm; b) – the scale bar represents 1 mm; f), g) and h) – the scale represents 500 µm.

Although no sufficient data regarding phenological observations or temperature measurements was gathered at site, to elaborate a solid hypothesis, it is possible that the rising temperatures of the last years might be disrupting the timing of important developmental stages in the oaks growth cycle, such as anticipating dormancy and release upon which untypically high early winter temperatures could result in forcing requirements being met and bud burst occurring much earlier than expected, as it was observed in this study. As mentioned previously, the mechanisms and pathways which control dormancy and flowering are extremely complex and still widely unknown in tree species such as *Q. robur*.

The phenological observations here presented provide a visual framework of the developmental phases whose molecular mechanisms are approached in this study. However, a more comprehensive and rigorous record of the phenological phases and climacteric conditions at site could prove essential for a better understanding of the relation between molecular regulation mechanisms and exogenous stimuli, further uncovering the intricate web of regulatory mechanisms responsible for the development cycle in *Q. robur* and other perennial tree species.

#### **4.2. Identification of *Q. robur* homologs relevant to dormancy and flowering time regulation**

Dormancy and flowering time are interconnected molecular processes controlled by a complex web of regulator genes. These mechanisms are capable of promoting or delaying bud break and flower development, ensuring that these events occur under the most favorable conditions (D. Horvath, 2009; D. P. Horvath et al., 2003; Singh et al., 2017, 2021). Several gene families involved in these processes have been identified and functionally characterized in *A. thaliana* as well as in other plant species (Bowman et al., 1989; D. P. Horvath et al., 2008; G. Kumar et al., 2016; C. Li & Lu, 2014; Y. Li et al., 2016, 2017; Z. Liu et al., 2020; Melzer et al., 2008; Mo et al., 2021; Pa enicová et al., 2003; Sobral et al., 2020; Yang et al., 2008; N. Yu et al., 2020). Hence, a screening of the available *Q. robur* genome and transcriptome databases was made to identify homologs of the *A. thaliana* gene hubs controlling the mechanisms responsible for bud set/break and flower induction/repression.

The *FT*; *SQUAMOSA-PROMOTER BINDING PROTEIN-LIKE (SPL)*; *CO*; *SOC1*; and *LFY* are genes known to have a central role in promoting bud break and flowering induction, whilst the *SVP* and *FLC* have been described to be flowering repressors and dormancy maintenance promoters (Cardon et al., 1999; G.

Kumar et al., 2016; J. Lee et al., 2008; C. Li & Lu, 2014; Y. Li et al., 2016; Michaels & Amasino, 1999; Pa enicová et al., 2003; Singh et al., 2017; Weigel et al., 1992; R. Wu, Tomes, et al., 2017; R. Wu, Wang, et al., 2017; F. Xu et al., 2012).

The *Q. robur* homologs were retrieved from both the Oak genome and NCBI databases by BLAST search with the above-mentioned *A. thaliana* proteins, as well as homologs of the closely related *Q. suber*, identified in Sobral et al., (2020) as queries.

Preliminary alignments and a phylogenetic analysis were made to filter the blast results of redundant sequences. Once the *Q. robur* homologs were retrieved, a phylogenetic analysis was conducted with the homologs retrieved by BLAST search from other Fagaceae trees (*Quercus suber* (Qs); *Quercus rubra* (Qru); *Quercus lobata* (Ql); *Castanea mollissima* (Cm); *C. sativa* (Csa); *Fagus crenata* (Fc)) as well as other perennial trees (*Populus trichocarpa* (Pt); *P. persica* (Pp); *Malus domestica* (Md); *Vitis vinifera* (Vv); *Juglans regia* (Jr); *Citrus unshiu* (Ci); *Gingko biloba* (Gb); *Actinidia chinensis* (Ac); *Amborella trichopoda* (Amt); *Corylus avellana* (Ca); *Glycine max* (Gm); *Mangifera indica* (Mi); *Medicago truncatula* (Mt); *Pyrus cummunis* (Pc); *Pynus radiata* (Pr); *Pyrus brestchneideri* (Pb)) and homologs in herbaceous species (*Petunia hibrida* (Ph); *Solanum lycopersicum* (Sl); *Arabidopsis thaliana* (At); *Argyranthemum frutescens* (Af); *Antirrhinum majus* (Amj); *Cucumis sativus* (Cs)) that had been previously functionally characterized and related to dormancy/budbreak and flowering induction.

#### 4.2.1. FT family

The FT phylogenetic tree was constructed by retrieving *Q. robur* homologs of the *A. thaliana* PEBP gene family which contains the *FT* gene as well as *MOTHER OF FT AND TFL1* (*MFT*); *BROTHER OF FT AND TFL1* (*BFT*); *TWIN SISTER OF FT* (*TSF*); *A. THALIANA CENTRORADIALIS* (*ATC*) and *TFL1*. Despite the previously mentioned role of *FT* in promoting flowering, *TFL1* has been described as a flowering repressor responsible for the maintenance of the meristem identity by repressing floral identity genes *AP1/AP2* and *LFY* which are required for flowering initiation on the meristem (Mimida et al., 2001; Schultz & Haughn, 1993; Shannon & Meeks-Wagner, 1993). The remaining genes are less well characterized however overexpression of *BFT* and *ATC* delayed flowering and resulted in similar phenotypes to the ones observed in *TFL1* overexpression mutants (Karlgrén et al., 2011b; Mimida et al., 2001; S. J. Yoo et al., 2010), while both *MFT* and *TSF* are thought to be flowering promoters (A. Yamaguchi et al., 2005; S. Y.

Yoo et al., 2004). In the phylogenetic analysis conducted, 6 PEBPs genes were found in *Q. robur* genome homologous to the above-mentioned *A. thaliana* genes. The proteins encoded by these genes were named *QrFT*; *QrTFL1*; *QrMFT*; *QrMFTL*; *QrBFT*; *QrCEN* according to the grouping with the respective *A. thaliana* homologs. A phylogenetic tree was then constructed with the PEBP homolog proteins from other plant species (Fig. 10). The proteins were observed to be clustered into four clades: TFL1 clade; BFT clade, FT clade and the MFT clade. *Q. robur* homologs are represented in all clades, closely clustered with the homologs from the other Fagaceae species. *QrFT* was grouped into the FT clade along *AtFT* and *AtTSF*, while *QrBFT* can be found in the BFT clade. Two *Q. robur* homologs *QrTFL1* and *QrCEN* can be observed in TFL1 clade. Regarding the MFT clade, two *Q. robur* homologs were also observed with *QrMFT* more closely grouped with *AtMFT* and *QrMFTL* (*Qr MOTHER OF FT AND TFL1-like*) clustered in a different sub-clade.

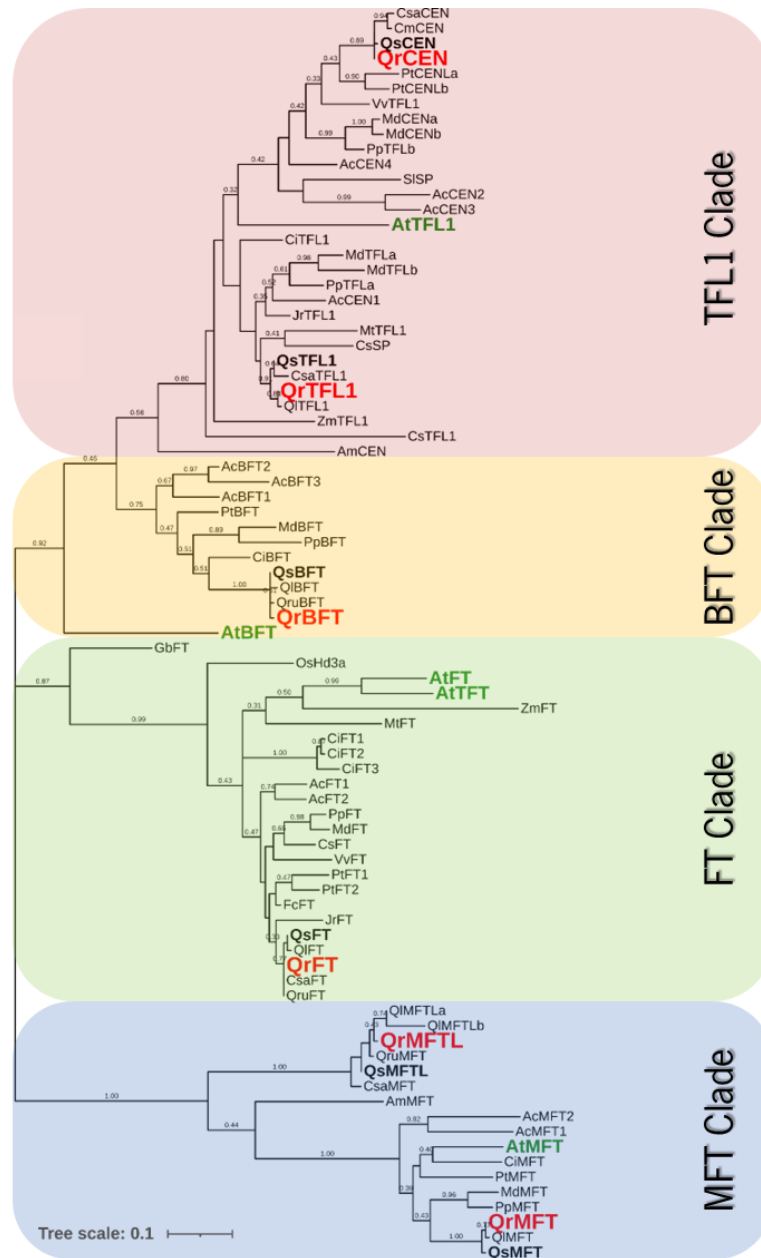


**Figure 10. Phylogenetic analysis of FT-like genes by Maximum Likelihood method.** The evolutionary history was inferred by using the Maximum Likelihood method and JTT matrix-based model (Jones et al., 1992). The tree with the highest log likelihood (-8333.29) is shown. The percentage of trees in which the associated taxa clustered together is shown next to the branches. Initial tree(s) for the heuristic search were obtained automatically by applying Neighbor-Join and BioNJ algorithms to a matrix of pairwise distances estimated using the JTT model, and then selecting the topology with superior log likelihood value. The tree is drawn to scale, with branch lengths measured in the number of substitutions per site. This analysis involved 83 amino acid sequences. There was a total of 225 positions in the final

dataset. Evolutionary analyses were conducted in MEGA X (S. Kumar et al., 2018). *Q. robur* proteins are highlighted in red and *A. thaliana* proteins are highlighted in green.

#### 4.2.2. SPL family

The SPL gene family is comprised of several transcription factors characterized by the presence of the highly conserved, 76 amino acids long, SBP domain and are involved in a vast range of processes central to plant development and growth (Klein et al., 1996; Yang et al., 2008; Preston & Hileman, 2013). SPL genes, (also named SBP-box genes) are ubiquitous among plants and other photosynthetic organisms, ranging from the less complex single cell photosynthetic algae and mosses through perennial woody trees (Kropat et al., 2005; C. Li & Lu, 2014; Riese et al., 2007; N. Yu et al., 2020) and in *A. thaliana* there have been identified, by genome sequencing, 16 SPL genes (*AtSPL1 - AtSPL16*) distributed through 8 major clades (I-VIII) (Cardon et al., 1999; Preston & Hileman, 2013; Salinas et al., 2012; Yang et al., 2008). The proteins encoded by these genes were used as query in the BLAST search on *Q. robur* databases and 11 homologs were identified and named according to their grouping with the *A. thaliana* SPL proteins: *QrSPL1*; *QrSPL2*; *QrSPL6*; *QrSPL7a*; *QrSPL7b*; *QrSPL8a*; *QrSPL8b*; *QrSPL9*; *QrSPL13*; *QrSPL14*; *QrSPL16*. Despite the presence of *Q. robur* homologs belonging to 7 different SPL clades (I; II; IV; V; VIII; VII; III) the phylogenetic tree was constructed with a broader focus on proteins belonging to the VI, VII and VIII clades, since these are the clades whose genes have been characterized to play important roles in flower development and flowering induction (Fig. 11) (Preston & Hileman, 2013; M. Xu et al., 2016). Despite the presence of clade VI proteins in other closely related Fagaceae species, including the *QsSPL4* identified in *Q. suber* (Sobral et al., 2020), on *Q. robur* no homologs belonging to this clade were found. Regarding clades VII and VIII, *Q. robur* proteins were identified belonging to both, with *QrSPL13* and *QrSPL16* grouped in clade VII and *QrSPL9* in VIII, clustered alongside the respective homologs from other Fagaceae trees.

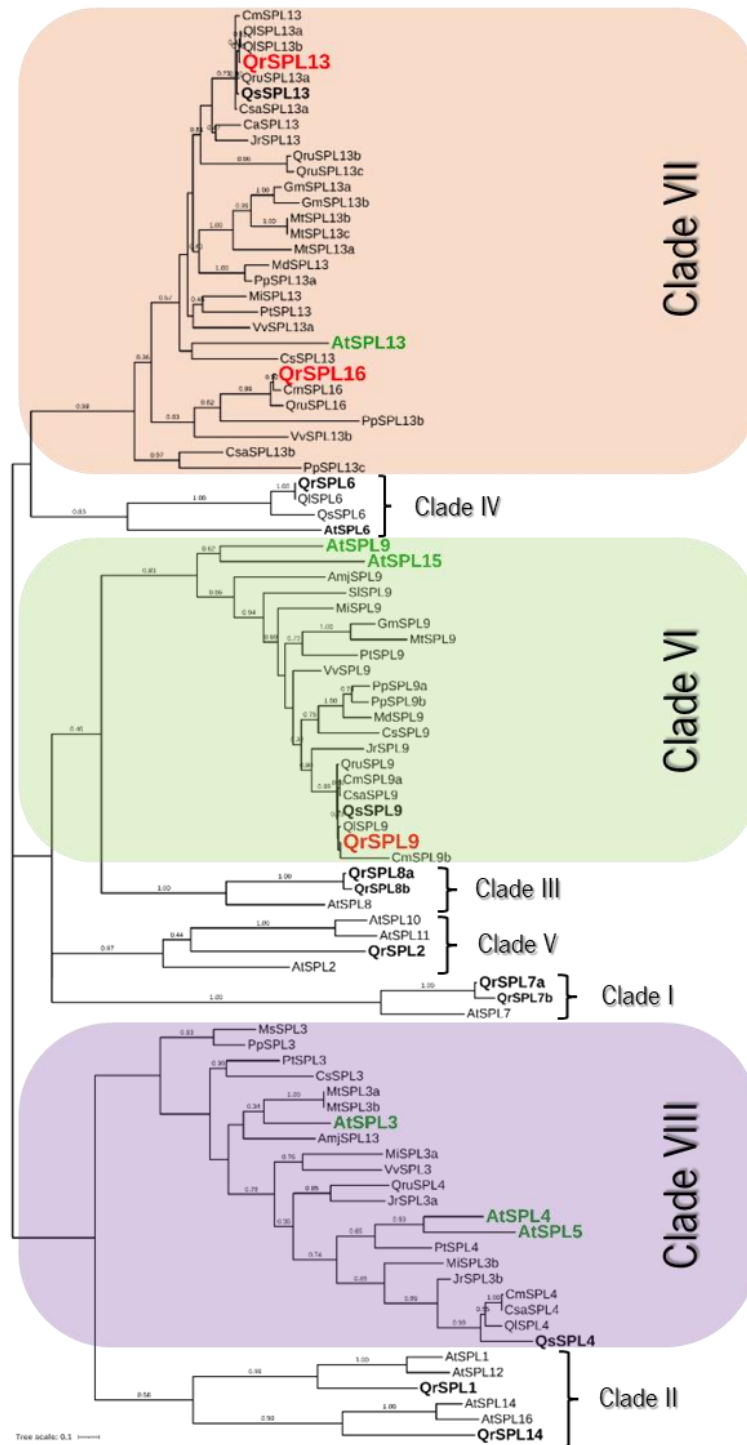


**Figure 11. Phylogenetic analysis of SPL-like genes by Maximum Likelihood method.** The evolutionary history was inferred by using the Maximum Likelihood method and JTT matrix-based model (Jones et al., 1992). The tree with the highest log likelihood (-52512.44) is shown. The percentage of trees in which the associated taxa clustered together is shown next to the branches. Initial tree(s) for the heuristic search were obtained automatically by applying Neighbor-Join and BioNJ algorithms to a matrix

of pairwise distances estimated using the JTT model, and then selecting the topology with superior log likelihood value. The tree is drawn to scale, with branch lengths measured in the number of substitutions per site. This analysis involved 92 amino acid sequences. There were a total of 1274 positions in the final dataset. Evolutionary analyses were conducted in MEGA X (S. Kumar et al., 2018). *Q. robur* proteins are highlighted in red and *A. thaliana* proteins are highlighted in green.

### 4.2.3. SOC1

The *A. thaliana* *SOC 1* is a type II MADS-box gene belonging to the TM3 subfamily of the MIKCC type genes that represent the majority of the better described MADS-box genes in plants. The TM3 subfamily also includes in *A. thaliana* the *AGL14*, *AGL19*, *AGL42*, *AGL71* and *AGL72* genes (Becker, 2003; Pa enicová et al., 2003). Despite the more extensively known role of *SOC1* as a flowering promoter central to both the photoperiod pathway, since *CO* promotes flowering partially by *SOC1* up regulation, the vernalization pathway, through *SOC1* repression by *FLC*, and the autonomous age pathway (Hepworth, 2002; J. Lee et al., 2008; J. Lee & Lee, 2010), *AGL42*, *AGL71* and *AGL72* have also been reported to promote flowering in *A. thaliana* as well as other homologs belonging to the same sub-clade from other species (Dorca-Fornell et al., 2011; Y. Li et al., 2016; Liu et al., 2020).

In the phylogenetic analysis conducted four *Q. robur* genes (*QrSOC1*, *QrAGL19*, *QrAGL42a*, *QrAGL42b*) were found belonging to the TM3 sub-family. A phylogenetic tree was then constructed with other TM3 sub-family proteins belonging to different plants species and the proteins belonging to the SVP MADS-box clade used as an outgroup. Upon analyzing the phylogenetic tree, the TM3-like proteins were observed to be clustered in three clades with *QrSOC1* grouped within the same clade as *AtSOC1* (SOC1 clade), *QrAGL19* belonging to the AGL14/19 clade and both *QrAGL42a* and *QrAGL42b* closely grouped with *AtAGL42* in the AGL42/71/72 clade (Fig. 12).

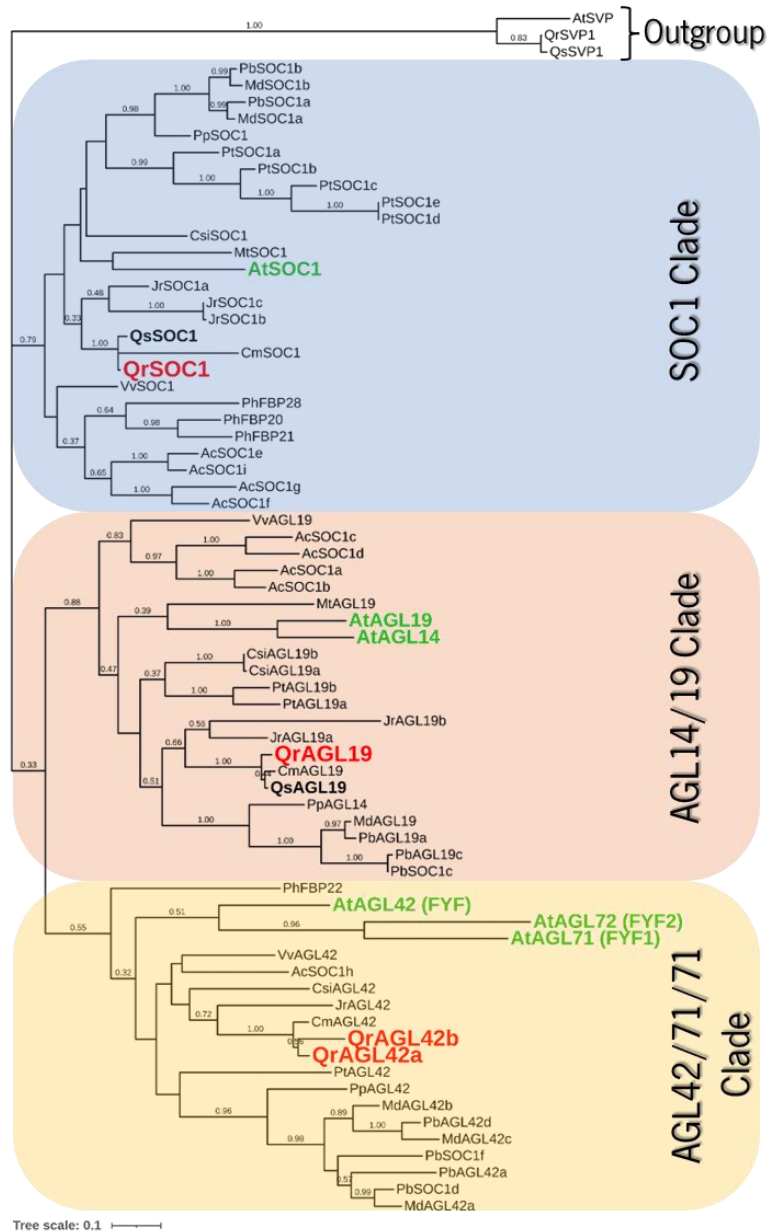


**Figure 12. Phylogenetic analysis of SOC1-like genes by Maximum Likelihood method.** The evolutionary history was inferred by using the Maximum Likelihood method and JTT matrix-based model (Jones et al., 1992). The tree with the highest log likelihood (-15071.71) is shown. The percentage of trees in which the associated taxa clustered together is shown next to the branches. Initial tree(s) for the heuristic search were obtained automatically by applying Neighbor-Join and BioNJ algorithms to a matrix of pairwise distances estimated using the JTT model, and then selecting the topology with superior log likelihood value. The tree is drawn to scale, with branch lengths measured in the number of substitutions per site. This analysis involved 72 amino acid sequences. There was a total of 329 positions in the final

dataset. Evolutionary analyses were conducted in MEGA X (S. Kumar et al., 2018). *Q. robur* proteins are highlighted in red and *A. thaliana* proteins are highlighted in green.

#### **4.2.4. *LEAFY* transcription factors**

*LFY* is a master regulator, transcription factor (TF), capable of binding to their usually condensed chromatin target sites before any other factors bind to, open, or modify said target site, typically initiating cell fate changes (Iwafuchi-Doi & Zaret, 2014; Soufi et al., 2015; N. Yamaguchi, 2021; Zaret & Carroll, 2011). Pioneer TFs are more extensively characterized in animals, with few being identified/characterized in plants, yet *LFY* stands out as an important pioneer TF in plants, capable of cell fate specification (Jin et al., 2021; Lai et al., 2021; N. Yamaguchi, 2021). In *A. thaliana*, *LFY* expression is thought to be suppressed by *TFL1* during the vegetative phase, impeding it from establishing the floral fate (Abe et al., 2005, 2019; Conti & Bradley, 2007; Kobayashi et al., 1999; N. Yamaguchi, 2021; Zhu et al., 2020).

In the phylogenetic analysis conducted, one *A. thaliana LFY* homolog was retrieved from the *Q. robur* databases, as was expected since most plant species studied only have one *LFY* representative (N. Yamaguchi, 2021). A phylogenetic tree was then constructed with *LFY* homologs from other plant species (Fig. 13). *QsLFY* was observed to be clustered along the other homologs from Fagaceae trees and in relative proximity to *AtLFY*.

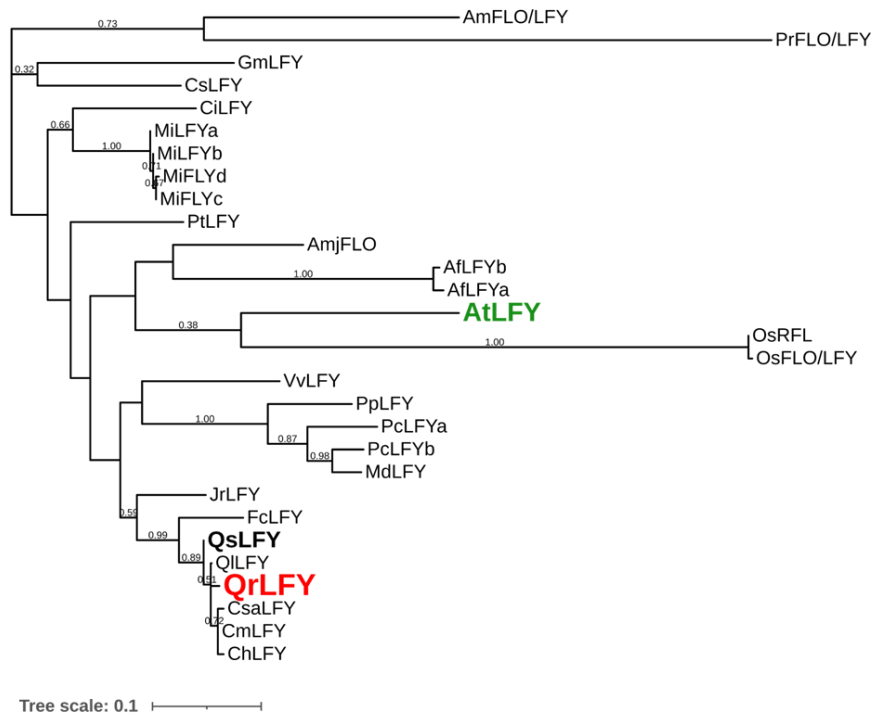


**Figure 13. Phylogenetic analysis of LFY-like genes by Maximum Likelihood method.** The evolutionary history was inferred by using the Maximum Likelihood method and JTT matrix-based model (Jones et al., 1992). The tree with the highest log likelihood (-7615.74) is shown. The percentage of trees in which the associated taxa clustered together is shown next to the branches. Initial tree(s) for the heuristic search were obtained automatically by applying Neighbor-Join and BioNJ algorithms to a matrix of pairwise distances estimated using the JTT model, and then selecting the topology with superior log likelihood value. The tree is drawn to scale, with branch lengths measured in the number of substitutions per site. This analysis involved 29 amino acid sequences. There was a total of 507 positions in the final dataset. Evolutionary analyses were conducted in MEGA X (S. Kumar et al., 2018). *Q. robur* proteins are highlighted in red and *A. thaliana* proteins are highlighted in green.

#### 4.2.5. SVP family

*SVP* genes are members of the *STMADS11* subfamily of MIKCC type MADS-box genes. In *A. thaliana* there are two genes belonging to this family, one is *SVP*, and the other is named *AGL24* (Becker, 2003). While *SVP* acts as a flowering repressor, despite their close phylogenetic proximity, *AGL24* reportedly has the opposite effect, acting as a flowering promoter, jointly activating *LFY* with *SOC1* (H.

Yu et al., 2002, 2004). SVP homologs were also reported to be involved in the maintenance of dormancy in perennial woody trees (R. Wu, Tomes, et al., 2017; R. Wu, Wang, et al., 2017; R.-M. Wu et al., 2012). In the phylogenetic analysis conducted six *Q. robur* proteins belonging to the *STMADS11* subfamily were retrieved. A phylogenetic tree was then constructed with homologs from several plant species. Tree major clades were observed, as reported in studies focusing on the characterization of the *SVP family* (X. Liu et al., 2018; Quesada-Traver et al., 2022). In the SVP 1 clade, which contains the *A. thaliana SVP* protein, one *Q. robur* homolog, *QrSVP1*, was found. One *Q. robur* homolog, *QrSVP5*, was observed to be grouped in the SVP 2 clade, along with the *A. thaliana AGL24* protein. Furthermore, the SVP 3 also contains the DAM subclade which groups the DAM proteins from the Rosaceae *P. persica* and *M. domestica* trees. Regarding the SVP 3 clade, four *Q. robur* homologs were retrieved belonging to this clade corresponding to *QrSVP2*, *QrSVP3*, *QrSVP4* and *QrSVP6*. Furthermore all *Q. robur* SVP proteins were grouped alongside respective homologs from other closely related Fagaceae species such as *Q. robur* and/or *C. sativa* (Fig. 14).

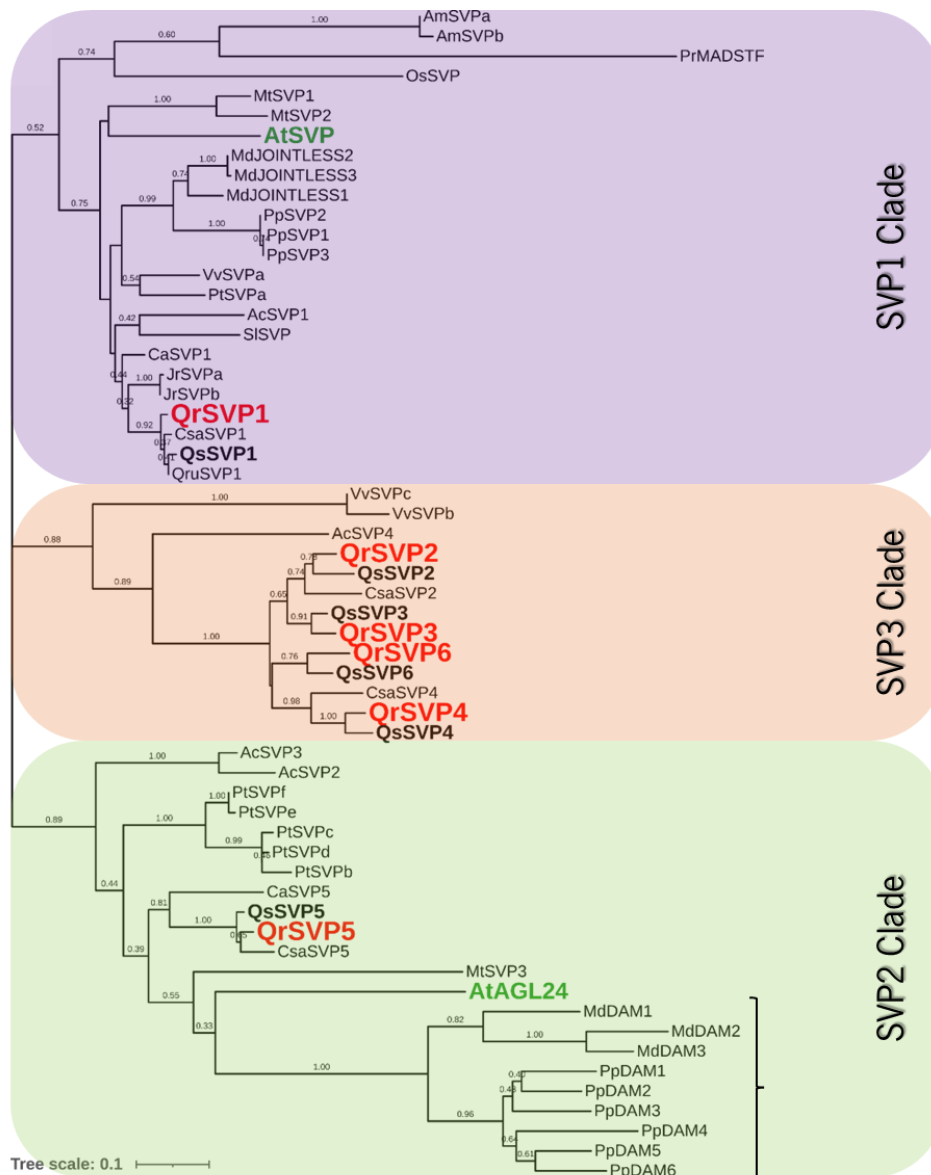


**Figure 14. Phylogenetic analysis of SVP-like genes by Maximum Likelihood method.** The evolutionary history was inferred by using the Maximum Likelihood method and JTT matrix-based model (Jones et al., 1992). The tree with the highest log likelihood (-10145.18) is shown. The percentage of trees in which the associated taxa clustered together is shown next to the branches. Initial tree(s) for the heuristic search were obtained automatically by applying Neighbor-Join and BioNJ algorithms to a matrix of pairwise distances estimated using the JTT model, and then selecting the topology with superior log likelihood value. The tree is drawn to scale, with branch lengths measured in the number of substitutions per site. This analysis involved 59 amino acid sequences. There was a total of 504 positions in the final dataset. Evolutionary analyses were conducted in MEGA X (S. Kumar et al., 2018). *Q. robur* proteins are highlighted in red and *A. thaliana* proteins are highlighted in green.

#### 4.2.6. FLC family

*FLC*, like the above-mentioned *SVPs* and *SOC1*, are a MIKCC type MADS-box gene. The *FLC-like* gene subfamily in *A. thaliana thaliana* contains six genes: *FLC*, *FLOWERING LOCUS M* (FLM), *AGAMOUS-LIKE 31* (AGL31), and the unnamed *At5G65060*, *At5G65070* and *At5G65080* (Becker, 2003). The role of *FLC* in *A. thaliana* is well known, being a suppressor of *SOC1* and *FT* and consequentially repressing flowering (Hepworth, 2002; Searle et al., 2006), *FLC* has a central role in the vernalization and autonomous pathways since its expression is downregulated by vernalization and some genes belonging to the autonomous pathway were observed to suppress *FLC*, inducing flowering (Becker, 2003; Hepworth, 2002; Michaels & Amasino, 1999, 2001; Searle et al., 2006; Sheldon et al., 1999). Two proteins homologous to *A. thaliana FLC* were retrieved from the *Q. robur* databases: *QrFLCa* and *QrFLCb*. Both *Q. robur* proteins were not closely grouped with the *AtFLC* or any other *A. thaliana FLC-like* family member, being grouped together with other woody perennials. Despite the distant relation, *QrFLCa* was observed to be the more closely related to the *A. thaliana* homolog, and the more distant *QrFLCb* closely clustered with the *FLC* homologs from the other Fagaceae species (Fig. 15).

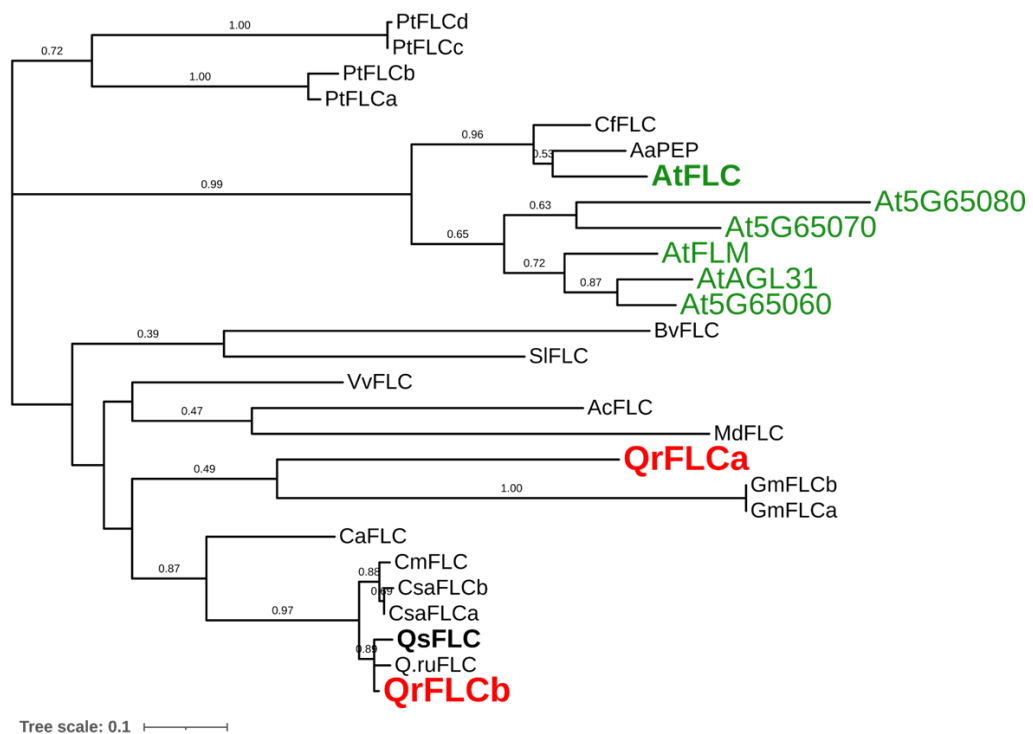


**Figure 15. Phylogenetic analysis of FLC-like genes by Maximum Likelihood method.** The evolutionary history was inferred by using the Maximum Likelihood method and JTT matrix-based model (Jones et al., 1992). The tree with the highest log likelihood (-5938.05) is shown. The percentage of trees

in which the associated taxa clustered together is shown next to the branches. Initial tree(s) for the heuristic search were obtained automatically by applying Neighbor-Join and BioNJ algorithms to a matrix of pairwise distances estimated using the JTT model, and then selecting the topology with superior log likelihood value. The tree is drawn to scale, with branch lengths measured in the number of substitutions per site. This analysis involved 27 amino acid sequences. There was a total of 298 positions in the final dataset. Evolutionary analyses were conducted in MEGA X (S. Kumar et al., 2018). *Q. robur* proteins are highlighted in red and *A. thaliana* proteins are highlighted in green.

### **4.3. Expression analysis of flowering and dormancy regulator genes in *Q. robur***

With the phylogenetic analysis of *Q. robur* homologs concluded, 4 genes, *QrFT*, *QrSOC1*, *QrSVP1*, and *QrFLC*, belonging to 4 distinct gene families were selected among potential dormancy and flowering regulators for expression analysis. They were selected due to their close association with genes linked to dormancy and flowering regulation in other perennial trees, including the closely related *Q. suber* (Sobral et al., 2020). Compatibility between the primers used to amplify the homolog *QsFT*, *QsSOC1*, *QsSVP1*, and *QsFLC* genes in *Q. suber*, was tested by nucleotide alignment, with the compatibility of the respective primers being further confirmed by PCR amplification in *Q. robur* samples. Despite no *Q. robur* homolog being identified belonging to the clade VI of SPL family in this thesis, the primers used in Sobral et al., (2020) to amplify *QsSPL4*, were still tested. An amplification of a PCR product using these primers with *Q. robur* genomic DNA would suggest that there is in fact a copy of SPL4 in the genome of this species, but it may have not been annotated yet. Clade VI contains the genes most closely associated with flowering regulation in plants, and all *Quercus* species analyzed were observed to have an homolog belonging to that clade, including the *QsSPL4*, which overexpression caused early flowering in *A. thaliana* mutants (C. Li & Lu, 2014; Preston & Hileman, 2013; Sobral et al., 2020; N. Yu et al., 2020). *QrSHP* expression was also analyzed due to their potential role in, and indication of flower organ development. Expression analysis of *Q. robur* homologs *QrFT*, *QrSOC1*, *QrSVP1*, *QrSPL4*, *QrFLC* and *QrSHP* was firstly conducted by PCR amplification of the monthly cDNA samples. *QrFT* expression was analyzed in leaf samples. *QrACTIN*, was used to normalize the expression levels between the different samples, while the remaining genes were analyzed in bud samples with *QrPP2A3* as the house-keeping gene. These reference genes were selected according to an expression analysis study of constitutive genes in several tissues of the closely related *Q. suber*, which deemed *ACTIN* and *PP2A3* to be the most suitable for expression

normalizing when analyzing leaf and bud samples, respectively (Marum et al., 2012). PCR amplification products were visualized in an electrophoresis gel (Fig. 16). However, to better observe and display the expression patterns of these genes during the year-long growth cycle of *Q. robur*, a semi-quantitative RT-PCR analysis was performed and analyzed by scanning densitometry using the ImageJ software (Gassmann et al., 2009; Schneider et al., 2012). This was carried out by measuring the optical density of each band by calculating the area of the associated absorbance peaks. The percentage of each peak area was calculated in relation to the total measured peak area for each respective gene. These calculations were also applied to both housekeeping genes. The relative expression quantification was finally obtained by dividing each peak area percentage by the respective peak area percentage measured in the constitutive gene (*QrACTIN* or *QrPP2A3*). The results from this analysis are displayed in the graphs of figure 17.

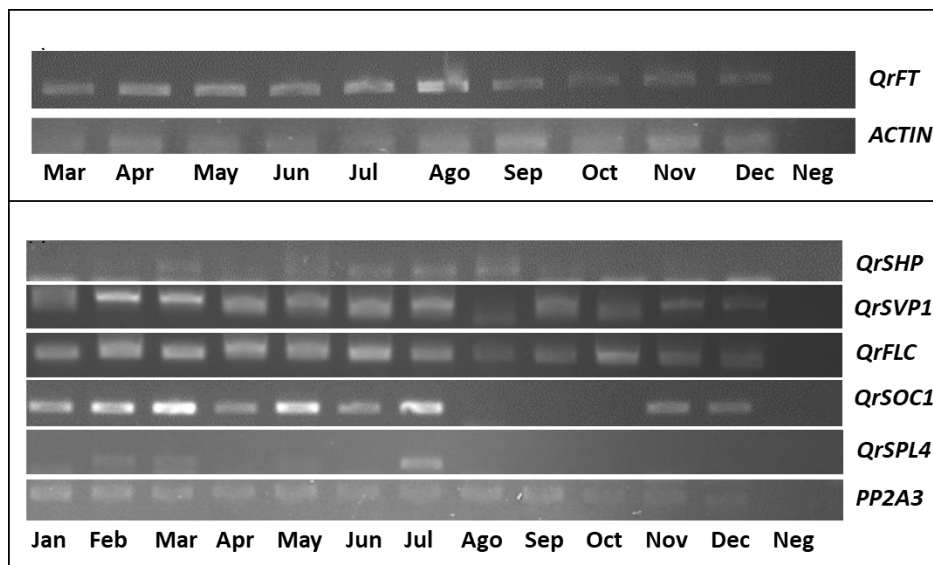


**Figure 16. Analysis of the expression of potential dormancy and flowering regulator genes in *Q. robur*.** a) *QrFT* expression was analysed in leaf samples with *QrACTIN* as the normalizing gene. b) The expression of *QrSHP*, *QrSVP1*, *QrFLC*, *QrSOC1* and *QrSPL4* was analyzed in bud samples with *PP2A3* as the normalizing gene. PCR analysis of the expression of potential flower development and growth promoters (*QrFT*, *QrSOC1*, *QrSPL4*, *QrSHP*), and potential flowering repressors and dormancy promoter genes (*QrFLC* and *QrSVP1*) in *Q.robur* monthly cDNA samples during the year of 2021. Each lane corresponds to the respective month listed below, with the last lane being the negative control.

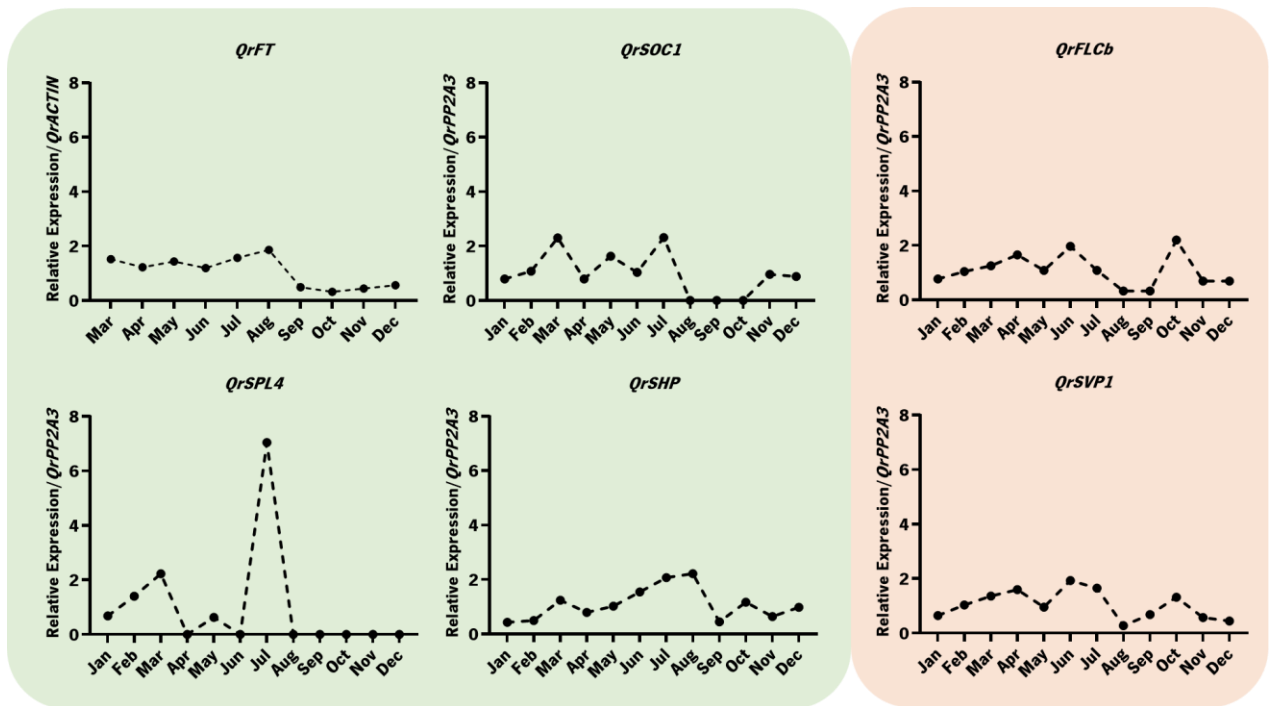


**Figure 17. Relative expression of potential flowering and bud dormancy regulator genes in *Q. robur* throughout 2021.** a)-d) Potential flower/bud development promoters. (a)- *QrFT* relative expression, with *QrACTIN* as the reference gene; b)- *QrSPL4* relative expression with *QrPP2A3* as the reference gene; c)- *QrSOC1* relative expression with *QrPP2A3* as the reference gene; d)- *QrSHP* relative expression with *QrPP2A3* as the reference gene.) e)-f) Potential flowering/dormancy release repressors. (e)- *QrFLCb* relative expression with *QrPP2A3* as the reference gene; f)- *QrSVP1* relative expression with *QrPP2A3* as the reference gene.) Relative expression levels were obtained by scanning the densitometry of the gel bands presented in Figure 12 using the ImageJ software.

Contrary to the remaining analyzed genes, *QrFT* expression was analyzed in leaf samples, since FT is thought to be mainly expressed in leaf tissues before being transported to the SAM (Abe et al., 2005; Wigge et al., 2005). *QrFT* was expressed throughout all samples (Fig. 17 – a). The months of January and February were absent in this analysis since no suitable leaf samples could be retrieved during this period in 2021. *QrFT* expression levels appear to be higher in spring and summer months (lanes 4 to 8, Fig. 17 – a) with the highest expression observed in August and declining in September, remaining low in the following autumn months. The expression pattern here observed is consistent with what is expected from a perennial tree, since FT is described in several woody perennial trees as a flowering and flower/bud

development promoter, and *QrFT* relative expression levels during phases of active development were higher than the ones observed in the months associated with growth cessation and dormancy. This is also consistent with the observed expression of *QsFT* in cork oak (Sobral et al., 2020), which further supports the functional conservation of *FT* genes in dormancy/growth regulation across Fagaceae trees. In Sobral et al., (2020), expression analysis in adult *Q. suber* leaf samples showed two *QsFT* expression peaks in March and August, while no *QsFT* expression peaks were observed in juvenile trees. This suggests that *QsFT* is involved in flower induction events, and that two such events could be occurring in *Q. suber*, one during the buds swelling phase, and other before growth cessation. Despite the mentioned difference, *QrFT* expression levels remained relatively similar throughout the active growth months with no significant expression peak being observed that could strongly point to any specific development or induction event as it was observed in *Q. suber* (Sobral et al., 2020). This does not necessarily rule out the possibility of multiple flower development events during *Q. robur* annual cycle since the observed expression of other flowering promoters, and the phenological observations in this study pointed otherwise. However, it is unlikely that such events would represent separate male and female flowering induction events, as suggested in *Q. suber*, since unlike the former, *Q. robur* flowers are neither unisexual by inception or have male and female flowering separated by months (Boavida et al., 2001; Sobral et al., 2020; Sobral & Costa, 2017; M. Varela et al., 2016).

Out of the 12 monthly samples analyzed, *QrSPL4* expression was only observed in January, February, March, May and July (Figure 17 b)). *QrSPL4* relative expression rises from January to February and reaches the first peak in March. *QrSPL4* was observed to be expressed again in May however with a low expression level, then peaking and registering the highest expression level in July. SPL clade VI genes in *A. thaliana* are suggested to promote flowering and floral meristem identity, by promoting the expression of *FT*, and floral meristem identity genes *LFY*, *API* and *FUL*. In Sobral et al., (2020), overexpression of *QsSPL4* lead to early flowering and increased *FT* expression in *A. thaliana* mutants, suggesting that the functions of *A. thaliana* clade VI *SPL* genes might be conserved in *Q. suber* and that *QsSPL4* might also be promoting flowering through *FT* upregulation. *Q. suber* adult bud samples differentially high *QsSPL4* expression levels reported in March also suggested that *QsSPL* could be involved in flower development during the buds swelling phase. Considering the observed *QrSPL4* expression peaks (Fig. 17 – b)), it is possible that they might also related to flowering induction events. The initial rise of *QrSPL4* relative expression in late winter culminating in the first peak in March might be associated with flower development during the buds swelling phase, as was reported in *Q. suber*, and

thus further suggesting a possible function conservation of these genes among these oaks and Fagaceae trees. Whereas the July peak could be related to a floral induction event in the newly formed buds. A sequencing of *QrSPL4* amplification product should however be conducted in future analysis to further confirm if the amplification observed here corresponds to a clade VI *SPL* gene, as no such gene was identified in the current databases, and if so, identify it.

*QrSOC1* was expressed in all samples except from August to October where no *QrSOC1* amplification was observed (Fig. 17- c)). Three peaks were observed in the relative expression *QrSOC1*, in March, May and July. Expression increases from January and peaks in March, then *QrSOC1* expression declines in April, rising again in May and July. As mentioned before, there is no *QrSOC1* expression from August until November and December when *QrSOC1* expression is observed again, yet at relatively low levels. *SOC1* is described in *A. thaliana* to promote flowering by, together with *AGL24*, activating *LFY* expression (J. Lee et al., 2008; J. Lee & Lee, 2010; C. Liu et al., 2008). The expression of *QrSOC1* observed is consistent with what was observed with *QrSPL4* with the first expression peak in March probably being related to a flower development in the buds swelling phase and the expression peak in July being related to a floral induction event before bud growth cessation.

The slight increase in relative expression observed in the May samples of both *QrSPL4* and *QrSOC1* were more subtle than the ones observed in March and July, however they could still prove to be relevant since both *QrSVP1* and *QrFLCb*, homologs of known repressor genes of *SOC1* expression in *A. thaliana*, registered a drop in their relative expression levels in May. Thus, the slight increase in *QrSPL4* and *QrSOC1* expression observed in May could possibly be indicating a flower induction or developmental event occurring in that month.

*QrFLCb* was observed to be expressed in all monthly samples. *QrFLCb* relative expression levels were observed to gradually increase from January to June (Fig. 17 – e)), except for May where *QrFLCb* expression slightly decreases. After the first expression peak in June, *QrFLCb* relative expression level drops in July and reaches the lowest values in August and September, before spiking to the highest expression level in October and returning to lower expression levels in November and December. *FLC* has been characterized in *A. thaliana* as an important flowering repressor, central to both autonomous and vernalization pathways, repressing *SOC1* and *FT* (Hepworth, 2002; Michaels & Amasino, 1999; Samach & Wigge, 2005; Searle et al., 2006). Several transcriptome and expression analysis studies in woody perennials have also pointed to role conservation of *FLC* homologs in the negative control of budbreak

and flowering (Díaz-Riquelme et al., 2012; G. Kumar et al., 2016; Voogd et al., 2022; T. Zhao et al., 2021). Regarding the expression pattern observed, it was expected that *QrFLCb* would have higher expression levels during the months of bud growth arrest and decreased with the progressive accumulation of cold temperature in the winter months. Despite the highest expression being observed in the October samples, which could possibly be related to bud dormancy set, *QrFLCb* expression was not differentially expressed between phases of bud growth and dormancy, even being slightly higher during months of bud growth. However, comparative analysis of *QrFLCb* and *QrSOC1* expression patterns during bud growth period could point to a possible conservation of the *QrFLCb* role in repressing *QrSOC1*, since the first expression peaks of *QrFLCb* were observed in April and June, months that corresponded to drops in the expression of *QrSOC1*. No obvious correlation between the expression patterns of *QrFLCb* and *QrFT* could be observed that would confirm *QrFLCb* repression of *QrFT*.

*QrSVP1* was expressed in all monthly samples (Fig 17 – f). Despite the observed drop in *QrSVP1* expression on the May sample, *QrSVP1* relative expression was observed to gradually increase from the beginning of the year until June, when the maximum relative expression was recorded. Expression levels were observed to remain relatively high in July, then, in August, *QrSVP1* expression drops to its lowest value, spiking again in October (Fig. 17 – f). *SVP* is described in *A. thaliana* to be a flowering repressor mainly repressing *FT* and *SOC1* expression, with *SVP*-like genes also being described in multiple perennial species as a potential repressor of dormancy release and bud break (Falavigna et al., 2019; C. Liu et al., 2009; X. Liu et al., 2018; R. Wu, Tomes, et al., 2017; R. Wu, Wang, et al., 2017; R.-M. Wu et al., 2012). Expression analysis of *SVP*-like genes has also been conducted in the closely related *Q. suber* with some *SVP* genes exhibiting expression spikes in September and October, supporting their role in growth cessation/dormancy induction and dormancy maintenance before bud break (Sobral et al., 2020 ).

*QrSVP1* expression peak in October might be comparable to the high *QsSVP1* expression level observed in cork oak in Sobral et al, (2020). This can be indicative of the conservation of *SVP1* role in dormancy establishment or as a repressor of dormancy release during the early stages of bud dormancy, amongst Fagaceae trees. However, the lower *QrSVP1* expression levels observed during late winter and relative higher expression levels observed from April to July, months associated with flowering induction events and meristem development, are at odds with the most commonly proposed role of *SVP* in flowering repression and dormancy maintenance. Recent studies have also reported up-regulation of *SVP*-like genes expression during active growth phases in other perennial species, specifically *P. mume* (Y. Li et al.,

2017), *P. avium* (J. Wang et al., 2021), *Poncirus trifoliata* (trifoliate orange) (Z.-M. Li et al., 2010) and mango (Mo et al., 2021). Moreover, overexpression of these genes in *A. thaliana* was observed to result in flower deformations for all of the species mentioned above, which points to a possible role of some *SVP* genes in flower organ development (Y. Li et al., 2017; Z.-M. Li et al., 2010; J. Wang et al., 2021). Curiously, despite the lack of data regarding the expression of *Q. suber SVP* genes during summer in Sobral et al., (2020), since the analysis was solely focused on dormancy periods, the over expression of *QsSVP4* similarly resulted in flower deformations. Adding to this, the fact that several of the proteins coded by the above-mentioned genes have been reported to interact with ABCDE genes further reinforces the suggestion for a role of *SVP*-like genes in flower development (Mo et al., 2021; R. Wu et al., 2014).

*QrSHP* relative expression was observed to be lower from January to February before displaying the first expression peak in March. *QrSHP* relative expression then gradually and consistently increases until August where the maximum relative expression level was observed, before plummeting in the September samples. Expression then rises in October, with *QrSHP* being consistently expressed throughout the remainder of the year (Fig. 17 – d).

The MADS-box class D gene, *SHP* is a floral organ identity gene associated in *A. thaliana* with female flower formation, necessary for conferring ovule identity to the flower meristematic cells (Liljgren et al., 2000; Pinyopich et al., 2003). *SHP* homologs have also been observed to be expressed during later stages of dormancy in multiple perennial species, including Chinese cherry (*Prunus pseudocerasus*), sweet cherry, peach, and apricot, suggesting that the floral differentiation progressively accompanies dormancy transition (Canton et al., 2021; Zhu et al., 2015). In the closely related *Q. suber*, *QsSHP* was observed to be involved in the formation of both female and male flowers, while also reported to be expressed during dormancy (Sobral et al., 2020). Thus, the expression pattern of *QrSHP*, specifically its expression during dormancy, seems to reinforce the suggestion of floral development being gradually induced with dormancy progression. Furthermore, the slightly higher expression observed in March and high expression levels during July and August further suggests a flowering induction event during the buds swelling phase and another before dormancy induction, as hinted by *QrSOC1* and *QrSPL4* relative expression patterns. Similarly to *QrSHP*, in Sobral et al, 2020, *QsSHP* was reported to have high expression levels before dormancy induction and during the buds swelling phase, further suggesting a possible conservation of *SHP* function between these two species and conceivably across other Fagaceae species.

It is, however, important to note that the semi-quantitative method used for expression analysis in this thesis does not produce the most accurate results, and before any significant conclusion is made, the analysis needs to be repeated to grant statistical significance to the results.

#### **4.4. Testing the interaction between *QsPI* promoter and *QsHTH***

For future Y1H assay analysis of the Protein–DNA interaction between *QsPI* and *QsHTH*, the cloning of *QsHTH* was performed for compatibility with the Matchmaker Gold Yeast One-Hybrid System kit (Clontech, USA). This Y1H assay consists in cloning a target DNA sequence, or bait sequence into the pAbai vector, (Fig. 18 - a)), which when transformed into the Y1H Gold yeast strain will integrate its genome by homologous recombination, (Fig. 19). This yeast strain also contains an inactive *ura3-52* locus that can only be repaired by homologous recombination with the wild type *URA3* gene present in the pAbai vector, therefore, successfully transformed Y1H Gold/pBait-Abai should grow in a yeast synthetic drop-out (SD) medium lacking Uracil (-URA). The candidate protein for DNA-binding, or prey protein, is cloned into a specific AD- prey plasmid, such as pGAD424 (Fig. 18 – b)), and it is expressed as a fusion protein containing the yeast GAL4 transcription activation domain (GAL4 AD). After transforming the AD-prey plasmid in the Bait strain, if the prey protein binds to the bait sequence, the GAL4 AD will activate the expression of AbA gene (*AUR-1C*), present in the pAbai, allowing cell growth on media containing the Aureobasidin A (AbA) cyclic depsipeptide antibiotic, which is toxic to yeast at low concentrations.

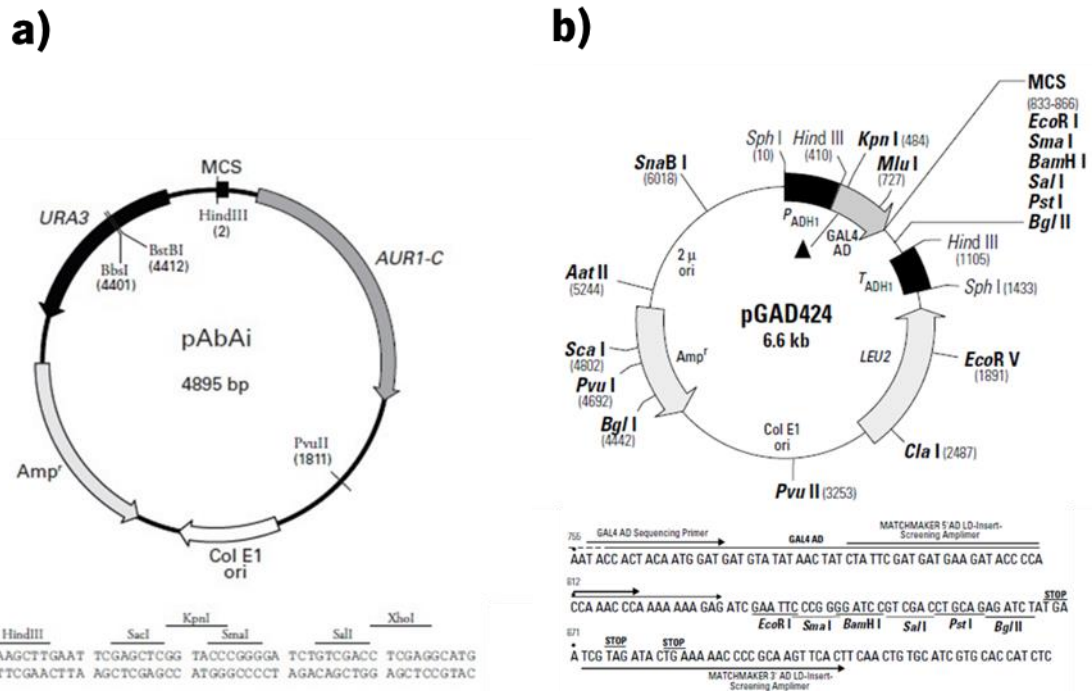


**Figure 18. Maps of the pAbAi and the pGAD424 Vectors.** a)- pAbAi. pAbAi is a yeast reporter vector, designed for use with the Matchmaker Gold Yeast One-Hybrid Library Screening System and can be used in one-hybrid assays to identify and characterize DNA-binding proteins. The vector contains a multiple cloning site (MCS; lower panel), the AUR1-C gene, an antibiotic resistance gene that confers resistance to Aureobasidin A (AbA), and the URA3 gene. b)- pGAD424. pGAD424 regenerates a hybrid protein containing a target sequence fused to the GAL4 activation domain, for Yeast One-Hybrid assays. pGAD424 contains a *ADHI* promoter, a MCS (lower panel), the GAL4 AD, *ADHI* transcription terminator signal and two antibiotic resistant genes that confer resistance to leucine (*LEU2*) and ampicillin (*bla*). Adapted from Clontech Laboratories (2012).

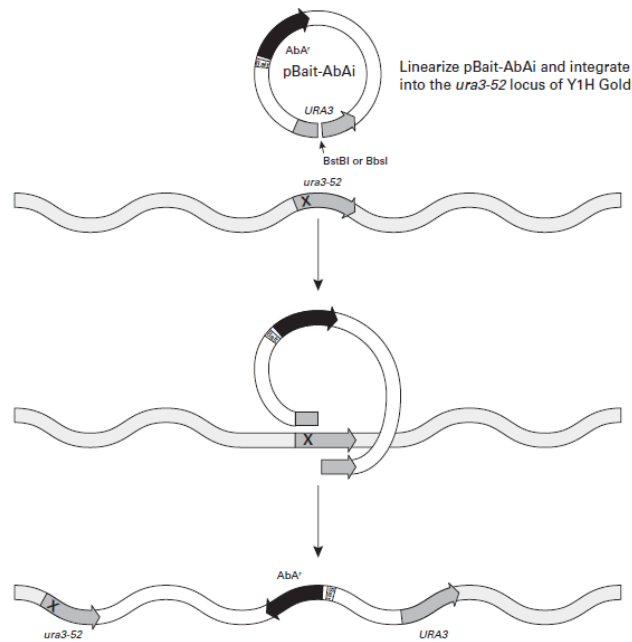


**Figure 19. Schematic representation of the bait strain creation.** The inactive *ura3-52* locus of Y1HGOLD is repaired by homologous recombination with the wild type *URA3* gene present in the pBait-AbAi vector. Transformation of Y1HGOLD with a pBait-AbAi vector linearized with BstBI or BbsI, results in colonies that can grow in the absence of uracil on SD/-Ura agar plates. Adapted from Clontech Laboratories, 2012.

#### 4.4.1. Cloning Qs HTH into pGAD424

In order to obtain the QsHTH fusion protein containing the yeast GAL4 AD, a plan was made to clone the Qs HTH protein coding sequence into the pGAD424 vector (Fig. 18 – b)). In this vector transcription is activated by the constitutive ADH1 promoter which will enable high expression levels of the fusion protein in yeast host cells. The MCS is located at the 3'- end of the GAL4 AD sequence open reading frame, allowing the protein of interest ligated into the MCS to be expressed as a fusion protein. Transcription stops at the ADH1 transcription termination signal.

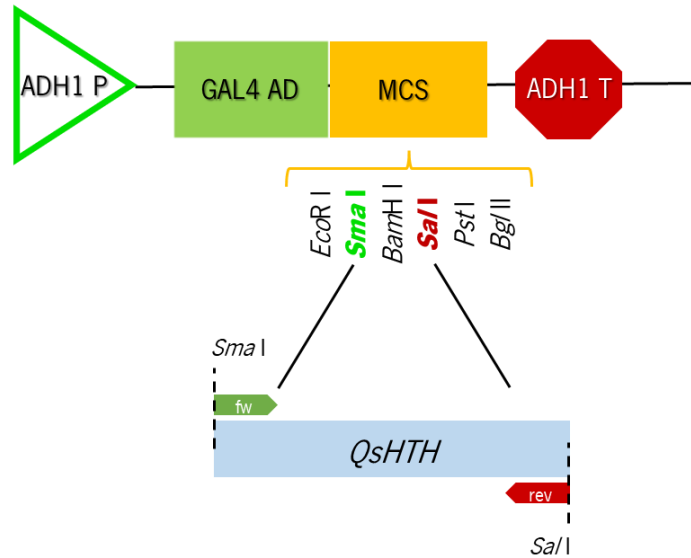


**Figure 20. Representation of the strategy employed for cloning *QsHTH* into pGAD424.** The pGAD424 plasmid contains within its sequence the ADH1 promoter, the GAL4 activation domain, a multiple cloning site, and the ADH1 terminator. Primers were designed to amplify the *QsHTH* coding sequence and to introduce the recognition sites for *Sma*I and *Sal*I restriction enzymes in the amplification products.

Primers were designed to amplify the entire open reading frame of *QsHTH* and to insert the restriction enzymes *Sma*I (5') and *Sal*I (3') recognition sites (Fig. 20). Amplification was carried out by PCR with NZYTaQ II 2× Green Master Mix, to reduce mutation risk, and the lower primer annealing temperature (48°C) was chosen. The expected amplification product size of 1.744kbp was observed in figure 21 – a). Because the Amplification of *QsHTH* was proving a difficult step to achieve, the *QsHTH* was extracted from the gel and purified (since another band of bigger size was present) and ligated to the pGEM-Teasy for a quick transformation in *E. coli* DH10B competent cells to safeguard the sequence. A colony PCR was done, and the two positive colonies, lanes 11 and 12 observed in figure 22, were stored as a glycerol stock.

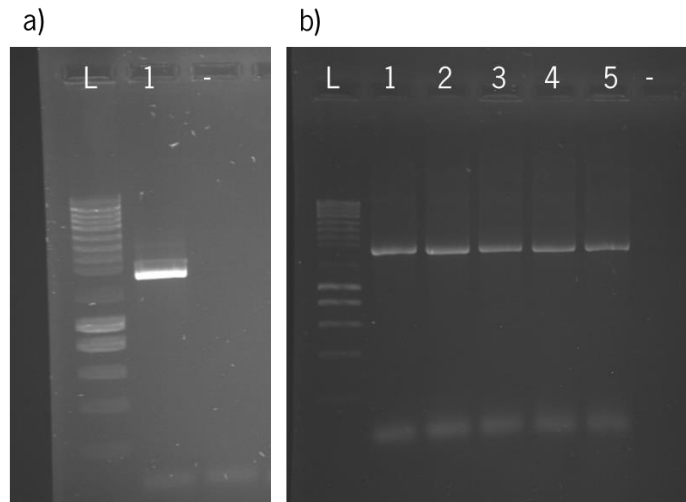


**Figure 21. PCR amplification of *QsHTH* open reading frame.** Amplification was carried out with the lower primer annealing temperature of 48°C. Electrophoresis run was performed with samples loaded into a 1.5 % agarose gel along with 1 kb Plus DNA Ladder (New England Biolabs) (L). The expected amplification product size of 1.744kbp is observed in lanes 1 in a) and lanes 1 to 5 in b).

A subsequent PCR was done with the same conditions using the remaining PCR product (15  $\mu$ L) distributed in 5 tubes (3  $\mu$ L each) in order to obtain a higher concentration of the amplification product (Fig 21 - b)). The PCR amplification products were added to the same tube following amplification, then purified and digested with *Sma*I and *Sal*I endonucleases. The pGAD424 vector was then also linearized with the same endonucleases and the digestion product purified.



**Figure 22. Colony PCR confirming *QsHTH* transformation into *E. coli* DH10 $\beta$  competent cells.** Amplification was carried out using the *QsHTH* forward and reverse primers, with 20 selected colonies (lanes 1-20) being used as template cDNA. The Electrophoresis run was performed with samples loaded into a 1.5 % agarose gel along with 1 kb Plus DNA Ladder (New England Biolabs) (L), and a negative control (-). Colonies 11 and 12 displayed the expected 1.744kbp amplification product.

The previously digested target sequence and pGAD424 vector were then ligated and transformed into *E. coli* DH10 $\beta$  competent cells along with two control situations, one consisting of the empty vector and the T4 ligase (Control 1) and another with only the empty vector (Control 2). The transformants were plated in selective medium containing ampicillin (100  $\mu\text{g mL}^{-1}$ ) and two colonies transformed with the pGAD424+*QsHTH* construct.

To screen for positive colonies and confirm the integration of the target sequence in the pGAD424 vector, a colony PCR was performed using the primers pGAD424 FW and pGAD424 REV, that flank the MCS of the plasmid, with the expected amplicon size of 1.895kbp. Both colonies were confirmed positive with the expected amplification product size observed (Fig. 23).

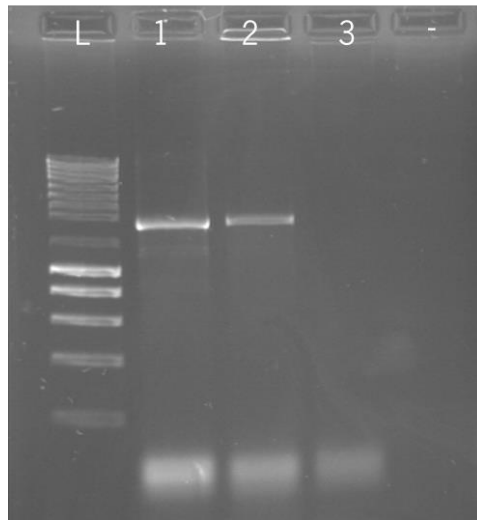


**Figure 23. Colony PCR confirming pGAD424+QsHTH transformation into *E. coli* DH10 $\beta$  competent cells.** Amplification was carried out using the pGAD424 forward and reverse primers, with the 3 colonies (lanes 1-3) being used as template cDNA. The Electrophoresis run was performed with samples loaded into a 1.5 % agarose gel along with 1 kb Plus DNA Ladder (New England Biolabs) (L), and a negative control (-). Colonies 1 and 2 both displayed the expected 1.895kbp amplification product.

#### 4.4.2. Integrating pAbai-F3pQsPI in Y1H Gold genome

A fragment of *QsPISTILLATA* promoter(F3p*QsPi*) region had already been previously cloned into the pAbai vector in an unpublished doctoral dissertation (H. Silva, 2018), and used in the construction of a smart cDNA library of potential interacting proteins where QsHTH was identified. The construct, that was stored in an *E. coli* XL1-Blue glycerol stock, was extracted, purified, and linearized with Bpil restriction enzyme for integration in the Y1H Gold's genome. Following the transformation of the digested pAbai-F3pQsPI plasmid into *Saccharomyces cerevisiae* Y1HGold strain competent cells, transformants were plated onto SD -ura selective medium and a Colony PCR was preformed to screen for positive colonies. The primers used for the colony PCR were pAbai FW and pAbai REV that flank the pAbai MCS and the expected amplification size of 879 bp was observed on lanes 14 and 15 Fig 23, confirming those colonies as positive for the integration of the pAbai-F3pQsPi in Y1H Gold genome.

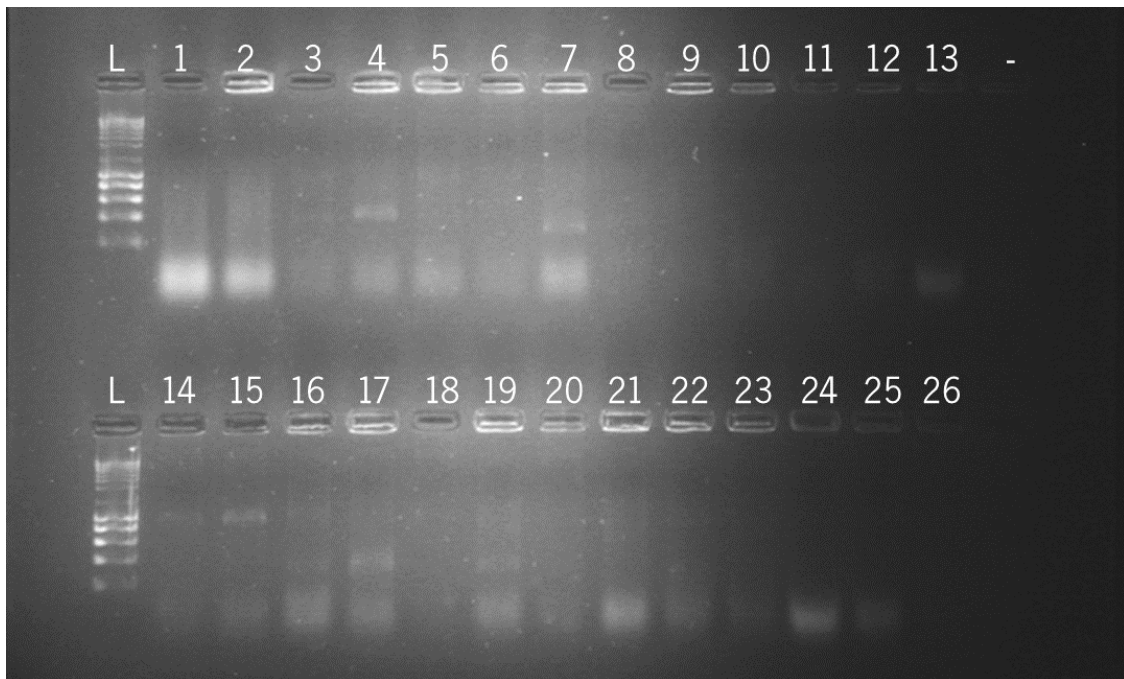


**Figure 24. Ccolony PCR confirming the integration of the pAbai+F3QsPI plasmid into Y1Hgold genome.** Amplification was carried out using the pAbai forward and reverse primers, with 26 selected colonies (lanes 1-26) being used as template cDNA. The Electrophoresis run was performed with samples loaded into a 1.5 % agarose gel along with 1 kb Plus DNA Ladder (New England Biolabs) (L), and a negative control ( - ). The yeast colonies represented in in lanes 14 and 15 both displayed the expected amplification product size of 879 bp.

The positive colony will have to be tested for the background Aureobasidin A resistance gene expression level, by plating in progressive concentration of Aureobasidin A and determining the minimum concentration at which the no growth was observed. Then, all required procedures will be concluded and the interaction between QsHTH and the promoter region of *QsPi* could finally be tested by transforming pGAD424+QsHTH in the yeast strain transformed with pAbai-F3pQsPi and plating it in the required selective medium, containing the minimum AbA concentration previously determined. If interaction between QsHTH and F3p*QsPi* occurs, then so will colony growth, while stronger interaction will result in greater growth, and vice versa.

## 5. Conclusion

Oak species such as *Q. robur* and *Q. suber* are not only cornerstone species in the forest ecosystems they inhabit, but also have been and will continue to be both economically and culturally important to the populations that rely on their resources. However, despite their relevance, there is still much to uncover regarding the regulatory mechanisms of these trees.

Regarding *Q. robur*, not much is currently known about the complex web of mechanisms and genetic pathways regulating its dormancy and flowering in response to environmental and endogenous signals. Thus, the identification and phylogenetic analysis of several *Q. robur* genes carried out in this thesis aimed to retrieve multiple potential flower and dormancy regulators. These genes are closely related to other previously identified genes, suggested as part of these pathways in *A. thaliana* and different perennial tree species. Regarding the identified genes, two potential flowering/growth promoters *QrFT*, *QrSOC1*, as well as *QrSPL4*, a clade VI *SPL* gene not yet characterized and amplified with *Q. suber* *SPL4* primers; and 2 flowering/growth repressors, *QrSVP1* and *QrFLCb*, were selected for expression analysis. Moreover, the study of the different *Q. robur* *SVP* homologs could also prove to be relevant in the understanding of the functional specification within the STMADS-11 family regarding flowering repression and flower development, as evidenced in the *SVP-like* and *DAM* genes of Rosaceae species (Jiménez et al., 2009; J. Liu et al., 2020; Xiang et al., 2016).

Nonetheless, multiple other genes were found to be potentially involved in these processes, and further expand our knowledge of them, particularly genes such as *QrTFL1*, *QrAGL19* and *QrSPL9*. Since only a few homologous genes have already been suggested to be involved in dormancy and/or flowering, with the role of these genes being largely unknown in perennial species, their study could provide an important framework for future studies aiming to further uncover these mechanisms.

Relative expression analysis revealed all potential flowering/growth promoters mentioned above (*QrFT*, *QrSPL4*, *QrSOC1*) to be up regulated during months associated with floral and vegetative growth. The *QrFT* expression drop observed in September and the low *FT* expression levels throughout fall and winter months could likely be indicating dormancy induction. Whereas *QrFT* relative expression remained relatively constant throughout the growing phase, *QrSPL4* and *QrSOC1* both displayed 2 expression peaks during the same period, registered in March and July.

Furthermore, relative expression analysis of *QrSHP*, homolog of a flower organ identity gene in *A. thaliana* also revealed a peak in March, as well as the highest expression levels during July and August. This coupled with the male catkin in early development observed inside an enclosed bud in August 2021 (Fig. 9 – b)), and the occurrence of summer flowering, observed in July 2022 (Fig. 9 – k)), strongly suggests that at least two flower induction or developmental events are taking place, one in the buds swelling phase, before bud burst, and another in summer, before growth arrest, with a possible third one related to the May samples. The expression of *QrSHP* during autumn and winter could also point to a gradual process of floral development integrated with dormancy release.

Regarding the expression analysis of potential floral repressors, both *QrSVP* and *QrFLCb* relative expression patterns were observed to be identical throughout the year. Despite both being described as floral repressors in *A. thaliana* and suggested to promote bud dormancy maintenance in several perennial species (Falavigna et al., 2019; G. Kumar et al., 2016; Y. Li et al., 2017; X. Liu et al., 2018; Michaels & Amasino, 1999; Voogd et al., 2022; J. Wang et al., 2021), *QrSVP1* and *QrFLCb* relative expression levels were observed to be higher during phases of active growth and flower development. Whereas both *QrSVP1* and *QrFLCb* showed an expression spike in October, that could be suggestive of dormancy induction. These high expression levels observed during spring and summer, backed by similar expression profiles and functional studies of *SVP*-like genes in other perennials, could possibly suggest a role for these genes in floral organ development. *QrSVP1* and *QrFLCb* highest expression levels during the vegetative growth phase correspond to the same monthly samples where *QrSOC1* expression was observed to decrease, which might suggest the conservation of *A. thaliana SVP* and *FLC* role in repressing *SOC1*.

However, it is important to highlight that more extensive research into these mechanisms is needed in order to better understand them and to construct a clearer picture of these pathways in *Q. robur*. For instance, a real time quantitative PCR analysis should be conducted in other to obtain more accurate results. More trees should also be analyzed in future studies, as well as repeating this analysis, to improve the statistical robustness of the results. Future studies in *Q. robur* dormancy and/or flowering associated genes, such as functional analysis with *A. thaliana* mutants and DNA binding assays to assert the interactions between these regulators, would also help to further discern their role in Dormancy and flowering.

The relative expression analysis conducted in this thesis was able to provide some insights into the regulatory web of genes responsible for the orchestration of bud dormancy and flowering, that could be

proven to be important to further uncover these mechanisms in *Q. robur* and to a larger extent, temperate perennial trees.

Concerning the flower reproductive identity of *Q. suber*, *QsHTH*, a potential regulator of *QsPi*, which has been suggested as responsible for male flower identity (Sobral et al., 2020; Sobral & Costa, 2017), was successfully cloned into a pGAD 424 vector. The promoter fragment of *QsPi*, where *QsHTH* is postulated to bind, was also successfully integrated into the Y1H gold *S. cerevisiae* genome in this thesis, thus providing all required components for testing the interaction of *QsHTH* and *QsPi* in a future Y1h assay.

Understanding the mechanisms underlying dormancy and flowering in ecologically and economically important Fagaceae trees such as *Q. robur* and *Q. suber* could prove to be fundamental in solving some of the future problems posed by the rapid climatic change and emergence of new diseases in such long-lived forest trees. In this thesis, several potential dormancy and flowering regulator genes were identified in *Q. robur*, with relative expression analysis suggesting the involvement of some in the processes approached here. The cloning of *QsHTH* as also helped laying groundwork for uncovering the mechanisms regulating *QPi*, and to extent, flower reproductive organ identity. To sum up, this thesis provided valuable insight into some of the processes coordinating bud dormancy and flowering in Fagaceae trees, however, extensive research is still needed into several diverse variables to better understand these complex webs of regulatory processes.

## 6. Bibliography

- Abe, M., Kobayashi, Y., Yamamoto, S., Daimon, Y., Yamaguchi, A., Ikeda, Y., Ichinoki, H., Notaguchi, M., Goto, K., & Araki, T. (2005). FD, a bZIP Protein Mediating Signals from the Floral Pathway Integrator FT at the Shoot Apex. *Science*, *309*(5737), 1052–1056. <https://doi.org/10.1126/science.1115983>
- Abe, M., Kosaka, S., Shibuta, M., Nagata, K., Uemura, T., Nakano, A., & Kaya, H. (2019). Transient activity of the florigen complex during the floral transition in *Arabidopsis thaliana*. *Development*, *146*(7). <https://doi.org/10.1242/dev.171504>
- Akiba, T., Hibara, K.-I., Kimura, F., Tsuda, K., Shibata, K., Ishibashi, M., Moriya, C., Nakagawa, K., Kurata, N., Itoh, J.-I., & Ito, Y. (2014). Organ fusion and defective shoot development in oni3 mutants of rice. *Plant and Cell Physiology*, *55*(1), 42–51. <https://doi.org/10.1093/pcp/pct154>
- Allard, A., Bink, M. C. A. M., Martinez, S., Kelner, J.-J., Legave, J.-M., di Guardo, M., Di Pierro, E. A., Laurens, F., van de Weg, E. W., & Costes, E. (2016). Detecting QTLs and putative candidate genes involved in budbreak and flowering time in an apple multiparental population. *Journal of Experimental Botany*, *67*(9), 2875–2888. <https://doi.org/10.1093/jxb/erw130>
- Anh Tuan, P., Bai, S., Saito, T., Imai, T., Ito, A., & Moriguchi, T. (2016). Involvement of *EARLY BUD-BREAK*, an AP2/ERF Transcription Factor Gene, in Bud Break in Japanese Pear (*Pyrus pyrifolia* Nakai) Lateral Flower Buds: Expression, Histone Modifications and Possible Target Genes. *Plant and Cell Physiology*, *57*(5), 1038–1047. <https://doi.org/10.1093/pcp/pcw041>
- Baskin, J. M., & Baskin, C. C. (2004). A classification system for seed dormancy. *Seed Science Research*, *14*(1), 1–16. <https://doi.org/10.1079/SSR2003150>
- Becker, A. (2003). The major clades of MADS-box genes and their role in the development and evolution of flowering plants. *Molecular Phylogenetics and Evolution*, *29*(3), 464–489. [https://doi.org/10.1016/S1055-7903\(03\)00207-0](https://doi.org/10.1016/S1055-7903(03)00207-0)
- BENEDICT, C., SKINNER, J. S., MENG, R., CHANG, Y., BHALERAO, R., HUNER, N. P. A., FINN, C. E., CHEN, T. H. H., & HURRY, V. (2006). The CBF1-dependent low temperature signalling pathway, regulon and increase in freeze tolerance are conserved in *Populus* spp. *Plant, Cell and Environment*, *29*(7), 1259–1272. <https://doi.org/10.1111/j.1365-3040.2006.01505.x>
- Bertin, R. I. (1993). Incidence of Monoecy and Dichogamy in Relation to Self-Fertilization in Angiosperms. *American Journal of Botany*, *80*(5), 557. <https://doi.org/10.2307/2445372>
- Bielenberg, D. G., Wang, Y. (Eileen), Li, Z., Zhebentyayeva, T., Fan, S., Reighard, G. L., Scorza, R., & Abbott, A. G. (2008). Sequencing and annotation of the evergrowing locus in peach [*Prunus persica* (L.) Batsch] reveals a cluster of six MADS-box transcription factors as candidate genes for regulation of terminal bud formation. *Tree Genetics & Genomes*, *4*(3), 495–507. <https://doi.org/10.1007/s11295-007-0126-9>

- Bielenberg, D. G., Wang, Y., Fan, S., Reighard, G. L., Scorza, R., & Abbott, A. G. (2004). A Deletion Affecting Several Gene Candidates is Present in the Evergrowing Peach Mutant. *Journal of Heredity*, *95*(5), 436–444. <https://doi.org/10.1093/jhered/esh057>
- Blázquez, M. A., Green, R., Nilsson, O., Sussman, M. R., & Weigel, D. (1998). Gibberellins Promote Flowering of Arabidopsis by Activating the *LEAFY* Promoter. *The Plant Cell*, *10*(5), 791–800. <https://doi.org/10.1105/tpc.10.5.791>
- Boavida, L. C., Silva, J. P., & Feijó, J. A. (2001). Sexual reproduction in the cork oak ( *Quercus suber* L). II. Crossing intra- and interspecific barriers. *Sexual Plant Reproduction*, *14*(3), 143–152. <https://doi.org/10.1007/s004970100100>
- Böhlenius, H., Huang, T., Charbonnel-Campaa, L., Brunner, A. M., Jansson, S., Strauss, S. H., & Nilsson, O. (2006). *CO/FT*Regulatory Module Controls Timing of Flowering and Seasonal Growth Cessation in Trees. *Science*, *312*(5776), 1040–1043. <https://doi.org/10.1126/science.1126038>
- Böhm, S. M., & Kalko, E. K. V. (2009). Patterns of resource use in an assemblage of birds in the canopy of a temperate alluvial forest. *Journal of Ornithology*, *150*(4), 799–814. <https://doi.org/10.1007/s10336-009-0401-7>
- Böhm, S. M., Wells, K., & Kalko, E. K. V. (2011). Top-Down Control of Herbivory by Birds and Bats in the Canopy of Temperate Broad-Leaved Oaks (*Quercus robur*). *PLoS ONE*, *6*(4), e17857. <https://doi.org/10.1371/journal.pone.0017857>
- Bowman, J. L., Alvarez, J., Weigel, D., Meyerowitz, E. M., & Smyth, D. R. (1993). Control of flower development in *Arabidopsis thaliana* by *APETALA1* and interacting genes. *Development*, *119*(3), 721–743. <https://doi.org/10.1242/dev.119.3.721>
- Bowman, J. L., Smyth, D. R., & Meyerowitz, E. M. (1989). Genes directing flower development in Arabidopsis. *The Plant Cell*, *1*(1), 37–52. <https://doi.org/10.1105/tpc.1.1.37>
- Brunner, A. M., Evans, L. M., Hsu, C.-Y., & Sheng, X. (2014). Vernalization and the chilling requirement to exit bud dormancy: shared or separate regulation? *Frontiers in Plant Science*, *5*. <https://doi.org/10.3389/fpls.2014.00732>
- Busov, V., Carneros, E., & Yakovlev, I. (2016). EARLY BUD-BREAK1 (EBB1) defines a conserved mechanism for control of bud-break in woody perennials. *Plant Signaling & Behavior*, *11*(2), e1073873. <https://doi.org/10.1080/15592324.2015.1073873>
- Cannon, C. H., Brendel, O., Deng, M., Hipp, A. L., Kremer, A., Kua, C.-S., Plomion, C., Romero-Severson, J., & Sork, V. L. (2018). Gaining a global perspective on Fagaceae genomic diversification and adaptation. *New Phytologist*, *218*(3), 894–897. <https://doi.org/10.1111/nph.15101>
- Canton, M., Forestan, C., Bonghi, C., & Varotto, S. (2021). Meta-analysis of RNA-Seq studies reveals genes with dominant functions during flower bud endo- to eco-dormancy transition in Prunus species. *Scientific Reports*, *11*(1), 13173. <https://doi.org/10.1038/s41598-021-92600-6>

- Cardon, G., Höhmann, S., Klein, J., Nettesheim, K., Saedler, H., & Huijser, P. (1999). Molecular characterisation of the Arabidopsis SBP-box genes. *Gene*, *237*(1), 91–104. [https://doi.org/10.1016/S0378-1119\(99\)00308-X](https://doi.org/10.1016/S0378-1119(99)00308-X)
- Castède, S., Campoy, J. A., Le Dantec, L., Quero-García, J., Barreneche, T., Wenden, B., & Dirlwanger, E. (2015). Mapping of Candidate Genes Involved in Bud Dormancy and Flowering Time in Sweet Cherry (*Prunus avium*). *PLOS ONE*, *10*(11), e0143250. <https://doi.org/10.1371/journal.pone.0143250>
- Caudullo, G., Welk, E., & San-Miguel-Ayanz, J. (2017). Chorological maps for the main European woody species. *Data in Brief*, *12*, 662–666. <https://doi.org/10.1016/j.dib.2017.05.007>
- Cavender-Bares, J., Fallon, B., González-Rodríguez, A., Hipp, A., Hoerner, F., Kaproth, M., Manos, P., Meireles, J., McVay, J., & Pearse, I. (2016). Diversity, Distribution and Ecosystem Services of the North American Oaks. *International Oaks*, No. 27, 37–48.
- Celton, J.-M., Martinez, S., Jammes, M.-J., Bechti, A., Salvi, S., Legave, J.-M., & Costes, E. (2011). Deciphering the genetic determinism of bud phenology in apple progenies: a new insight into chilling and heat requirement effects on flowering dates and positional candidate genes. *New Phytologist*, *192*(2), 378–392. <https://doi.org/10.1111/j.1469-8137.2011.03823.x>
- Cline, M. G., & Deppong, D. O. (1999). The Role of Apical Dominance in Paradormancy of Temperate Woody Plants: A Reappraisal. *Journal of Plant Physiology*, *155*(3), 350–356. [https://doi.org/10.1016/S0176-1617\(99\)80116-3](https://doi.org/10.1016/S0176-1617(99)80116-3)
- Coen, E. S., & Meyerowitz, E. M. (1991). The war of the whorls: genetic interactions controlling flower development. *Nature*, *353*(6339), 31–37. <https://doi.org/10.1038/353031a0>
- Conde, D., Le Gac, A., Perales, M., Dervinis, C., Kirst, M., Maury, S., González-Melendi, P., & Allona, I. (2017). Chilling-responsive DEMETER-LIKE DNA demethylase mediates in poplar bud break. *Plant, Cell & Environment*, *40*(10), 2236–2249. <https://doi.org/10.1111/pce.13019>
- Conde, D., Moreno-Cortés, A., Dervinis, C., Ramos-Sánchez, J. M., Kirst, M., Perales, M., González-Melendi, P., & Allona, I. (2017). Overexpression of DEMETER, a DNA demethylase, promotes early apical bud maturation in poplar. *Plant, Cell & Environment*, *40*(11), 2806–2819. <https://doi.org/10.1111/pce.13056>
- Considine, M. J., & Considine, J. A. (2016). On the language and physiology of dormancy and quiescence in plants. *Journal of Experimental Botany*, *67*(11), 3189–3203. <https://doi.org/10.1093/jxb/erw138>
- Conti, L., & Bradley, D. (2007). TERMINAL FLOWER1 Is a Mobile Signal Controlling *Arabidopsis* Architecture. *The Plant Cell*, *19*(3), 767–778. <https://doi.org/10.1105/tpc.106.049767>

- Cooke, J. E. K., ERIKSSON, M. E., & JUNTILLA, O. (2012). The dynamic nature of bud dormancy in trees: environmental control and molecular mechanisms. *Plant, Cell & Environment*, *35*(10), 1707–1728. <https://doi.org/10.1111/j.1365-3040.2012.02552.x>
- de la Fuente, L., Conesa, A., Lloret, A., Badenes, M. L., & Rios, G. (2015). Genome-wide changes in histone H3 lysine 27 trimethylation associated with bud dormancy release in peach. *Tree Genetics & Genomes*, *11*(3), 45. <https://doi.org/10.1007/s11295-015-0869-7>
- De Schepper, V., De Swaef, T., Bauweraerts, I., & Steppe, K. (2013). Phloem transport: a review of mechanisms and controls. *Journal of Experimental Botany*, *64*(16), 4839–4850. <https://doi.org/10.1093/jxb/ert302>
- Delpierre, N., Vitasse, Y., Chuine, I., Guillemot, J., Bazot, S., Rutishauser, T., & Rathgeber, C. B. K. (2016). Temperate and boreal forest tree phenology: from organ-scale processes to terrestrial ecosystem models. *Annals of Forest Science*, *73*(1), 5–25. <https://doi.org/10.1007/s13595-015-0477-6>
- Díaz-Riquelme, J., Grimplet, J., Martínez-Zapater, J. M., & Carmona, M. J. (2012). Transcriptome variation along bud development in grapevine (*Vitis vinifera*L.). *BMC Plant Biology*, *12*(1), 181. <https://doi.org/10.1186/1471-2229-12-181>
- do Amaral Franco, J., & da Luz da Rocha Afonso, M. (1994). *Nova flora de Portugal. 3,1: Alismataceae - Iridaceae*. Sociedade Astória.
- Doğramacı, M., Horvath, D. P., Chao, W. S., Foley, M. E., Christoffers, M. J., & Anderson, J. V. (2010). Low temperatures impact dormancy status, flowering competence, and transcript profiles in crown buds of leafy spurge. *Plant Molecular Biology*, *73*(1–2), 207–226. <https://doi.org/10.1007/s11103-010-9621-8>
- Dorca-Fornell, C., Gregis, V., Grandi, V., Coupland, G., Colombo, L., & Kater, M. M. (2011). The Arabidopsis SOC1-like genes AGL42, AGL71 and AGL72 promote flowering in the shoot apical and axillary meristems. *The Plant Journal*, *67*(6), 1006–1017. <https://doi.org/10.1111/j.1365-313X.2011.04653.x>
- Eaton, E., Caudullo, G., Oliveira, S., & de Rigo, D. (2016). *Quercus robur* and *Quercus petraea* in Europe: distribution, habitat, usage and threats. In J. San-Miguel-Ayanz, D. de Rigo, G. Caudullo, T. Houston Durrant, & A. Mauri (Eds.), *European Atlas of Forest Tree Species*. Publ. Off. EU, Luxembourg, pp. e01c6df+.
- Edgar, R. C. (2004). MUSCLE: multiple sequence alignment with high accuracy and high throughput. *Nucleic Acids Research*, *32*(5), 1792–1797. <https://doi.org/10.1093/nar/gkh340>
- Eriksson, M. E., Hoffman, D., Kaduk, M., Mauriat, M., & Moritz, T. (2015). Transgenic hybrid aspen trees with increased gibberellin ( <sc>GA</sc> ) concentrations suggest that <sc>GA</sc> acts in parallel with <sc>FLOWERING LOCUS T</sc> 2 to control shoot elongation. *New Phytologist*, *205*(3), 1288–1295. <https://doi.org/10.1111/nph.13144>

- Fadón, E., Fernandez, E., Behn, H., & Luedeling, E. (2020). A Conceptual Framework for Winter Dormancy in Deciduous Trees. *Agronomy*, *10*(2), 241. <https://doi.org/10.3390/agronomy10020241>
- Fadón, E., Herrero, M., & Rodrigo, J. (2018). Dormant Flower Buds Actively Accumulate Starch over Winter in Sweet Cherry. *Frontiers in Plant Science*, *9*. <https://doi.org/10.3389/fpls.2018.00171>
- Falavigna, V. da S., Guitton, B., Costes, E., & Andrés, F. (2019). I Want to (Bud) Break Free: The Potential Role of DAM and SVP-Like Genes in Regulating Dormancy Cycle in Temperate Fruit Trees. *Frontiers in Plant Science*, *9*. <https://doi.org/10.3389/fpls.2018.01990>
- Fang, Y., Hu, J., Xu, J., Yu, H., Shi, Z., Xiong, G., Zhu, L., Zeng, D., Zhang, G., Gao, Z., Dong, G., Yan, M., Guo, L., Wang, Y., & Qian, Q. (2015). Identification and characterization of *Mini1*, a gene regulating rice shoot development. *Journal of Integrative Plant Biology*, *57*(2), 151–161. <https://doi.org/10.1111/jipb.12230>
- Fernandez, E., Cuneo, I. F., Luedeling, E., Alvarado, L., Farias, D., & Saa, S. (2019). Starch and hexoses concentrations as physiological markers in dormancy progression of sweet cherry twigs. *Trees*, *33*(4), 1187–1201. <https://doi.org/10.1007/s00468-019-01855-0>
- Flanagan, C. A., Hu, Y., & Ma, H. (1996). Specific expression of the AGL1 MADS-box gene suggests regulatory functions in Arabidopsis gynoecium and ovule development. *The Plant Journal*, *10*(2), 343–353. <https://doi.org/10.1046/j.1365-313X.1996.10020343.x>
- Foley, M. E., Anderson, J. V., & Horvath, D. P. (2009). The effects of temperature, photoperiod, and vernalization on regrowth and flowering competence in *Euphorbia esula* (Euphorbiaceae) crown buds. *Botany*, *87*(10), 986–992. <https://doi.org/10.1139/B09-055>
- FOSTER, T. (2003). A Morphological and Quantitative Characterization of Early Floral Development in Apple (*Malus x domestica* Borkh.). *Annals of Botany*, *92*(2), 199–206. <https://doi.org/10.1093/aob/mcg120>
- Fu, Y. S. H., Campioli, M., Vitasse, Y., De Boeck, H. J., Van den Berge, J., AbdElgawad, H., Asard, H., Piao, S., Deckmyn, G., & Janssens, I. A. (2014). Variation in leaf flushing date influences autumnal senescence and next year's flushing date in two temperate tree species. *Proceedings of the National Academy of Sciences*, *111*(20), 7355–7360. <https://doi.org/10.1073/pnas.1321727111>
- Gabay, G., Dahan, Y., Izhaki, Y., Isaacson, Tal, Elkind, Y., Ben-Ari, G., & Flaishman, M. A. (2017). Identification of QTLs associated with spring vegetative budbreak time after dormancy release in pear (*Pyrus communis* L.). *Plant Breeding*, *136*(5), 749–758. <https://doi.org/10.1111/pbr.12499>
- Gassmann, M., Grenacher, B., Rohde, B., & Vogel, J. (2009). Quantifying Western blots: Pitfalls of densitometry. *ELECTROPHORESIS*, *30*(11), 1845–1855. <https://doi.org/10.1002/elps.200800720>

- Gil, L., & Varela, M. (2008a). EUFORGEN Technical Guidelines for genetic conservation and use for cork oak (*Quercus suber*). *Biodiversity International, Rome, Italy*, 1–6.
- Gil, L., & Varela, M. C. (2008b). Technical guidelines for genetic conservation and use \_CORK OAK. *EUFORGEN, EUFORGEN*.
- Hanano, S., & Goto, K. (2011). *Arabidopsis* TERMINAL FLOWER1 Is Involved in the Regulation of Flowering Time and Inflorescence Development through Transcriptional Repression . *The Plant Cell*, *23*(9), 3172–3184. <https://doi.org/10.1105/tpc.111.088641>
- Harder, L. D., Barrett, S. C. H., & Cole, W. W. (2000). The mating consequences of sexual segregation within inflorescences of flowering plants. *Proceedings of the Royal Society of London. Series B: Biological Sciences*, *267*(1441), 315–320. <https://doi.org/10.1098/rspb.2000.1002>
- Hartmann, U., Hohmann, S., Nettesheim, K., Wisman, E., Saedler, H., & Huijser, P. (2000). Molecular cloning of SVP: a negative regulator of the floral transition in *Arabidopsis*. *The Plant Journal*, *21*(4), 351–360. <https://doi.org/10.1046/j.1365-313x.2000.00682.x>
- Heide, O. M., & Prestrud, A. K. (2005). Low temperature, but not photoperiod, controls growth cessation and dormancy induction and release in apple and pear. *Tree Physiology*, *25*(1), 109–114. <https://doi.org/10.1093/treephys/25.1.109>
- Hepworth, S. R. (2002). Antagonistic regulation of flowering-time gene SOC1 by CONSTANS and FLC via separate promoter motifs. *The EMBO Journal*, *21*(16), 4327–4337. <https://doi.org/10.1093/emboj/cdf432>
- Horvath, D. (2009). Common mechanisms regulate flowering and dormancy. *Plant Science*, *177*(6), 523–531. <https://doi.org/10.1016/j.plantsci.2009.09.002>
- Horvath, D. P., Anderson, J. V., Chao, W. S., & Foley, M. E. (2003). Knowing when to grow: signals regulating bud dormancy. *Trends in Plant Science*, *8*(11), 534–540. <https://doi.org/10.1016/j.tplants.2003.09.013>
- Horvath, D. P., Chao, W. S., Suttle, J. C., Thimmapuram, J., & Anderson, J. V. (2008). Transcriptome analysis identifies novel responses and potential regulatory genes involved in seasonal dormancy transitions of leafy spurge (*Euphorbia esula* L.). *BMC Genomics*, *9*(1), 536. <https://doi.org/10.1186/1471-2164-9-536>
- Hsu, C.-Y., Adams, J. P., Kim, H., No, K., Ma, C., Strauss, S. H., Drnevich, J., Vandervelde, L., Ellis, J. D., Rice, B. M., Wickett, N., Gunter, L. E., Tuskan, G. A., Brunner, A. M., Page, G. P., Barakat, A., Carlson, J. E., dePamphilis, C. W., Luthe, D. S., & Yuceer, C. (2011). *FLOWERING LOCUS T* duplication coordinates reproductive and vegetative growth in perennial poplar. *Proceedings of the National Academy of Sciences*, *108*(26), 10756–10761. <https://doi.org/10.1073/pnas.1104713108>
- <https://www.arbolapp.es/en/species/info/quercus-suber/>. (n.d.).

<https://www.euforgen.org/species/quercus-robur/>. (n.d.).

<https://www.euforgen.org/species/quercus-suber/>. (n.d.).

<https://www.ncbi.nlm.nih.gov/>. (n.d.).

Instituto Português do Mar e da Atmosfera, I. P. D. de C. e A. C. (2022). *Boletim Climatológico Mensal – Janeiro 2022*.

Irish, V. F., & Sussex, I. M. (1990). Function of the *apetala-1* gene during *Arabidopsis* floral development. *The Plant Cell*, 2(8), 741–753. <https://doi.org/10.1105/tpc.2.8.741>

Iwafuchi-Doi, M., & Zaret, K. S. (2014). Pioneer transcription factors in cell reprogramming. *Genes & Development*, 28(24), 2679–2692. <https://doi.org/10.1101/gad.253443.114>

Jiménez, S., Lawton-Rauh, A. L., Reighard, G. L., Abbott, A. G., & Bielenberg, D. G. (2009). Phylogenetic analysis and molecular evolution of the dormancy associated MADS-box genes from peach. *BMC Plant Biology*, 9(1), 81. <https://doi.org/10.1186/1471-2229-9-81>

Jin, R., Klasfeld, S., Zhu, Y., Fernandez Garcia, M., Xiao, J., Han, S.-K., Konkol, A., & Wagner, D. (2021). LEAFY is a pioneer transcription factor and licenses cell reprogramming to floral fate. *Nature Communications*, 12(1), 626. <https://doi.org/10.1038/s41467-020-20883-w>

Jones, D. T., Taylor, W. R., & Thornton, J. M. (1992). The rapid generation of mutation data matrices from protein sequences. *Bioinformatics*, 8(3), 275–282. <https://doi.org/10.1093/bioinformatics/8.3.275>

Junttila, O., & Jensen, E. (1988). Gibberellins and photoperiodic control of shoot elongation in *Salix*. *Physiologia Plantarum*, 74(2), 371–376. <https://doi.org/10.1111/j.1399-3054.1988.tb00645.x>

Kardailsky, I., Shukla, V. K., Ahn, J. H., Dagenais, N., Christensen, S. K., Nguyen, J. T., Chory, J., Harrison, M. J., & Weigel, D. (1999). Activation Tagging of the Floral Inducer *FT*. *Science*, 286(5446), 1962–1965. <https://doi.org/10.1126/science.286.5446.1962>

Karlgren, A., Gyllenstrand, N., Källman, T., Sundström, J. F., Moore, D., Lascoux, M., & Lagercrantz, U. (2011a). Evolution of the PEBP Gene Family in Plants: Functional Diversification in Seed Plant Evolution. *Plant Physiology*, 156(4), 1967–1977. <https://doi.org/10.1104/pp.111.176206>

Karlgren, A., Gyllenstrand, N., Källman, T., Sundström, J. F., Moore, D., Lascoux, M., & Lagercrantz, U. (2011b). Evolution of the PEBP Gene Family in Plants: Functional Diversification in Seed Plant Evolution. *Plant Physiology*, 156(4), 1967–1977. <https://doi.org/10.1104/pp.111.176206>

Kawagoe, T., & Suzuki, N. (2005). Self-Pollen on a Stigma Interferes with Outcrossed Seed Production in a Self-Incompatible Monoecious Plant, *Akebia quinata* (Lardizabalaceae). *Functional Ecology*, 19(1), 49–54. <http://www.jstor.org/stable/3599270>

- Kim, D.-H., Doyle, M. R., Sung, S., & Amasino, R. M. (2009). Vernalization: Winter and the Timing of Flowering in Plants. *Annual Review of Cell and Developmental Biology*, *25*(1), 277–299. <https://doi.org/10.1146/annurev.cellbio.042308.113411>
- Kitamura, Y., Takeuchi, T., Yamane, H., & Tao, R. (2016). Simultaneous down-regulation of *DORMANCY-ASSOCIATED MADS-box6* and *SOC1* during dormancy release in Japanese apricot (*Prunus mume*) flower buds. *The Journal of Horticultural Science and Biotechnology*, *91*(5), 476–482. <https://doi.org/10.1080/14620316.2016.1173524>
- Klein, J., Saedler, H., & Huijser, P. (1996). A new family of DNA binding proteins includes putative transcriptional regulators of the *Antirrhinum majus* floral meristem identity gene *SQUAMOSA*. *Molecular and General Genetics MGG*, *250*(1), 7–16. <https://doi.org/10.1007/BF02191820>
- Kobayashi, Y., Kaya, H., Goto, K., Iwabuchi, M., & Araki, T. (1999). A Pair of Related Genes with Antagonistic Roles in Mediating Flowering Signals. *Science*, *286*(5446), 1960–1962. <https://doi.org/10.1126/science.286.5446.1960>
- Kobayashi, Y., & Weigel, D. (2007). Move on up, it's time for change—mobile signals controlling photoperiod-dependent flowering. *Genes & Development*, *21*(19), 2371–2384. <https://doi.org/10.1101/gad.1589007>
- Krolkowski, K. A., Victor, J. L., Wagler, T. N., Lolle, S. J., & Pruitt, R. E. (2003). Isolation and characterization of the *Arabidopsis* organ fusion gene *HOTHEAD*. *The Plant Journal*, *35*(4), 501–511. <https://doi.org/10.1046/j.1365-313X.2003.01824.x>
- Kropat, J., Tottey, S., Birkenbihl, R. P., Depège, N., Huijser, P., & Merchant, S. (2005). A regulator of nutritional copper signaling in *Chlamydomonas* is an SBP domain protein that recognizes the GTAC core of copper response element. *Proceedings of the National Academy of Sciences*, *102*(51), 18730–18735. <https://doi.org/10.1073/pnas.0507693102>
- Kumar, G., Arya, P., Gupta, K., Randhawa, V., Acharya, V., & Singh, A. K. (2016). Comparative phylogenetic analysis and transcriptional profiling of MADS-box gene family identified DAM and FLC-like genes in apple (*Malus domestica*). *Scientific Reports*, *6*(1), 20695. <https://doi.org/10.1038/srep20695>
- Kumar, S., Stecher, G., Li, M., Knyaz, C., & Tamura, K. (2018). MEGA X: Molecular Evolutionary Genetics Analysis across Computing Platforms. *Molecular Biology and Evolution*, *35*(6), 1547–1549. <https://doi.org/10.1093/molbev/msy096>
- Kumar, S. V., Lucyshyn, D., Jaeger, K. E., Alós, E., Alvey, E., Harberd, N. P., & Wigge, P. A. (2012). Transcription factor PIF4 controls the thermosensory activation of flowering. *Nature*, *484*(7393), 242–245. <https://doi.org/10.1038/nature10928>
- Kumar, S. V., & Wigge, P. A. (2010). H2A.Z-Containing Nucleosomes Mediate the Thermosensory Response in *Arabidopsis*. *Cell*, *140*(1), 136–147. <https://doi.org/10.1016/j.cell.2009.11.006>

- Kurokura, T., Mimida, N., Battey, N. H., & Hytönen, T. (2013). The regulation of seasonal flowering in the Rosaceae. *Journal of Experimental Botany*, *64*(14), 4131–4141. <https://doi.org/10.1093/jxb/ert233>
- Clontech Laboratories. (2012). *Matchmaker® Gold Yeast One-Hybrid Library Screening System User Manual*. [www.clontech.com](http://www.clontech.com)
- Lai, X., Blanc-Mathieu, R., GrandVuillemin, L., Huang, Y., Stigliani, A., Lucas, J., Thévenon, E., Loue-Manifel, J., Turchi, L., Daher, H., Brun-Hernandez, E., Vachon, G., Latrasse, D., Benhamed, M., Dumas, R., Zubieta, C., & Parcy, F. (2021). The LEAFY floral regulator displays pioneer transcription factor properties. *Molecular Plant*, *14*(5), 829–837. <https://doi.org/10.1016/j.molp.2021.03.004>
- Lang, G. A. (1987). Dormancy: A New Universal Terminology. *HortScience*, *22*(5), 817–820. <https://doi.org/10.21273/HORTSCI.22.5.817>
- Lang, G. A., Early, J. D., Martin, G. C., & Darnell, R. L. (1987). Endo-, Para-, and Ecodormancy: Physiological Terminology and Classification for Dormancy Research. *HortScience*, *22*(3), 371–377. <https://doi.org/10.21273/HORTSCI.22.3.371>
- Lee, H., Suh, S.-S., Park, E., Cho, E., Ahn, J. H., Kim, S.-G., Lee, J. S., Kwon, Y. M., & Lee, I. (2000). The AGAMOUS-LIKE 20 MADS domain protein integrates floral inductive pathways in *Arabidopsis*. *Genes & Development*, *14*(18), 2366–2376. <https://doi.org/10.1101/gad.813600>
- Lee, J. H., Yoo, S. J., Park, S. H., Hwang, I., Lee, J. S., & Ahn, J. H. (2007). Role of *SVP* in the control of flowering time by ambient temperature in *Arabidopsis*. *Genes & Development*, *21*(4), 397–402. <https://doi.org/10.1101/gad.1518407>
- Lee, J., & Lee, I. (2010). Regulation and function of SOC1, a flowering pathway integrator. *Journal of Experimental Botany*, *61*(9), 2247–2254. <https://doi.org/10.1093/jxb/erq098>
- Lee, J., Oh, M., Park, H., & Lee, I. (2008). SOC1 translocated to the nucleus by interaction with AGL24 directly regulates *LEAFY*. *The Plant Journal*, *55*(5), 832–843. <https://doi.org/10.1111/j.1365-313X.2008.03552.x>
- Li, C., & Lu, S. (2014). Molecular characterization of the SPL gene family in *Populus trichocarpa*. *BMC Plant Biology*, *14*(1), 131. <https://doi.org/10.1186/1471-2229-14-131>
- Li, D., Liu, C., Shen, L., Wu, Y., Chen, H., Robertson, M., Helliwell, C. A., Ito, T., Meyerowitz, E., & Yu, H. (2008). A Repressor Complex Governs the Integration of Flowering Signals in *Arabidopsis*. *Developmental Cell*, *15*(1), 110–120. <https://doi.org/10.1016/j.devcel.2008.05.002>
- Li, J., Xu, Y., Niu, Q., He, L., Teng, Y., & Bai, S. (2018). Abscisic Acid (ABA) Promotes the Induction and Maintenance of Pear (*Pyrus pyrifolia* White Pear Group) Flower Bud Endodormancy. *International Journal of Molecular Sciences*, *19*(1), 310. <https://doi.org/10.3390/ijms19010310>

- Li, Y., Xu, Z., Yang, W., Cheng, T., Wang, J., & Zhang, Q. (2016). Isolation and Functional Characterization of SOC1-like Genes in *Prunus mume*. *Journal of the American Society for Horticultural Science*, *141*(4), 315–326. <https://doi.org/10.21273/JASHS.141.4.315>
- Li, Y., Zhou, Y., Yang, W., Cheng, T., Wang, J., & Zhang, Q. (2017). Isolation and functional characterization of SVP-like genes in *Prunus mume*. *Scientia Horticulturae*, *215*, 91–101. <https://doi.org/10.1016/j.scienta.2016.12.013>
- Li, Z.-M., Zhang, J.-Z., Mei, L., Deng, X.-X., Hu, C.-G., & Yao, J.-L. (2010). PtSVP, an SVP homolog from trifoliolate orange (*Poncirus trifoliata* L. Raf.), shows seasonal periodicity of meristem determination and affects flower development in transgenic *Arabidopsis* and tobacco plants. *Plant Molecular Biology*, *74*(1–2), 129–142. <https://doi.org/10.1007/s11103-010-9660-1>
- Liljgren, S. J., Ditta, G. S., Eshed, Y., Savidge, B., Bowman, J. L., & Yanofsky, M. F. (2000). SHATTERPROOF MADS-box genes control seed dispersal in *Arabidopsis*. *Nature*, *404*(6779), 766–770. <https://doi.org/10.1038/35008089>
- Liljgren, S. J., Gustafson-Brown, C., Pinyopich, A., Ditta, G. S., & Yanofsky, M. F. (1999). Interactions among *APETALA1*, *LEAFY*, and *TERMINAL FLOWER1* Specify Meristem Fate. *The Plant Cell*, *11*(6), 1007–1018. <https://doi.org/10.1105/tpc.11.6.1007>
- Lin, M.-K., Belanger, H., Lee, Y.-J., Varkonyi-Gasic, E., Taoka, K.-I., Miura, E., Xoconostle-Cázares, B., Gendler, K., Jorgensen, R. A., Phinney, B., Lough, T. J., & Lucas, W. J. (2007). FLOWERING LOCUS T Protein May Act as the Long-Distance Florigenic Signal in the Cucurbits. *The Plant Cell*, *19*(5), 1488–1506. <https://doi.org/10.1105/tpc.107.051920>
- Liu, C., Chen, H., Er, H. L., Soo, H. M., Kumar, P. P., Han, J.-H., Liou, Y. C., & Yu, H. (2008). Direct interaction of *AGL24* and *SOC1* integrates flowering signals in *Arabidopsis*. *Development*, *135*(8), 1481–1491. <https://doi.org/10.1242/dev.020255>
- Liu, C., Xi, W., Shen, L., Tan, C., & Yu, H. (2009). Regulation of Floral Patterning by Flowering Time Genes. *Developmental Cell*, *16*(5), 711–722. <https://doi.org/10.1016/j.devcel.2009.03.011>
- Liu, J., Ren, M., Chen, H., Wu, S., Yan, H., Jalal, A., & Wang, C. (2020). Evolution of *SHORT VEGETATIVE PHASE* ( *SVP* ) genes in Rosaceae: Implications of lineage-specific gene duplication events and function diversifications with respect to their roles in processes other than bud dormancy. *The Plant Genome*, *13*(3). <https://doi.org/10.1002/tpg2.20053>
- Liu, X., Sun, Z., Dong, W., Wang, Z., & Zhang, L. (2018). Expansion and Functional Divergence of the *SHORT VEGETATIVE PHASE* ( *SVP* ) Genes in Eudicots. *Genome Biology and Evolution*, *10*(11), 3026–3037. <https://doi.org/10.1093/gbe/evy235>
- Liu, Z., Wu, X., Cheng, M., Xie, Z., Xiong, C., Zhang, S., Wu, J., & Wang, P. (2020). Identification and functional characterization of SOC1-like genes in *Pyrus bretschneideri*. *Genomics*, *112*(2), 1622–1632. <https://doi.org/10.1016/j.ygeno.2019.09.011>

- Liu, Z., Zhu, H., & Abbott, A. (2015). Dormancy Behaviors and Underlying Regulatory Mechanisms: From Perspective of Pathways to Epigenetic Regulation. In *Advances in Plant Dormancy* (pp. 75–105). Springer International Publishing. [https://doi.org/10.1007/978-3-319-14451-1\\_4](https://doi.org/10.1007/978-3-319-14451-1_4)
- Lloret, A., Badenes, M. L., & Ríos, G. (2018a). Modulation of Dormancy and Growth Responses in Reproductive Buds of Temperate Trees. *Frontiers in Plant Science*, *9*. <https://doi.org/10.3389/fpls.2018.01368>
- Lloret, A., Badenes, M. L., & Ríos, G. (2018b). Modulation of Dormancy and Growth Responses in Reproductive Buds of Temperate Trees. *Frontiers in Plant Science*, *9*. <https://doi.org/10.3389/fpls.2018.01368>
- Lundell, R., Hänninen, H., Saarinen, T., Åström, H., & Zhang, R. (2020). Beyond rest and quiescence (endodormancy and ecodormancy): A novel model for quantifying plant–environment interaction in bud dormancy release. *Plant, Cell & Environment*, *43*(1), 40–54. <https://doi.org/10.1111/pce.13650>
- Marañón, T., & Muñoz-Rojas, M. (2012). *Oak trees and woodlands providing ecosystem services in Southern Spain Novel approaches for harnessing native soil microbial communities to restore biodiverse degraded ecosystems in drylands View project Analysis of nutrient cycles in oak forests affected by decline: linking community changes with ecosystem functioning View project*. <https://www.researchgate.net/publication/259298749>
- Marum, L., Miguel, A., Ricardo, C. P., & Miguel, C. (2012). Correction: Reference Gene Selection for Quantitative Real-time PCR Normalization in *Quercus suber*. *PLoS ONE*, *7*(9). <https://doi.org/10.1371/annotation/13c5a136-9db4-43a9-aad3-f73acb064d0a>
- Meetings*. (2012). <http://colloque4.inra.fr/iufro2012>
- Melzer, S., Lens, F., Gennen, J., Vanneste, S., Rohde, A., & Beeckman, T. (2008). Flowering-time genes modulate meristem determinacy and growth form in *Arabidopsis thaliana*. *Nature Genetics*, *40*(12), 1489–1492. <https://doi.org/10.1038/ng.253>
- Menzel, A., SPARKS, T. H., ESTRELLA, N., KOCH, E., AASA, A., AHAS, R., ALM-KÜBLER, K., BISSOLLI, P., BRASLAVSKÁ, O., BRIEDE, A., CHMIELEWSKI, F. M., CREPINSEK, Z., CURNEL, Y., DAHL, Å., DEFILA, C., DONNELLY, A., FILELLA, Y., JATCZAK, K., MÅGE, F., ... ZUST, A. (2006). European phenological response to climate change matches the warming pattern. *Global Change Biology*, *12*(10), 1969–1976. <https://doi.org/10.1111/j.1365-2486.2006.01193.x>
- Mhamdi, A., & Van Breusegem, F. (2018). Reactive oxygen species in plant development. *Development*, *145*(15). <https://doi.org/10.1242/dev.164376>
- Michaels, S. D., & Amasino, R. M. (1999). *FLOWERING LOCUS C* Encodes a Novel MADS Domain Protein That Acts as a Repressor of Flowering. *The Plant Cell*, *11*(5), 949–956. <https://doi.org/10.1105/tpc.11.5.949>

- Michaels, S. D., & Amasino, R. M. (2001). Loss of *FLOWERING LOCUS C* Activity Eliminates the Late-Flowering Phenotype of *FRIGIDA* and Autonomous Pathway Mutations but Not Responsiveness to Vernalization. *The Plant Cell*, *13*(4), 935–941. <https://doi.org/10.1105/tpc.13.4.935>
- Michaels, S. D., Himelblau, E., Kim, S. Y., Schomburg, F. M., & Amasino, R. M. (2005). Integration of Flowering Signals in Winter-Annual Arabidopsis. *Plant Physiology*, *137*(1), 149–156. <https://doi.org/10.1104/pp.104.052811>
- Mimida, N., Goto, K., Kobayashi, Y., Araki, T., Ahn, J. H., Weigel, D., Murata, M., Motoyoshi, F., & Sakamoto, W. (2001). Functional divergence of the *TFL1*-like gene family in *Arabidopsis* revealed by characterization of a novel homologue. *Genes to Cells*, *6*(4), 327–336. <https://doi.org/10.1046/j.1365-2443.2001.00425.x>
- Mo, X., Luo, C., Yu, H., Chen, J., Liu, Y., Xie, X., Fan, Z., & He, X. (2021). Isolation and Functional Characterization of Two SHORT VEGETATIVE PHASE Homologous Genes from Mango. *International Journal of Molecular Sciences*, *22*(18), 9802. <https://doi.org/10.3390/ijms22189802>
- Mohamed, R., Wang, C.-T., Ma, C., Shevchenko, O., Dye, S. J., Puzey, J. R., Etherington, E., Sheng, X., Meilan, R., Strauss, S. H., & Brunner, A. M. (2010). Populus CEN/TFL1 regulates first onset of flowering, axillary meristem identity and dormancy release in Populus. *The Plant Journal*, *62*(4), 674–688. <https://doi.org/10.1111/j.1365-313X.2010.04185.x>
- Moon, J., Lee, H., Kim, M., & Lee, I. (2005). Analysis of Flowering Pathway Integrators in Arabidopsis. *Plant and Cell Physiology*, *46*(2), 292–299. <https://doi.org/10.1093/pcp/pci024>
- Moon, J., Suh, S.-S., Lee, H., Choi, K.-R., Hong, C. B., Paek, N.-C., Kim, S.-G., & Lee, I. (2003). The *SOC1* MADS-box gene integrates vernalization and gibberellin signals for flowering in *Arabidopsis*. *The Plant Journal*, *35*(5), 613–623. <https://doi.org/10.1046/j.1365-313X.2003.01833.x>
- Morin, X., Roy, J., Sonié, L., & Chuine, I. (2010). Changes in leaf phenology of three European oak species in response to experimental climate change. *New Phytologist*, *186*(4), 900–910. <https://doi.org/10.1111/j.1469-8137.2010.03252.x>
- Natividade, J. V. (1950). Subercultura. *Ministério Da Economia - Direção Geral Dos Serviços Florestais e Aquícolas*. Lisboa., 101–104.
- Ng, M., & Yanofsky, M. F. (2001). Activation of the Arabidopsis B Class Homeotic Genes by *APETALA1*. *The Plant Cell*, *13*(4), 739–753. <https://doi.org/10.1105/tpc.13.4.739>
- Niu, Q., Li, J., Cai, D., Qian, M., Jia, H., Bai, S., Hussain, S., Liu, G., Teng, Y., & Zheng, X. (2016). Dormancy-associated MADS-box genes and microRNAs jointly control dormancy transition in pear (*Pyrus pyrifolia* white pear group) flower bud. *Journal of Experimental Botany*, *67*(1), 239–257. <https://doi.org/10.1093/jxb/erv454>
- Pařenicová, L., de Folter, S., Kieffer, M., Horner, D. S., Favalli, C., Busscher, J., Cook, H. E., Ingram, R. M., Kater, M. M., Davies, B., Angenent, G. C., & Colombo, L. (2003). Molecular and Phylogenetic

- Analyses of the Complete MADS-Box Transcription Factor Family in Arabidopsis. *The Plant Cell*, 15(7), 1538–1551. <https://doi.org/10.1105/tpc.011544>
- Parmesan, C. (2007). Influences of species, latitudes and methodologies on estimates of phenological response to global warming. *Global Change Biology*, 13(9), 1860–1872. <https://doi.org/10.1111/j.1365-2486.2007.01404.x>
- Pelaz, S., Ditta, G. S., Baumann, E., Wisman, E., & Yanofsky, M. F. (2000). B and C floral organ identity functions require SEPALLATA MADS-box genes. *Nature*, 405(6783), 200–203. <https://doi.org/10.1038/35012103>
- Pérez, F. J., Vergara, R., & Or, E. (2009). On the mechanism of dormancy release in grapevine buds: a comparative study between hydrogen cyanamide and sodium azide. *Plant Growth Regulation*, 59(2), 145–152. <https://doi.org/10.1007/s10725-009-9397-5>
- Pinyopich, A., Ditta, G. S., Savidge, B., Liljegren, S. J., Baumann, E., Wisman, E., & Yanofsky, M. F. (2003). Assessing the redundancy of MADS-box genes during carpel and ovule development. *Nature*, 424(6944), 85–88. <https://doi.org/10.1038/nature01741>
- Preston, J. C., & Hileman, L. C. (2013). Functional Evolution in the Plant SQUAMOSA-PROMOTER BINDING PROTEIN-LIKE (SPL) Gene Family. *Frontiers in Plant Science*, 4. <https://doi.org/10.3389/fpls.2013.00080>
- Quesada-Traver, C., Lloret, A., Carretero-Paulet, L., Badenes, M. L., & Ríos, G. (2022). Evolutionary origin and functional specialization of Dormancy-Associated MADS box (DAM) proteins in perennial crops. *BMC Plant Biology*, 22(1), 473. <https://doi.org/10.1186/s12870-022-03856-7>
- Ramos, A., Pérez-Solís, E., Ibáñez, C., Casado, R., Collada, C., Gómez, L., Aragoncillo, C., & Allona, I. (2005). Winter disruption of the circadian clock in chestnut. *Proceedings of the National Academy of Sciences*, 102(19), 7037–7042. <https://doi.org/10.1073/pnas.0408549102>
- Rede DRAPN. (n.d.). *Leituras meteorológicas e parâmetros agrometeorológicos diários*. . <https://Drapnsiapd.Utad.Pt/Sia/Meteorologia/Leituras>.
- Richard Southwood, T. E., WINT, G. R., KENNEDY, C. E. J., & GREENWOOD, S. R. (2004). Seasonality, abundance, species richness and specificity of the phytophagous guild of insects on oak (*Quercus*) canopies. *European Journal of Entomology*, 101(1), 43–50. <https://doi.org/10.14411/eje.2004.011>
- Riese, M., Höhmann, S., Saedler, H., Münster, T., & Huijser, P. (2007). Comparative analysis of the SBP-box gene families in *P. patens* and seed plants. *Gene*, 401(1–2), 28–37. <https://doi.org/10.1016/j.gene.2007.06.018>
- Rinne, P. L. H., Welling, A., Vahala, J., Ripel, L., Ruonala, R., Kangasjärvi, J., & van der Schoot, C. (2011a). Chilling of Dormant Buds Hyperinduces *FLOWERING LOCUS T* and Recruits GA-Inducible 1,3-β-

- Glucanases to Reopen Signal Conduits and Release Dormancy in *Populus*. *The Plant Cell*, *23*(1), 130–146. <https://doi.org/10.1105/tpc.110.081307>
- Rinne, P. L. H., Welling, A., Vahala, J., Ripel, L., Ruonala, R., Kangasjärvi, J., & van der Schoot, C. (2011b). Chilling of Dormant Buds Hyperinduces *FLOWERING LOCUS T* and Recruits GA-Inducible 1,3- $\beta$ -Glucanases to Reopen Signal Conduits and Release Dormancy in *Populus*. *The Plant Cell*, *23*(1), 130–146. <https://doi.org/10.1105/tpc.110.081307>
- Rives, J., Fernandez-Rodriguez, I., Rieradevall, J., & Gabarrell, X. (2013). Integrated environmental analysis of the main cork products in southern Europe (Catalonia – Spain). *Journal of Cleaner Production*, *51*, 289–298. <https://doi.org/10.1016/j.jclepro.2013.01.015>
- Rocheta, M., Sobral, R., Magalhães, J., Amorim, M. I., Ribeiro, T., Pinheiro, M., Egas, C., Morais-Cecílio, L., & Costa, M. M. R. (2014). Comparative transcriptomic analysis of male and female flowers of monoecious *Quercus suber*. *Frontiers in Plant Science*, *5*. <https://doi.org/10.3389/fpls.2014.00599>
- Rodriguez-A., J., Sherman, W. B., Scorza, R., Wisniewski, M., & Okie, W. R. (1994). 'Evergreen' Peach, Its Inheritance and Dormant Behavior. *Journal of the American Society for Horticultural Science*, *119*(4), 789–792. <https://doi.org/10.21273/JASHS.119.4.789>
- Rogers, R. (2004). TEMPERATE ECOSYSTEMS | Fagaceae. In *Encyclopedia of Forest Sciences* (pp. 1419–1427). Elsevier. <https://doi.org/10.1016/B0-12-145160-7/00192-7>
- Rohde, A., & Bhalerao, R. P. (2007). Plant dormancy in the perennial context. *Trends in Plant Science*, *12*(5), 217–223. <https://doi.org/10.1016/j.tplants.2007.03.012>
- Rohde, A., Prinsen, E., De Rycke, R., Engler, G., Van Montagu, M., & Boerjan, W. (2002). PtABI3 Impinges on the Growth and Differentiation of Embryonic Leaves during Bud Set in Poplar. *The Plant Cell*, *14*(8), 1885–1901. <https://doi.org/10.1105/tpc.003186>
- Saito, T., Bai, S., Ito, A., Sakamoto, D., Saito, T., Ubi, B. E., Imai, T., & Moriguchi, T. (2013). Expression and genomic structure of the dormancy-associated MADS box genes MADS13 in Japanese pears (*Pyrus pyrifolia* Nakai) that differ in their chilling requirement for endodormancy release. *Tree Physiology*, *33*(6), 654–667. <https://doi.org/10.1093/treephys/tpt037>
- Salinas, M., Xing, S., Höhmann, S., Berndtgen, R., & Huijser, P. (2012). Genomic organization, phylogenetic comparison and differential expression of the SBP-box family of transcription factors in tomato. *Planta*, *235*(6), 1171–1184. <https://doi.org/10.1007/s00425-011-1565-y>
- Samach, A., Onouchi, H., Gold, S. E., Ditta, G. S., Schwarz-Sommer, Z., Yanofsky, M. F., & Coupland, G. (2000). Distinct Roles of CONSTANS Target Genes in Reproductive Development of *Arabidopsis*. *Science*, *288*(5471), 1613–1616. <https://doi.org/10.1126/science.288.5471.1613>
- Samach, A., & Wigge, P. A. (2005). Ambient temperature perception in plants. *Current Opinion in Plant Biology*, *8*(5), 483–486. <https://doi.org/10.1016/j.pbi.2005.07.011>

- Sande Silva, J. (2007). *Os carvalhais: um património a conservar*. Fundação Luso-Americana, etc.
- Santamaría, M. E., Rodríguez, R., Cañal, M. J., & Toorop, P. E. (2011). Transcriptome analysis of chestnut (*Castanea sativa*) tree buds suggests a putative role for epigenetic control of bud dormancy. *Annals of Botany*, *108*(3), 485–498. <https://doi.org/10.1093/aob/mcr185>
- Santamaría, M., Hasbún, R., Valera, M., Meijón, M., Valledor, L., Rodríguez, J. L., Toorop, P. E., Cañal, M., & Rodríguez, R. (2009). Acetylated H4 histone and genomic DNA methylation patterns during bud set and bud burst in *Castanea sativa*. *Journal of Plant Physiology*, *166*(13), 1360–1369. <https://doi.org/10.1016/j.jplph.2009.02.014>
- Sasaki, R., Yamane, H., Ooka, T., Jotatsu, H., Kitamura, Y., Akagi, T., & Tao, R. (2011). Functional and Expressional Analyses of *PmDAM* Genes Associated with Endodormancy in Japanese Apricot. *Plant Physiology*, *157*(1), 485–497. <https://doi.org/10.1104/pp.111.181982>
- Schneider, C. A., Rasband, W. S., & Eliceiri, K. W. (2012). NIH Image to ImageJ: 25 years of image analysis. *Nature Methods*, *9*(7), 671–675. <https://doi.org/10.1038/nmeth.2089>
- Schultz, E. A., & Haughn, G. W. (1993). Genetic analysis of the floral initiation process (FLIP) in *Arabidopsis*. *Development*, *119*(3), 745–765. <https://doi.org/10.1242/dev.119.3.745>
- Searle, I., He, Y., Turck, F., Vincent, C., Fornara, F., Kröber, S., Amasino, R. A., & Coupland, G. (2006). The transcription factor FLC confers a flowering response to vernalization by repressing meristem competence and systemic signaling in *Arabidopsis*. *Genes & Development*, *20*(7), 898–912. <https://doi.org/10.1101/gad.373506>
- Shannon, S., & Meeks-Wagner, D. R. (1993). Genetic Interactions That Regulate Inflorescence Development in *Arabidopsis*. *The Plant Cell*, 639–655. <https://doi.org/10.1105/tpc.5.6.639>
- Sheldon, C. C., Burn, J. E., Perez, P. P., Metzger, J., Edwards, J. A., Peacock, W. J., & Dennis, E. S. (1999). The *FLF* MADS Box Gene: A Repressor of Flowering in *Arabidopsis* Regulated by Vernalization and Methylation. *The Plant Cell*, *11*(3), 445–458. <https://doi.org/10.1105/tpc.11.3.445>
- Shindo, C., Aranzana, M. J., Lister, C., Baxter, C., Nicholls, C., Nordborg, M., & Dean, C. (2005). Role of *FRIGIDA* and *FLOWERING LOCUS C* in Determining Variation in Flowering Time of *Arabidopsis*. *Plant Physiology*, *138*(2), 1163–1173. <https://doi.org/10.1104/pp.105.061309>
- Silva, H. (2018). *Characterization of flower induction and fertilization of Quercus suber* [Unpublished doctoral dissertation]. Universidade do Minho.
- Silva, H. G., Sobral, R. S., Magalhães, A. P., Morais-Cecílio, L., & Costa, M. M. R. (2020). Genome-Wide Identification of Epigenetic Regulators in *Quercus suber* L. *International Journal of Molecular Sciences*, *21*(11), 3783. <https://doi.org/10.3390/ijms21113783>

- Simpson, G. G., & Dean, C. (2002). *Arabidopsis*, the Rosetta Stone of Flowering Time? *Science*, *296*(5566), 285–289. <https://doi.org/10.1126/science.296.5566.285>
- Simpson, M. G. (2010). Diversity and Classification of Flowering Plants: Eudicots. In *Plant Systematics* (pp. 275–448). Elsevier. <https://doi.org/10.1016/B978-0-12-374380-0.50008-7>
- Singh, R. K., Bhalerao, R. P., & Eriksson, M. E. (2021). Growing in time: exploring the molecular mechanisms of tree growth. *Tree Physiology*, *41*(4), 657–678. <https://doi.org/10.1093/treephys/tpaa065>
- Singh, R. K., Maurya, J. P., Azeez, A., Miskolczi, P., Tylewicz, S., Stojkovič, K., Delhomme, N., Busov, V., & Bhalerao, R. P. (2018). A genetic network mediating the control of bud break in hybrid aspen. *Nature Communications*, *9*(1), 4173. <https://doi.org/10.1038/s41467-018-06696-y>
- Singh, R. K., Miskolczi, P., Maurya, J. P., & Bhalerao, R. P. (2019). A Tree Ortholog of SHORT VEGETATIVE PHASE Floral Repressor Mediates Photoperiodic Control of Bud Dormancy. *Current Biology*, *29*(1), 128-133.e2. <https://doi.org/10.1016/j.cub.2018.11.006>
- Singh, R. K., Svystun, T., AlDahmash, B., Jönsson, A. M., & Bhalerao, R. P. (2017). Photoperiod- and temperature-mediated control of phenology in trees – a molecular perspective. *New Phytologist*, *213*(2), 511–524. <https://doi.org/10.1111/nph.14346>
- Sobral, R., & Costa, M. M. R. (2017). Role of floral organ identity genes in the development of unisexual flowers of *Quercus suber* L. *Scientific Reports*, *7*(1), 10368. <https://doi.org/10.1038/s41598-017-10732-0>
- Sobral, R., Silva, H. G., Laranjeira, S., Magalhães, J., Andrade, L., Alinho, A. T., & Costa, M. M. R. (2020). Unisexual flower initiation in the monoecious *Quercus suber* L.: a molecular approach. *Tree Physiology*, *40*(9), 1260–1276. <https://doi.org/10.1093/treephys/tpaa061>
- Soufi, A., Garcia, M. F., Jaroszewicz, A., Osman, N., Pellegrini, M., & Zaret, K. S. (2015). Pioneer Transcription Factors Target Partial DNA Motifs on Nucleosomes to Initiate Reprogramming. *Cell*, *161*(3), 555–568. <https://doi.org/10.1016/j.cell.2015.03.017>
- Tanino, K. K., Kalcsits, L., Silim, S., Kendall, E., & Gray, G. R. (2010). Temperature-driven plasticity in growth cessation and dormancy development in deciduous woody plants: a working hypothesis suggesting how molecular and cellular function is affected by temperature during dormancy induction. *Plant Molecular Biology*, *73*(1–2), 49–65. <https://doi.org/10.1007/s11103-010-9610-y>
- Theissen, G., & Melzer, R. (2007). Molecular Mechanisms Underlying Origin and Diversification of the Angiosperm Flower. *Annals of Botany*, *100*(3), 603–619. <https://doi.org/10.1093/aob/mcm143>
- Tuan, P. A., Bai, S., Saito, T., Ito, A., & Moriguchi, T. (2017). Dormancy-Associated MADS-Box (DAM) and the Abscisic Acid Pathway Regulate Pear Endodormancy Through a Feedback Mechanism. *Plant and Cell Physiology*, *58*(8), 1378–1390. <https://doi.org/10.1093/pcp/pcx074>

- Tylewicz, S., Petterle, A., Marttila, S., Miskolczi, P., Azeez, A., Singh, R. K., Immanen, J., Mähler, N., Hvidsten, T. R., Eklund, D. M., Bowman, J. L., Helariutta, Y., & Bhalerao, R. P. (2018). Photoperiodic control of seasonal growth is mediated by ABA acting on cell-cell communication. *Science*, *360*(6385), 212–215. <https://doi.org/10.1126/science.aan8576>
- Tylewicz, S., Tsuji, H., Miskolczi, P., Petterle, A., Azeez, A., Jonsson, K., Shimamoto, K., & Bhalerao, R. P. (2015). Dual role of tree florigen activation complex component *FD* in photoperiodic growth control and adaptive response pathways. *Proceedings of the National Academy of Sciences*, *112*(10), 3140–3145. <https://doi.org/10.1073/pnas.1423440112>
- Valverde, F., Mouradov, A., Soppe, W., Ravenscroft, D., Samach, A., & Coupland, G. (2004). Photoreceptor Regulation of CONSTANS Protein in Photoperiodic Flowering. *Science*, *303*(5660), 1003–1006. <https://doi.org/10.1126/science.1091761>
- Van Benthem, F., Clarke, G. C. S., & Punt, W. (1984). Fagaceae. *Review of Palaeobotany and Palynology*, *42*(1–4), 87–110. [https://doi.org/10.1016/0034-6667\(84\)90063-0](https://doi.org/10.1016/0034-6667(84)90063-0)
- van Dyk, M. M., Soeker, M. K., Labuschagne, I. F., & Rees, D. J. G. (2010). Identification of a major QTL for time of initial vegetative budbreak in apple (*Malus x domestica* Borkh.). *Tree Genetics & Genomes*, *6*(3), 489–502. <https://doi.org/10.1007/s11295-009-0266-1>
- Varela, M. C., & Valdivieso, T. (1996). Phenological phases of *Quercus suber* L. flowering. *Forest Genetics*, *3*, 93–102.
- Varela, M., Valdivieso, T., Novelli, E., & Trindade, C. (2016). Flower Bud Differentiation in *Quercus suber* L. *South-East European Forestry*, *7*(1). <https://doi.org/10.15177/seeefor.16-02>
- Vergara, R., Noriega, X., Aravena, K., Prieto, H., & Pérez, F. J. (2017). ABA Represses the Expression of Cell Cycle Genes and May Modulate the Development of Endodormancy in Grapevine Buds. *Frontiers in Plant Science*, *8*. <https://doi.org/10.3389/fpls.2017.00812>
- Vila-Viçosa, C. M., Capelo, J. H., Alves, P., Almeida, R. S., & Vázquez, F. M. (2022). New annotated checklist of the Portuguese oaks (*Quercus* L., Fagaceae). *Mediterranean Botany, Online first*, 1–46. <https://doi.org/10.5209/mbot.79286>
- Voogd, C., Brian, L. A., Wu, R., Wang, T., Allan, A. C., & Varkonyi-Gasic, E. (2022). A MADS-box gene with similarity to *FLC* is induced by cold and correlated with epigenetic changes to control budbreak in kiwifruit. *New Phytologist*, *233*(5), 2111–2126. <https://doi.org/10.1111/nph.17916>
- Wang, D., Gao, Z., Du, P., Xiao, W., Tan, Q., Chen, X., Li, L., & Gao, D. (2016). Expression of ABA Metabolism-Related Genes Suggests Similarities and Differences Between Seed Dormancy and Bud Dormancy of Peach (*Prunus persica*). *Frontiers in Plant Science*, *6*. <https://doi.org/10.3389/fpls.2015.01248>
- Wang, J., Jiu, S., Xu, Y., Sabir, I. A., Wang, L., Ma, C., Xu, W., Wang, S., & Zhang, C. (2021). SVP-like gene PavSVP potentially suppressing flowering with PavSEP, PavAP1, and PavJONITLESS in sweet

- cherries (*Prunus avium* L.). *Plant Physiology and Biochemistry*, *159*, 277–284. <https://doi.org/10.1016/j.plaphy.2020.12.013>
- Weigel, D., Alvarez, J., Smyth, D. R., Yanofsky, M. F., & Meyerowitz, E. M. (1992). LEAFY controls floral meristem identity in *Arabidopsis*. *Cell*, *69*(5), 843–859. [https://doi.org/10.1016/0092-8674\(92\)90295-N](https://doi.org/10.1016/0092-8674(92)90295-N)
- Wen, L. H., Zhong, W. J., Huo, X. M., Zhuang, W. B., Ni, Z. J., & Gao, Z. H. (2016). Expression analysis of ABA- and GA-related genes during four stages of bud dormancy in Japanese apricot (*Prunus mume* Sieb. et Zucc). *The Journal of Horticultural Science and Biotechnology*, *91*(4), 362–369. <https://doi.org/10.1080/14620316.2016.1160546>
- Westerberg, L. M., Mohammadi, U. H., Bergman, K.-O., & Milberg, P. (2017). Spatial pattern of occurrence of epiphytic lichens on oaks in a heterogeneous landscape. *Acta Oecologica*, *84*, 64–71. <https://doi.org/10.1016/j.actao.2017.09.005>
- Wigge, P. A., Kim, M. C., Jaeger, K. E., Busch, W., Schmid, M., Lohmann, J. U., & Weigel, D. (2005). Integration of Spatial and Temporal Information During Floral Induction in *Arabidopsis*. *Science*, *309*(5737), 1056–1059. <https://doi.org/10.1126/science.1114358>
- Wilkinson, M., Eaton, E. L., & Morison, J. I. L. (2017). Variation in the date of budburst in *Quercus robur* and *Q. petraea* across a range of provenances grown in Southern England. *European Journal of Forest Research*, *136*(1), 1–12. <https://doi.org/10.1007/s10342-016-0998-z>
- Wisniewski, M., Norelli, J., & Artlip, T. (2015). Overexpression of a peach CBF gene in apple: a model for understanding the integration of growth, dormancy, and cold hardiness in woody plants. *Frontiers in Plant Science*, *6*. <https://doi.org/10.3389/fpls.2015.00085>
- Wu, R., Tomes, S., Karunairetnam, S., Tustin, S. D., Hellens, R. P., Allan, A. C., Macknight, R. C., & Varkonyi-Gasic, E. (2017). SVP-like MADS Box Genes Control Dormancy and Budbreak in Apple. *Frontiers in Plant Science*, *08*. <https://doi.org/10.3389/fpls.2017.00477>
- Wu, R., Wang, T., McGie, T., Voogd, C., Allan, A. C., Hellens, R. P., & Varkonyi-Gasic, E. (2014). Overexpression of the kiwifruit SVP3 gene affects reproductive development and suppresses anthocyanin biosynthesis in petals, but has no effect on vegetative growth, dormancy, or flowering time. *Journal of Experimental Botany*, *65*(17), 4985–4995. <https://doi.org/10.1093/jxb/eru264>
- Wu, R., Wang, T., Warren, B. A. W., Allan, A. C., Macknight, R. C., & Varkonyi-Gasic, E. (2017). Kiwifruit SVP2 gene prevents premature budbreak during dormancy. *Journal of Experimental Botany*, *68*(5), 1071–1082. <https://doi.org/10.1093/jxb/erx014>
- Wu, R.-M., Walton, E. F., Richardson, A. C., Wood, M., Hellens, R. P., & Varkonyi-Gasic, E. (2012). Conservation and divergence of four kiwifruit SVP-like MADS-box genes suggest distinct roles in kiwifruit bud dormancy and flowering. *Journal of Experimental Botany*, *63*(2), 797–807. <https://doi.org/10.1093/jxb/err304>

- Wu, S.-W., Kumar, R., Iswanto, A. B. B., & Kim, J.-Y. (2018). Callose balancing at plasmodesmata. *Journal of Experimental Botany*. <https://doi.org/10.1093/jxb/ery317>
- Xiang, Y., Huang, C.-H., Hu, Y., Wen, J., Li, S., Yi, T., Chen, H., Xiang, J., & Ma, H. (2016). Evolution of Rosaceae Fruit Types Based on Nuclear Phylogeny in the Context of Geological Times and Genome Duplication. *Molecular Biology and Evolution*, msw242. <https://doi.org/10.1093/molbev/msw242>
- Xu, F., Rong, X., Huang, X., & Cheng, S. (2012). Recent Advances of Flowering Locus T Gene in Higher Plants. *International Journal of Molecular Sciences*, 13(3), 3773–3781. <https://doi.org/10.3390/ijms13033773>
- Xu, M., Hu, T., Zhao, J., Park, M.-Y., Earley, K. W., Wu, G., Yang, L., & Poethig, R. S. (2016). Developmental Functions of miR156-Regulated SQUAMOSA PROMOTER BINDING PROTEIN-LIKE (SPL) Genes in *Arabidopsis thaliana*. *PLOS Genetics*, 12(8), e1006263. <https://doi.org/10.1371/journal.pgen.1006263>
- Xu, Y., Liu, S., Liu, Y., Ling, S., Chen, C., & Yao, J. (2017). HOTHEAD-Like HTH1 is Involved in Anther Cutin Biosynthesis and is Required for Pollen Fertility in Rice. *Plant and Cell Physiology*, 58(7), 1238–1248. <https://doi.org/10.1093/pcp/pcx063>
- Yamaguchi, A., Kobayashi, Y., Goto, K., Abe, M., & Araki, T. (2005). TWIN SISTER OF FT (TSF) Acts as a Floral Pathway Integrator Redundantly with FT. *Plant and Cell Physiology*, 46(8), 1175–1189. <https://doi.org/10.1093/pcp/pci151>
- Yamaguchi, N. (2021). LEAFY, a Pioneer Transcription Factor in Plants: A Mini-Review. *Frontiers in Plant Science*, 12. <https://doi.org/10.3389/fpls.2021.701406>
- Yang, Z., Wang, X., Gu, S., Hu, Z., Xu, H., & Xu, C. (2008). Comparative study of SBP-box gene family in *Arabidopsis* and rice. *Gene*, 407(1–2), 1–11. <https://doi.org/10.1016/j.gene.2007.02.034>
- Yoo, S. J., Chung, K. S., Jung, S. H., Yoo, S. Y., Lee, J. S., & Ahn, J. H. (2010). BROTHER OF FT AND TFL1 (BFT) has TFL1-like activity and functions redundantly with TFL1 in inflorescence meristem development in *Arabidopsis*. *The Plant Journal*, 63(2), 241–253. <https://doi.org/10.1111/j.1365-313X.2010.04234.x>
- Yoo, S. Y., Kardailsky, I., Lee, J. S., Weigel, D., & Ahn, J. H. (2004). Acceleration of flowering by overexpression of MFT (MOTHER OF FT AND TFL1). *Molecules and Cells*, 17(1), 95–101.
- Yordanov, Y. S., Ma, C., Strauss, S. H., & Busov, V. B. (2014). EARLY BUD-BREAK 1 (EBB1) is a regulator of release from seasonal dormancy in poplar trees. *Proceedings of the National Academy of Sciences*, 111(27), 10001–10006. <https://doi.org/10.1073/pnas.1405621111>
- Yu, H., Ito, T., Wellmer, F., & Meyerowitz, E. M. (2004). Repression of AGAMOUS-LIKE 24 is a crucial step in promoting flower development. *Nature Genetics*, 36(2), 157–161. <https://doi.org/10.1038/ng1286>

- Yu, H., Xu, Y., Tan, E. L., & Kumar, P. P. (2002). AGAMOUS-LIKE 24, a dosage-dependent mediator of the flowering signals. *Proceedings of the National Academy of Sciences*, *99*(25), 16336–16341. <https://doi.org/10.1073/pnas.212624599>
- Yu, N., Yang, J.-C., Yin, G.-T., Li, R.-S., & Zou, W.-T. (2020). Genome-wide characterization of the SPL gene family involved in the age development of *Jatropha curcas*. *BMC Genomics*, *21*(1), 368. <https://doi.org/10.1186/s12864-020-06776-8>
- Zaret, K. S., & Carroll, J. S. (2011). Pioneer transcription factors: establishing competence for gene expression. *Genes & Development*, *25*(21), 2227–2241. <https://doi.org/10.1101/gad.176826.111>
- Zawaski, C., & Busov, V. B. (2014). Roles of Gibberellin Catabolism and Signaling in Growth and Physiological Response to Drought and Short-Day Photoperiods in *Populus* Trees. *PLoS ONE*, *9*(1), e86217. <https://doi.org/10.1371/journal.pone.0086217>
- Zawaski, C., Kadmiel, M., Pickens, J., Ma, C., Strauss, S., & Busov, V. (2011). Repression of gibberellin biosynthesis or signaling produces striking alterations in poplar growth, morphology, and flowering. *Planta*, *234*(6), 1285–1298. <https://doi.org/10.1007/s00425-011-1485-x>
- Zhao, K., Zhou, Y., Li, Y., Zhuo, X., Ahmad, S., Han, Y., Yong, X., & Zhang, Q. (2018). Crosstalk of PmCBFs and PmDAMs Based on the Changes of Phytohormones under Seasonal Cold Stress in the Stem of *Prunus mume*. *International Journal of Molecular Sciences*, *19*(2), 15. <https://doi.org/10.3390/ijms19020015>
- Zhao, T., Yang, X., Yang, X., Rao, P., An, X., & Chen, Z. (2021). Identification of key flowering-related genes and their seasonal expression in *Populus tomentosa* reproductive buds suggests dual roles in floral development and dormancy. *Industrial Crops and Products*, *161*, 113175. <https://doi.org/10.1016/j.indcrop.2020.113175>
- Zheng, C., Halaly, T., Acheampong, A. K., Takebayashi, Y., Jikumaru, Y., Kamiya, Y., & Or, E. (2015). Abscisic acid (ABA) regulates grape bud dormancy, and dormancy release stimuli may act through modification of ABA metabolism. *Journal of Experimental Botany*, *66*(5), 1527–1542. <https://doi.org/10.1093/jxb/eru519>
- Zheng, C., Kwame Acheampong, A., Shi, Z., Halaly, T., Kamiya, Y., Ophir, R., Galbraith, D. W., & Or, E. (2018a). Distinct gibberellin functions during and after grapevine bud dormancy release. *Journal of Experimental Botany*, *69*(7), 1635–1648. <https://doi.org/10.1093/jxb/ery022>
- Zheng, C., Kwame Acheampong, A., Shi, Z., Halaly, T., Kamiya, Y., Ophir, R., Galbraith, D. W., & Or, E. (2018b). Distinct gibberellin functions during and after grapevine bud dormancy release. *Journal of Experimental Botany*, *69*(7), 1635–1648. <https://doi.org/10.1093/jxb/ery022>
- Zhu, Y., Klasfeld, S., Jeong, C. W., Jin, R., Goto, K., Yamaguchi, N., & Wagner, D. (2020). TERMINAL FLOWER 1-FD complex target genes and competition with FLOWERING LOCUS T. *Nature Communications*, *11*(1), 5118. <https://doi.org/10.1038/s41467-020-18782-1>

- Zhu, Y., Li, Y., Xin, D., Chen, W., Shao, X., Wang, Y., & Guo, W. (2015). RNA-Seq-based transcriptome analysis of dormant flower buds of Chinese cherry (*Prunus pseudocerasus*). *Gene*, *555*(2), 362–376. <https://doi.org/10.1016/j.gene.2014.11.032>
- Zhuang, W., Gao, Z., Wang, L., Zhong, W., Ni, Z., & Zhang, Z. (2013). Comparative proteomic and transcriptomic approaches to address the active role of GA4 in Japanese apricot flower bud dormancy release. *Journal of Experimental Botany*, *64*(16), 4953–4966. <https://doi.org/10.1093/jxb/ert284>

## 7. Supplementary material

**Table 1. List of primers used for expression analysis and molecular procedures.**

<b>PRIMER</b>	<b>PRIMER SEQUENCE (5'-3')</b>
<b>QSHTH FW</b>	AATGGGTACTATTGGGT
<b>QSHTH RV</b>	GTCGACTCAATTATTTGAG
<b>PGAD424 FW</b>	CTATTCGATGATGAAGATACCC
<b>PGAD424 RV</b>	GAACTGCGGGGTTTTTCAG
<b>PABAI FW</b>	TTTGTCTGTGCAGTTGGGT
<b>PABAI RV</b>	TCGGCTACATGGCAGTTTGG
<b>QS SPL4 FW</b>	ACCATAGGAGGCACAAGGTG
<b>QS SPL4 RV</b>	CGGCAACTCCTCTTTGTTTC
<b>QSFT FW</b>	GATGCACCAAGTCCAAGTGA
<b>QSFT RV</b>	TTGACGGAACAACACGAAAC
<b>QS SOC1 FW</b>	GCAGCTGAAAATGCAAGGCT
<b>QS SOC1 RV</b>	GCTCTTTGTTCTCCCTTCT
<b>QS SVP1 FW</b>	GGACTTACCCGTGTGCTTGA
<b>QS SVP1 RV</b>	ATGTCCGAGTCCACAAGACC
<b>QSFLC FW</b>	GGAGTCCATAATGAGCCTTCA
<b>QSFLC RV</b>	GGATGGGCCAACTGATGAT
<b>QS SHP1.FW</b>	AGGGAAGTTGAGCGCAAAA
<b>QS SHP1.RV</b>	CTGGGAGGTAGTTCCGATCA
<b>QS ACT F1</b>	GCTGGATTCTGGTGATGGTGTGAGC
<b>QS ACT R1</b>	GCTTCAATGAGAGATGGCTGGAAGAGG
<b>QSPP2AA3 FW</b>	GGGTTCCCAACATCAAGTTC
<b>QSPP2AA3 RV</b>	TGACCTGATCACTTGACTGC

**Table 2. Gene accession list.**

FT		
Species	Identifier	Gene Accessions
<i>Actinidia chinensis</i>	<i>AcBFT1</i>	ARE72520.1
	<i>AcBFT2</i>	ARE72521.1
	<i>AcBFT3</i>	ARE72522.1
	<i>AcCEN1</i>	ARE72516.1
	<i>AcCEN2</i>	ARE72517.1
	<i>AcCEN3</i>	ARE72518.1
	<i>AcCEN4</i>	ARE72519.1
	<i>AcFT1</i>	ARE72514.1
	<i>AcFT2</i>	ARE72515.1
<i>Amborella trichopoda</i>	<i>AcMFT1</i>	ARE72523.1
	<i>AcMFT2</i>	ARE72524.1
	<i>AmCEN</i>	XP_011628408.1
<i>Arabidopsis thaliana</i>	<i>AmMFT</i>	XP_006841865.2
	<i>AtBFT</i>	AT5G62040.1
	<i>AtFT</i>	AT1G65480.1
	<i>AtMFT</i>	AT1G18100.1
	<i>AtTFL1</i>	AT5G03840.1
<i>Citrus unshiu</i>	<i>AtTFT</i>	AAF03937.1
	<i>CiBFT</i>	A0A2H5NM19
	<i>CiFT1</i>	BAA77836.1
	<i>CiFT2</i>	BAF96644.1

	<i>CiFT3</i>	BAF96645.1
	<i>CiMFT</i>	A9ECZ7
	<i>CiTFL1</i>	AOA2H5MYR6
<i>Castanea mollissima</i>	<i>CmCEN</i>	Cm_g49231.t1
<i>Castanea sativa</i>	<i>CsaCEN</i>	TRINITY_DN77437_c0_g1_i1
	<i>CsaFT</i>	TRINITY_DN18605_c0_g1_i1
	<i>CsaMFT</i>	TRINITY_DN68730_c0_g2_i1
	<i>CsaTFL1</i>	TRINITY_DN95552_c0_g1_i1
<i>Cucumis sativus</i>	<i>CsFT</i>	NP_001292686.1
	<i>CsSP</i>	NP_001267654.1
	<i>CsTFL1</i>	BAH28254.1
<i>Fagus crenata</i>	<i>FcFT</i>	BAP28173.1
<i>Gingko biloba</i>	<i>GbFT</i>	ANS56339.1
<i>Juglans regia</i>	<i>JrFT</i>	01182017_WALNUT_00002262-RA_mRNA
	<i>JrTFL1</i>	XP_018811176.1
<i>Malus domestica</i>	<i>MdBFT</i>	NP_001280770.1
	<i>MdCENa</i>	NP_001280940.1
	<i>MdCENb</i>	NP_001280813.1
	<i>MdFT</i>	BAI77730.1
	<i>MdMFT</i>	XP_008374830.1
	<i>MdTFLa</i>	NP_001280887.1
	<i>MdTFLb</i>	NP_001280794.1
<i>Medicago truncatula</i>	<i>MtFT</i>	XP_013451589.1
	<i>MtTFL1</i>	XP_003625808.1
<i>Oryza sativa</i>	<i>OsHd3a</i>	BAO03040.1

	<i>PpBFT</i>	XP_007221173.1
	<i>PpFT</i>	ACH73165.1
<i>Prunus persica</i>	<i>PpMFT</i>	XP_007209687.1
	<i>PpTFLa</i>	XP_007202664.1
	<i>PpTFLb</i>	XP_007206006.1
	<i>PtBFT</i>	XP_002321903.2
	<i>PtCENLa</i>	XP_006384827.1
<i>Populus trichocarpa</i>	<i>PtCENLb</i>	XP_002312811.1
	<i>PtFT1</i>	XP_002311264.1
	<i>PtFT2</i>	XP_002316173.1
	<i>PtMFT</i>	XP_002321507.1
	<i>QIBFT</i>	XP_030933076.1
	<i>QIFT</i>	XP_030971855.1
<i>Quercus lobata</i>	<i>QIMFT</i>	XP_030941190.1
	<i>QIMFTLa</i>	XP_030971914.1
	<i>QIMFTLb</i>	XP_030971915.1
	<i>QITFL1</i>	XP_030927808.1
	<i>QrBFT</i>	Qrob_P0372980.2
	<i>QrCEN</i>	XP_050280681.1
<i>Quercus robur</i>	<i>QrFT</i>	Qrob_P0763140.2
	<i>QrMFT</i>	Qrob_P0431520.2
	<i>QrMFTL</i>	Qrob_P0701880.2
	<i>QrTFL1</i>	Qrob_P0649270.2
<i>Quercus rubra</i>	<i>QruBFT</i>	120313 comp12577 c0 seq1 m.3461
	<i>QruFT</i>	120313 comp71155 c0 seq1

	<i>QruMFT</i>	120313 comp25656 c0 seq1 m.1723
<i>Quercus suber</i>	<i>QsBFT</i>	XP_023885678.1
	<i>QsCEN</i>	XP_023880417.1
	<i>QsFT</i>	XP_023899320.1
	<i>QsMFT</i>	XP_023927178.1
	<i>QsMFTL</i>	XP_023877038.1
	<i>QsTFL1</i>	XP_023905546.1
<i>Solanum lycopersicum</i>	<i>SISP</i>	sp O82088.1
<i>Vitis vinifera</i>	<i>VvFT</i>	ABF56526.1
	<i>VvTFL1</i>	AAM46142.1
<i>Zea mays</i>	<i>ZmFT</i>	PWZ45286.1
	<i>ZmTFL1</i>	ABI98712.1

*SOC*

Species	Identifier	Gene Accessions
<i>Actinidia chinensis</i>	<i>AcSOC1a</i>	AKH61954.1
	<i>AcSOC1b</i>	AKH61955.1
	<i>AcSOC1c</i>	AKH61956.1
	<i>AcSOC1d</i>	AKH61957.1
	<i>AcSOC1e</i>	AKH61958.1
	<i>AcSOC1f</i>	AKH61959.1
	<i>AcSOC1g</i>	AKH61960.1
	<i>AcSOC1h</i>	AKH61961.1
	<i>AcSOC1i</i>	AKH61962.1
<i>Arabidopsis thaliana</i>	<i>AtAGL14</i>	AT4G11880.1
	<i>AtAGL19</i>	AT4G22950.1

	<i>AtAGL42(FYF)</i>	AT5G62165.1
	<i>AtAGL71(FYF1)</i>	AT5G51870.3
	<i>AtAGL72(FYF2)</i>	AT5G51860.1
	<i>AtSOC1</i>	AT2G45660.1
<i>Castanea mollissima</i>	<i>CmAGL19</i>	KAF3952286.1
	<i>CmAGL42</i>	KAF3973569.1 hypothetical protein CMV 003024
	<i>CmSOC1</i>	KAF3966985.1 hypothetical protein CMV 008965
<i>Citrus sinensis</i>	<i>CsiAGL19a</i>	XP 006477355.1
	<i>CsiAGL19b</i>	XP 006477351.1
	<i>CsiAGL42</i>	KAH9678043.1
	<i>CsiSOC1</i>	NP 001275772.1
<i>Juglans regia</i>	<i>JrAGL19a</i>	XP 018820266.1
	<i>JrAGL19b</i>	XP 018820468.2
	<i>JrAGL42</i>	XP 018830813.1
	<i>JrSOC1a</i>	XP 018851690.1
	<i>JrSOC1b</i>	XP 018820384.1
	<i>JrSOC1c</i>	XP 018820387.1
<i>Malus domestica</i>	<i>MdAGL19</i>	NP 001280778.1
	<i>MdAGL42a</i>	XP 008376826.1
	<i>MdAGL42b</i>	XP 008376862.1
	<i>MdAGL42c</i>	NP 001280901.1
	<i>MdSOC1a</i>	NP 001280855.1
	<i>MdSOC1b</i>	NP 001315886.1
	<i>MtAGL19</i>	XP 013457660.1

<i>Medicago truncatula</i>	<i>MtSOC1</i>	XP 003623808.2
	<i>PbAGL19a</i>	XP 009345827.1
	<i>PbAGL19b (PbSOC1c)</i>	XP 009362848.2
	<i>PbAGL19c</i>	XP 048445115.1
	<i>PbAGL42a</i>	XP 009371259.2
<i>Pyrus brestchneideri</i>	<i>PbAGL42b (PbSOC1d)</i>	XP 009347895.1
	<i>PbAGL42c (PbSOC1f)</i>	XP 018501073.1
	<i>PbAGL42d</i>	XP 048427014.1
	<i>PbSOC1a</i>	XP 048431602.1
	<i>PbSOC1b</i>	XP 048432208.1
<i>Petunia hybrida</i>	<i>PhFBP20</i>	AAK21251.1
	<i>PhFBP21</i>	AAK21252.1
	<i>PhFBP22</i>	AAK21253.1
	<i>PhFBP28</i>	AAK21257.1
<i>Prunus persica</i>	<i>PpAGL14</i>	XP 020420482.1
	<i>PpAGL42</i>	XP 007219737.2
	<i>PpSOC1</i>	XP 007221064.2
<i>Populus trichocarpa</i>	<i>PtAGL19a</i>	XP 024461746.1
	<i>PtAGL19b</i>	XP 024452474.1
	<i>PtAGL42</i>	XP 002318261.1
	<i>PtSOC1a</i>	XP 002302552.3
	<i>PtSOC1b</i>	XP 024440079.1
	<i>PtSOC1c</i>	XP 024440080.1
	<i>PtSOC1d</i>	XP 024440072.1

	<i>PtSOC1e</i>	XP 024440073.1
<i>Quercus robur</i>	<i>QrAGL19</i>	XP 050267013.1
	<i>QrAGL42a</i>	XP 050251034.1
	<i>QrAGL42b</i>	XP 050251035.1
	<i>QrSOC1</i>	XP 050249824.1
<i>Quercus suber</i>	<i>QsAGL19</i>	XP 023876869.1
	<i>QsSOC1</i>	XP 023900830.1
<i>Vitis vinifera</i>	<i>VvAGL19</i>	XP 002275695.2
	<i>VvAGL42</i>	XP 010662337.1
	<i>VvSOC1</i>	NP 001267909.1

**SVP**

Species	Identifier	Gene Accessions
<i>Actinidia chinensis</i>	<i>AcSVP1</i>	AFA37967.1
	<i>AcSVP2</i>	AFA37968.1
	<i>AcSVP3</i>	AFA37969.1
	<i>AcSVP4</i>	AFA37970.1
<i>Amborella trichopoda</i>	<i>AmtSVPa</i>	XP 011629321.1
	<i>AmtSVPb</i>	XP 020517655.1
<i>Arabidopsis thaliana</i>	<i>AtSVP</i>	AFU85642.1
<i>Corylus avellana</i>	<i>CaSVP1</i>	Corav.7774
	<i>CaSVP5</i>	Corav.2037
<i>Castanea sativa</i>	<i>CsaSVP1</i>	TRINITY_DN1678_c6_g1_i1.p1
	<i>CsaSVP2 (AT)</i>	TRINITY DN77088 c0 g4 i1
	<i>CsaSVP4 (AT)</i>	TRINITY DN16223 c0 g1 i1
	<i>CsaSVP5 (AT SVP1)</i>	TRINITY_DN63368_c0_g1_i1

<i>Juglans regia</i>	<i>JrSVPa</i>	XP 018806751.1
	<i>JrSVPb</i>	XP 018806748.1
<i>Malus domestica</i>	<i>MdDAM1</i>	KP164996.1
	<i>MdDAM2</i>	KP164997
	<i>MdDAM3</i>	MD15G1384500
	<i>MdJOINTLESS1</i>	XP 028953815.1
	<i>MdJOINTLESS2</i>	XP 008363740.1
	<i>MdJOINTLESS3</i>	XP 028949096.1
<i>Oryza sativa</i>	<i>OsSVP</i>	AAQ23144.2
<i>Prunus persica</i>	<i>PpDAM1</i>	ABJ96361.2
	<i>PpDAM2</i>	ABJ96370.1
	<i>PpDAM3</i>	ABJ96371.1
	<i>PpDAM4</i>	ABJ96365.1
	<i>PpDAM5</i>	ABJ96359.1
	<i>PpDAM6</i>	ABJ96360.1
	<i>PpSVP1</i>	XP 020422314.1
	<i>PpSVP2</i>	XP 020422315.1
	<i>PpSVP3</i>	XP 007205845.2
<i>Populus trichocarpa</i>	<i>PtSVPa</i>	Pt1 POPTR 007G010800
	<i>PtSVPb</i>	Pt6 POPTR 005G155300
	<i>PtSVPc</i>	Pt4 POPTR 005G155300
	<i>PtSVPd</i>	Pt5 POPTR 005G155300
	<i>PtSVPe</i>	Pt3 POPTR 002G105600
	<i>PtSVPf</i>	Pt2 POPTR 002G105600
<i>Quercus robur</i>	<i>QrSVP1</i>	XP 050292150.1

	<i>QrSVP2</i>	XP 050260235.1
	<i>QrSVP3</i>	XP 050260244.1
	<i>QrSVP4</i>	XP 050260238.1
	<i>QrSVP5</i>	XP 050251974.1
	<i>QrSVP6</i>	XP 050260211.1
<i>Quercus rubra</i>	<i>QruSVP1</i>	120313 comp20213 c0 seq1 m.8705
<i>Quercus suber</i>	<i>QsSVP1</i>	QSP116365.0
	<i>QsSVP2</i>	QSP020714.0
	<i>QsSVP3</i>	XP 023916617.1
	<i>QsSVP4</i>	QSP012535.0
	<i>QsSVP5</i>	QSP056153.0
	<i>QsSVP6</i>	QSP095201.0
<i>Solanum lycopersicum</i>	<i>SISVP</i>	NP 001306770.1
<i>Vitis vinifera</i>	<i>VvSVPa</i>	XP 019073897.1
	<i>VvSVPb</i>	XP 010661297.2
	<i>VvSVPc</i>	XP 010648133.1

**FLC**

Species	Identifier	Gene Accessions
<i>Arabidopsis thaliana</i>	<i>AaPEP</i>	ACQ44228.1
<i>Actinidia chinensis</i>	<i>AcFLC</i>	PSS13690.1
<i>Beta vulgaris</i>	<i>BvFLC</i>	ABN04205.1
<i>Corylus avellana</i>	<i>CaFLC</i>	Corav.4981 Corylus avellana

<i>Cardamine flexuosa</i>	<i>CfFLC</i>	AGN29203.1
<i>Castanea mollissima</i>	<i>CmFLC</i>	Cm_g11184.t1
<i>Castanea sativa</i>	<i>CsaFLCa</i>	TRINITY_DN65955_c0_g1_i1
	<i>CsaFLCb</i>	TRINITY_DN65955_c0_g1_i2
<i>Glycine max</i>	<i>GmFLCa</i>	XP 014631160.1
	<i>GmFLCb</i>	XP 003524905.1
<i>Malus domestica</i>	<i>MdFLC</i>	QDB06341.1
<i>Populus trichocarpa</i>	<i>PtFLCa</i>	XP 024452986.1
	<i>PtFLCb</i>	XP 024452886.1
	<i>PtFLCc</i>	XP 024452565.1
	<i>PtFLCd</i>	XP 024452564.1
<i>Quercus robur</i>	<i>QrFLCa</i>	Qrob P0729180.2 83
	<i>QrFLCb</i>	XP 050276176.1
<i>Quercus rubra</i>	<i>QruFLC</i>	120313 comp11449 c0 seq1 m.2899
<i>Quercus suber</i>	<i>QsFLC</i>	XP 023903430.1
<i>Solanum lycopersicum</i>	<i>SIFLC</i>	XP 010321013.1
<i>Vitis vinifera</i>	<i>VvFLC</i>	NP 001268057.1

*LFY*

Species	Identifier	Gene Accessions
<i>Castanea henryi</i>	<i>ChLFY</i>	AFJ04412.1
<i>Argyranthemum frutescens</i>	<i>AfLFYa</i>	QBQ95415.1
	<i>AfLFYb</i>	QBQ95416.1
<i>Antirrhinus majus</i>	<i>AmjFLO</i>	P23915.1
<i>Amborella trichopoda</i>	<i>AmLFY</i>	NP 001292752.1

<i>Arabidopsis thaliana</i>	<i>AtLFY</i>	AAM27931.1
<i>Citrus unshiu</i>	<i>CiLFY</i>	ABJ97281.1
<i>Castanea mollissima</i>	<i>CmLFY</i>	maker-scaffold02060-augustus-gene-0.31-mRNA-1 protein
<i>Castanea mollissima</i>	<i>CsaLFY</i>	TRINITY_DN64373_c0_g1_i1
<i>Cucumis sativus</i>	<i>CsLFY</i>	NP_001292666.1
<i>Fagus crenata</i>	<i>FcLFY</i>	BAP28172.1
<i>Glycine max</i>	<i>GmLFY</i>	ABP94177.1
<i>Juglans regia</i>	<i>JrLFY</i>	AXR75691.1
<i>Malus domestica</i>	<i>MdLFY</i>	ABF84009.1
<i>Mangifera indica</i>	<i>MiLFYa</i>	ADX97319.1
	<i>MiLFYb</i>	ADX97318.1
	<i>MiLFYc</i>	ADX97315.1
	<i>MiLFYd</i>	ADX97316.1
<i>Oryza sativa</i>	<i>OsFLO/LFY</i>	XP_015635355.1
	<i>OsRFL</i>	AAY33607.1
<i>Pyrus cummunis</i>	<i>PcLFYa</i>	BAD10951.1
	<i>PcLFYb</i>	BAD10957.1
<i>Prunus persica</i>	<i>PpLFY</i>	ABY78032.1
<i>Pynus radiata</i>	<i>PrFLO/LFY</i>	sp O04116.1
<i>Populus trichocarpa</i>	<i>PtLFY</i>	AAB51533.1
<i>Quercus lobata</i>	<i>QILFY</i>	XP_030940803.1
<i>Quercus robur</i>	<i>QrLFY</i>	XP_050258338.1
<i>Quercus suber</i>	<i>QsLFY</i>	XP_023902312.1
<i>Vitits vinifera</i>	<i>VvLFY</i>	AAM46141.1

SPL

Species	Identifier	Gene Accessions
<i>Antirrhinum majus</i>	<i>AmjSPL13</i>	sp Q38741.1
	<i>AmjSPL9</i>	CAB56570.1
<i>Colrylus avellana</i>	<i>CaSPL13</i>	Corav.4743
<i>Castanea mollissima</i>	<i>CmSPL16</i>	Cm g1042.t1
	<i>CmSPL13</i>	Cm g8825.t1
	<i>CmSPL9a</i>	Cm g11422.t2
	<i>CmSPL9b</i>	Cm g11422.t1
	<i>CmSPLa</i>	Cm g16231.t1
<i>Castanea sativa</i>	<i>CsaSPL13a</i>	TRINITY_DN72534_c4_g2_i2
	<i>CsaSPL13b</i>	TRINITY_DN72534_c2_g1_i1
	<i>CsaSPL4</i>	TRINITY_DN76783_c1_g1_i3
	<i>CsaSPL9</i>	TRINITY_DN64862_c0_g1_i1
<i>Cucumis sativos</i>	<i>CsSPL13</i>	XP 004138255.1
	<i>CsSPL3</i>	XP 011653273.1
	<i>CsSPL9</i>	XP 004136576.1
<i>Glycine max</i>	<i>GmSPL13a</i>	XP 003525416.1
	<i>GmSPL13b</i>	XP 003532399.2
	<i>GmSPL9</i>	XP 003553428.1
<i>Juglans regia</i>	<i>JrSPL13</i>	01182017 WALNUT 00005162-RA mRNA protein
	<i>JrSPL3a</i>	XP 018850782.1
	<i>JrSPL3b</i>	01182017 WALNUT 00016104-RA mRNA protein
	<i>JrSPL9</i>	01182017 WALNUT 00022989-RA mRNA protein
<i>Malus domestica</i>	<i>MdSPL13</i>	NP 001281011.1
	<i>MdSPL3</i>	XP 008383704.1

	<i>MdSPL9</i>	XP 008392088.1
<i>Mangifera indica</i>	<i>MiSPL13</i>	XP 044491968.1
	<i>MiSPL3a</i>	XP 044473334.1
	<i>MiSPL3b</i>	XP 044466985.1
	<i>MiSPL9</i>	XP 044507349.1
	<i>MtSPL13a</i>	XP 003602795.1
<i>Medicago truncatula</i>	<i>MtSPL13b</i>	XP 024628067.1
	<i>MtSPL13c</i>	XP 024628066.1
	<i>MtSPL3a</i>	XP 024637451.1
	<i>MtSPL3b</i>	XP 013456994.1
	<i>MtSPL9</i>	XP 003625236.2
<i>Prunus persica</i>	<i>PpSPL13a</i>	XP 007209206.1
	<i>PpSPL13b</i>	XP 020415133.1
	<i>PpSPL13c</i>	XP 007224806.2
	<i>PpSPL3</i>	XP 007212177.1
	<i>PpSPL9a</i>	XP 007203426.1
	<i>PpSPL9b</i>	XP 007205341.1
<i>Populus trichocarpa</i>	<i>PtSPL13</i>	XP 002322273.3
	<i>PtSPL3</i>	XP 006377387.2
	<i>PtSPL4</i>	XP 002317486.3
	<i>PtSPL9</i>	XP 002322678.3
<i>Quercus lobata</i>	<i>QISPL13a</i>	XP 030937235.1
	<i>QISPL13b</i>	XP 030937234.1
	<i>QISPL4</i>	XP 030932880.1
	<i>QISPL6</i>	XP 030956853.1

	<i>QISPL9</i>	XP 030926912.1
	<i>QrSPL1</i>	XP 050264767.1
	<i>QrSPL14</i>	XP 050268044.1
	<i>QrSPL2</i>	XP 050276190.1
	<i>QrSPL6</i>	XP 050277562.1
	<i>QrSPL7a</i>	XP 050240237.1
<i>Quercus robur</i>	<i>QrSPL7b</i>	XP 050240236.1
	<i>QrSPL8a</i>	XP 050282265.1
	<i>QrSPL8b</i>	XP 050282266.1
	<i>QrSPL9</i>	XP 050244707.1
	<i>QrSPL13</i>	<i>XP 050257612.1</i>
	<i>QrSPL16</i>	<i>XP 050270745.1</i>
	<i>QruSPL13a</i>	120313 comp28334 c0 seq9 m.22992
	<i>QruSPL13b</i>	120313 comp28334 c0 seq3 m.22986
<i>Quercus rubra</i>	<i>QruSPL13c</i>	120313 comp28334 c0 seq2 m.22985
	<i>QruSPL4</i>	120313 comp11550 c0 seq1 m.2969
	<i>QruSPL9</i>	120313 comp23812 c0 seq1 m.13847
	<i>QruSPL16</i>	120313 comp28334 c0 seq10 m.22993
	<i>QsSPL13</i>	XP 023894488.1
<i>Quercus suber</i>	<i>QsSPL4</i>	XP 023889584.1
	<i>QsSPL6</i>	XP 023917881.1
	<i>QsSPL9</i>	XP 023919077.1
<i>Solanum lycopersicum</i>	<i>SISPL9</i>	XP 004249164.1
<i>Vitis vinifera</i>	<i>VvSPL13a</i>	XP 002280160.1
	<i>VvSPL13b</i>	XP 010660739.1

<i>W<sub>SPL3</sub></i>	XP 002282598.1
<i>W<sub>SPL9</sub></i>	NP 001267898.1

**Table 3. Scanning densitometry results.**

<i>QrSVP1</i>	AREA	%	NORM	<i>QrSOC1</i>	AREA	%	NORM
Jan	2643,477	7,116	0,642528	Jan	2508,163	8,764	0,791332
Feb	4876,477	13,126	1,035991	Feb	3894,113	13,607	1,073954
Mar	4627,527	12,456	1,36146	Mar	6018,234	21,029	2,298503
Apr	4465,113	12,019	1,594455	Apr	1708,991	5,972	0,792253
May	3761,698	10,125	0,951598	May	4948,355	17,291	1,625094
Jun	4641,406	12,493	1,927337	Jun	1913,941	6,688	1,03178
Jul	4148,527	11,167	1,648996	Jul	4476,134	15,641	2,309657
Aug	826,406	2,224	0,274432	Aug	0	0	0
Sep	3037,184	8,175	0,684845	Sep	0	0	0
Oct	1842,184	4,959	1,315734	Oct	0	0	0
Nov	1459,355	3,928	0,570019	Nov	1894,062	6,618	0,960383
Dec	821,577	2,211	0,44478	Dec	1256,184	4,389	0,882921
<i>QrSHP</i>	AREA	%	NORM	<i>QrFLC</i>	AREA	%	NORM
Jan	390,184	4,72	0,426185	Jan	3111,477	8,48	0,765688
Feb	516,527	6,249	0,493212	Feb	4821,113	13,139	1,037017
Mar	936,355	11,328	1,238168	Mar	4195,062	11,433	1,249645
Apr	491,477	5,946	0,788803	Apr	4566,82	12,446	1,651101
May	895,527	10,834	1,018233	May	4215,284	11,488	1,079699

Jun	825,719	9,99	1,541191	Jun	4678,82	12,752	1,967294
Jul	1158,77	14,019	2,070142	Jul	2681,527	7,308	1,079149
Aug	1482,305	17,933	2,212858	Aug	968,648	2,64	0,325765
Sep	439,598	5,318	0,445506	Sep	1416,891	3,862	0,323532
Oct	362,77	4,389	1,1645	Oct	3041,962	8,29	2,199522
Nov	363,941	4,403	0,638949	Nov	1737,062	4,734	0,686983
Dec	402,577	4,87	0,979682	Dec	1257,527	3,427	0,689399
<b>QrSPL4</b>	<b>AREA</b>	<b>%</b>	<b>NORM</b>	<b>QrPP2A3</b>	<b>AREA</b>	<b>%</b>	
Jan	228,87	7,542	0,680993	Jan	1059,648	11,075	
Feb	538,406	17,743	1,400395	Feb	1212,284	12,67	
Mar	618,87	20,395			875,406	9,149	
Apr	0	0	0	Apr	721,284	7,538	
May	202,213	6,664	0,626316	May	1018,062	10,64	
Jun	0	0	0	Jun	620,234	6,482	
Jul	1446,113	47,656	7,037212	Jul	647,991	6,772	
Aug	0	0	0	Aug	775,406	8,104	
Sep	0	0	0	Sep	1142,134	11,937	
Oct	0	0	0	Oct	360,619	3,769	
Nov	0	0	0	Nov	659,376	6,891	
Dec	0	0	0	Dec	475,648	4,971	
<b>QrFT</b>	<b>Peak Area</b>	<b>%</b>	<b>Norm</b>	<b>QrACT</b>	<b>Peak Area</b>	<b>%</b>	
Mar	2329,841	8,602	1,516305	1	1604,527	5,673	
Apr	3737,305	13,799	1,219963	2	3198,861	11,311	
May	3733,255	13,784	1,43136	3	2723,619	9,63	
Jun	2676,598	9,883	1,191153	4	2346,619	8,297	

Jul	3374,598	12,46	1,565523	5	2251,033	7,959
Aug	5732,477	21,166	1,859276	6	3219,569	11,384
Sep	1834,669	6,774	0,487619	7	3929,012	13,892
Oct	923,205	3,409	0,319734	8	3015,376	10,662
Nov	1693,347	6,252	0,438368	9	4033,589	14,262
Dec	1048,033	3,87	0,558603	10	1959,426	6,928

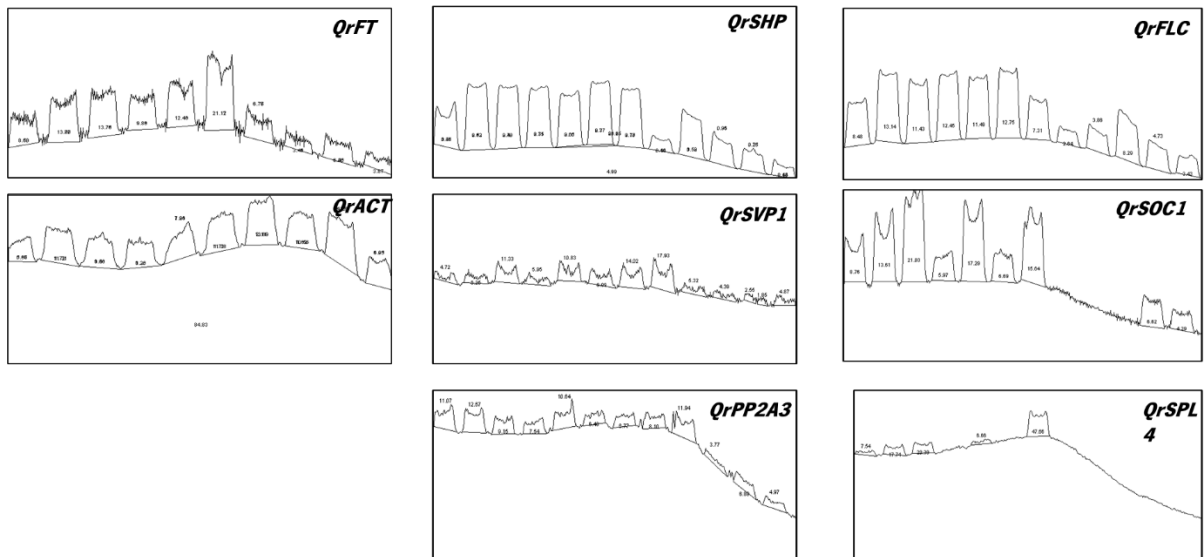


**Figure 1. Optical density graphs.** Obtained using the ImageJ software (Gassmann et al., 2009; Schneider et al., 2012).